



UNIVERSIDADE ESTADUAL DE CAMPINAS
FACULDADE DE CIÊNCIAS MÉDICAS

ALEXANDRE MOURA ASSIS

MECANISMOS ENVOLVIDOS NA DISFUNÇÃO DE NEURÔNIOS POMC NO
HIPOTÁLAMO DE CAMUNDONGOS OBESOS

*MECHANISMS OF POMC-EXPRESSING NEURONS DYSFUNCTION IN THE
HYPOTHALAMUS OF OBESE MICE*

CAMPINAS

2021

ALEXANDRE MOURA ASSIS

MECANISMOS ENVOLVIDOS NA DISFUNÇÃO DE NEURÔNIOS POMC NO
HIPOTÁLAMO DE CAMUNDONGOS OBESOS

*MECHANISMS OF POMC-EXPRESSING NEURONS DYSFUNCTION IN THE
HYPOTHALAMUS OF OBESE MICE*

Tese apresentada à Faculdade de Ciências Médicas da Universidade
Estadual de Campinas como parte dos requisitos exigidos para a
obtenção do título de Doutor em Ciências

ORIENTADOR: PROF. DR. LICIO AUGUSTO VELLOSO

ESTE TRABALHO CORRESPONDE À VERSÃO
FINAL DA TESE DEFENDIDA PELO
ALUNO ALEXANDRE MOURA ASSIS, E ORIENTADA PELO
PROF. DR. LICIO AUGUSTO VELLOSO.

CAMPINAS

Ficha catalográfica
Universidade Estadual de Campinas
Biblioteca da Faculdade de Ciências Médicas
Maristella Soares dos Santos - CRB 8/8402

Assis, Alexandre Moura, 1989-
As76m Mecanismos envolvidos na disfunção de neurônios POMC no hipotálamo de camundongos obesos / Alexandre Moura Assis. – Campinas, SP : [s.n.], 2021.

Orientador: Licio Augusto Velloso.
Tese (doutorado) – Universidade Estadual de Campinas, Faculdade de Ciências Médicas.

1. Obesidade. 2. Pró-opiomelanocortina. 3. Inflamação. 4. Metabolismo. 5. Leptina. I. Velloso, Licio Augusto, 1963-. II. Universidade Estadual de Campinas. Faculdade de Ciências Médicas. III. Título.

Informações para Biblioteca Digital

Título em outro idioma: Mechanisms of POMC-expressing neurons dysfunction in the hypothalamus of obese mice

Palavras-chave em inglês:

Obesity

Pro-opiomelanocortin

Inflammation

Metabolism

Leptin

Área de concentração: Fisiopatologia Médica

Titulação: Doutor em Ciências

Banca examinadora:

Licio Augusto Velloso [Orientador]

Eduardo Rochete Ropelle

Letícia Martins Ignácio de Souza

Aparecida Emiko Hirata

Egberto Gaspar de Moura

Data de defesa: 19-05-2021

Programa de Pós-Graduação: Fisiopatologia Médica

Identificação e informações acadêmicas do(a) aluno(a)

- ORCID do autor: <http://orcid.org/0000-0003-3300-3964>

- Currículo Lattes do autor: <http://lattes.cnpq.br/5560626716117484>

COMISSÃO EXAMINADORA DA DEFESA DE DOUTORADO
ALEXANDRE MOURA ASSIS

ORIENTADOR: PROF. DR. LICIO AUGUSTO VELLOSO

MEMBROS TITULARES:

- 1. PROF. DR. LICIO AUGUSTO VELLOSO**
 - 2. PROFA. DRA. LETÍCIA MARTINS IGNÁCIO DE SOUZA**
 - 3. PROF. DR. EGBERTO GASPAR DE MOURA**
 - 4. PROFA. DRA. APARECIDA EMIKO HIRATA**
 - 5. PROF. DR. EDUARDO ROCHETE ROPELLE**
-

Programa de Pós-Graduação em Fisiopatologia Médica da Faculdade de Ciências Médicas da Universidade Estadual de Campinas.

A ata de defesa com as respectivas assinaturas dos membros encontra-se no SIGA/Sistema de Fluxo de Dissertação/Tese e na Secretaria do Programa da FCM.

Data de Defesa: 19/05/2021

DEDICATÓRIA

Dedico esta Tese aos meus pais (Seu Sidney e D. Neide) que celebram cada pequeno êxito nesta jornada em pesquisa e acreditam piamente na dignidade que o trabalho duro proporciona. Obrigado pelo exemplo de tantas virtudes e por salvaguardar teus filhos.

Não me fora necessário dom, de onde quer que ele eventualmente pudesse vir, para profetizar que iríamos longe. E vamos longe! Vamos com a pressa de quem sabe o que quer, ainda que esta vida seja mesmo muito louca e por vezes tente resistir. Amo-te, Bruna.

AGRADECIMENTOS

Aos amigos de laboratório que compartilharam comigo, de perto ou de longe, a bancada, as incertezas e as cervejas. Parceiro Zeca, brilhante e audaz; Pedro, sempre disposto a me ajudar; Rafa Gaspar, sonhador e batalhador. Aos companheiros da labuta diária, já em outros caminhos: Daiane Engel, Nath Dragano e Joana Gaspar.

Ao Professor José Donato Jr. por colocar seu laboratório e os seus recursos à inteira disposição, muito aprendi com as rápidas visitas ao ICB/USP. Ao Fernando Simabuco pela habilidade técnica e disposição em ajudar no que for necessário. Ao Gerson, Erika e Marcio por manterem a máquina girando.

Ao Professor Licio Velloso, que me permitiu explorar a obesidade sob uma nova perspectiva, depositando muita confiança no meu trabalho e oferecendo as condições mais favoráveis para que eu pudesse prosperar.

Aos amigos de sempre, daquele velho Mosteiro. Gabriel, Marcus, Luis, Alex, Diego, Matteo e Marcel.

Aos amigos da Rockefeller University: Kristina Hedbacker, Estef, Lisa e Jerry. Ao Professor Paul Cohen e ao Franc Marchildon por disponibilizarem a estrutura de seu laboratório; ao professor Jeffrey Friedman, por abrir as portas do seu laboratório pra mim e oferecer imensas oportunidades na academia.

À Coordenação de Aperfeiçoamento de Pessoal de Nível Superior - Brasil (CAPES) e Fundação de Amparo à Pesquisa do Estado de São Paulo (FAPESP), processo número 2016/01245-5, pela concessão de bolsa no país e processo número 2019/12969-2, pela concessão de bolsa no exterior, que possibilitaram o desenvolvimento desta Tese.

O presente trabalho foi realizado com apoio da Coordenação de Aperfeiçoamento de Pessoal de Nível Superior - Brasil (CAPES) - Código de Financiamento 001 entre Maio/2016 e Dezembro/2017

ΕΠΪΓΡΑΦΕ

“(neurons are) the mysterious butterflies of the soul, the beating of whose wings may some day - who knows? – clarify the secrets of mental life”

Santiago Ramón y Cajal (1852-1934)

RESUMO

O hipotálamo integra sinais sistêmicos de hormônios e nutrientes em uma complexa rede neural que controla a ingestão alimentar e o gasto energético. A exposição crônica a uma dieta hiperlipídica é capaz de deflagrar uma resposta inflamatória no hipotálamo que dessensibiliza os neurônios POMC aos sinais anorexigênicos e, eventualmente, pode levar a perda neuronal por apoptose. Na primeira parte desta Tese, investigamos o papel da TRIL, uma proteína acessória do TLR4, na inflamação hipotalâmica associada ao consumo de dieta hiperlipídica e na função dos neurônios POMC. Demonstramos que a TRIL está predominantemente expressa em neurônios POMC e que o seu *knockdown* no núcleo arqueado resulta na redução da inflamação hipotalâmica, na melhora na homeostase glicêmica e na proteção contra a obesidade. Utilizando adenovírus associado Cre-dependente para o *knockdown* da TRIL especificamente nos neurônios POMC, observamos redução da massa de gordura e melhora na sinalização da leptina nestes neurônios.

A sensibilidade neuronal à glicose é fundamental para ativação pós-prandial de neurônios POMC e inibição do apetite por meio de seus sinais anorexigênicos. Na segunda parte desta Tese, examinamos o papel do PPAR δ como regulador indireto da ativação de neurônios POMC. Camundongos com deleção do PPAR δ em neurônios POMC utilizando *CRISPR-Cas9* não exibiram alteração na responsividade destes neurônios aos estímulos de glicose e leptina, no entanto, apresentaram melhora na homeostase sistêmica da glicose.

Esta Tese avaliou dois mecanismos potencialmente envolvidos com a disfunção do hipotálamo em obesidade e distúrbios metabólicos. Nossos resultados permitem concluir que a proteína TRIL participa da inflamação hipotalâmica gerada em resposta ao consumo de dieta hiperlipídica enquanto a inibição do PPAR δ em neurônios POMC é capaz de melhorar a homeostase sistêmica da glicose sem afetar sua resposta a leptina e glicose.

Palavras-chave: obesidade, proopiomelanocortina, inflamação, metabolismo, leptina

ABSTRACT

The hypothalamus integrates peripheral signals to a complex neural circuit that controls feeding and energy expenditure. The consumption of high-fat diet triggers an inflammatory response in the hypothalamus and promotes loss of nutrient sensing and apoptosis of POMC neurons after long-term high-fat diet feeding. Here, we investigated the role of TRIL, an accessory protein of TLR4, in the diet-induced hypothalamic inflammation and POMC neuronal function. We showed that TRIL is predominantly expressed in POMC neurons. After the knockdown of TRIL in the arcuate nucleus of the hypothalamus, there was a reduction in hypothalamic inflammation, improved systemic glucose tolerance and protection against diet-induced obesity. The POMC-specific knockdown of TRIL using Cre-dependent adeno-associated virus promoted body mass reduction and enhanced leptin signaling.

Glucose sensitivity is pivotal for the post-prandial activation and appetite-suppressant effects of POMC neurons. In the second part of this Thesis, we analyzed a putative role for PPAR δ as an indirect regulator of POMC neurons. CRISPR-Cas9-mediated deletion of PPAR δ in POMC neurons was not sufficient to alter glucose and leptin sensitivity, but reduced glucose intolerance in obese mice.

In this Thesis, we evaluated two mechanisms potentially involved in hypothalamic dysfunction in obesity and metabolic disorders. Altogether, our results show that TRIL is involved in the development of diet-induced hypothalamic inflammation whereas POMC PPAR δ is involved in the hypothalamic regulation of systemic glucose tolerance.

Keywords: obesity, proopiomelanocortin, inflammation, metabolism, leptin

SUMÁRIO

1. INTRODUÇÃO.....	11
2. CAPÍTULO 1: ARTIGO 1 - TLR4-interactor with leucine-rich repeats (TRIL) is involved in diet-induced hypothalamic inflammation.....	21
3. CAPÍTULO 2: ARTIGO 2 - POMC-specific deletion of PPAR δ attenuates diet-induced obesity and systemic glucose intolerance.....	56
4. CONCLUSÃO GERAL.....	75
5. REFERÊNCIAS.....	76
6. ANEXOS.....	80

INTRODUÇÃO

Obesidade: princípios e epidemiologia global

A obesidade é definida como um acúmulo excessivo de gordura corporal e está associada com redução na expectativa de vida, doenças cardiovasculares, diabetes *mellitus* tipo 2, câncer e outras doenças metabólicas (1–3). Embora não exista um padrão bem definido da relação temporal entre a progressão da obesidade e o início do desenvolvimento das doenças cardiometabólicas, estas parecem estar mais prevalentes nos indivíduos que apresentam deposição de gordura ectópica, isto é, em órgãos e tecidos como fígado, músculo esquelético e na região visceral (4,5).

De acordo com os estudos epidemiológicos mais recentes, a prevalência de obesidade aumentou em praticamente todos os países do mundo nos últimos 40 anos (6). Em números, estes estudos identificaram mais de 600 milhões de indivíduos adultos obesos e mais de 107 milhões de crianças obesas (7). As tendências de aumento no índice de massa corporal (IMC) populacional foram particularmente acentuadas em alguns países do sul da Ásia, Caribe e da América Latina (6). No Brasil, de acordo com os dados da Pesquisa Nacional em Saúde do IBGE em 2019, aproximadamente 22% dos homens e 30% das mulheres apresentam IMC acima de 30 kg/m² (8).

A considerável variação do peso corporal entre indivíduos de uma mesma população e a alta heritabilidade do IMC sugerem que fatores genéticos influenciam significativamente o desenvolvimento da obesidade. De fato, *Genome-wide association studies* (GWAS) já identificaram mais de 200 *loci* relacionados com níveis elevados de IMC (9,10). Alguns autores também argumentam que o genoma do homem contemporâneo herdou de nossos ancestrais alelos “econômicos”, ou seja, genes associados à maior capacidade de preservação de energia (11). Ainda que muitas variantes genéticas que predispõem o desenvolvimento da obesidade tenham sido identificadas nos últimos anos, a alta prevalência desta doença ao redor do mundo está majoritariamente associada com o ambiente obesogênico que surgiu a partir da década de 1970.

A motorização e redução da atividade física aliadas ao consumo de alimentos altamente palatáveis, ricos em calorias e pobres em nutrientes, constituem os

principais fatores ambientais associados ao balanço energético positivo e, em última instância, à obesidade. Debate-se há décadas quais macronutrientes, quando consumidos em excesso, tem maior influência no ganho de peso. O popular “*carbohydrate-insulin model of obesity*”, por exemplo, postula que o alto consumo de carboidratos eleva a secreção de insulina e direciona os ácidos graxos para lipogênese no tecido adiposo branco (TAB), enquanto outros tecidos metabolicamente ativos (músculo esquelético e cérebro, por exemplo) são privados da oxidação lipídica, desencadeando redução da taxa metabólica e favorecendo o ganho de peso (12,13). Por outro lado, dietas contendo menos carboidratos e mais gordura parecem não estar associadas com maior secreção de insulina, permitindo a distribuição e a metabolização de ácidos graxos em todos os tecidos, porém sua maior densidade energética estaria associada com menor saciedade e consumo inconsciente e excessivo de calorias (14).

Enquanto se debate a influência dos macronutrientes no balanço energético objetivando o desenho das melhores estratégias dietéticas para redução do peso corporal em obesos, o papel destes como moléculas de sinalização celular tem sido bastante investigados nos últimos anos (15,16). Inúmeros estudos experimentais e clínicos têm demonstrado consistentemente o papel que os lipídeos desempenham no desenvolvimento da obesidade e da resistência à insulina, não apenas pelo sua alta densidade calórica, mas também como efetores da ativação de vias inflamatórias (17–19). O receptor de reconhecimento padrão do sistema imunológico inato *Toll-like receptor 4* (TLR4), por exemplo, pode reconhecer e ser ativado por ácidos graxos saturados (20,21). Mediante tal ativação, o TLR4 estimula a transcrição gênica de diversas citocinas pró-inflamatórias, cuja produção crônica é um marco no caráter inflamatório da obesidade.

A natureza da inflamação associada à obesidade

A identificação de níveis elevados de *Tumor necrosis factor alpha* (TNF- α) no tecido adiposo branco de camundongos obesos deu início à uma nova era no estudo da obesidade (22). A natureza estéril da inflamação crônica e sub-clínica da obesidade é resultado da ativação de diversos componentes do sistema imunológico e, em particular, da ativação do TLR4 por ácidos graxos saturados provenientes da dieta e da liberação endógena pelo TAB.

O TLR4 utiliza a via do fator de diferenciação mielóide 88 (MyD88) para recrutar e ativar proteínas citoplasmáticas envolvidas na ativação da cinase β do inibidor do fator de transcrição NF- κ B (I κ B) que, por sua vez, fosforila e inibe o I κ B. Quando fosforilado, o I κ B permite a liberação no citoplasma das porções catalíticas p50 e p65 do fator nuclear *kappa* B (NF- κ B), um dos principais fatores de transcrição envolvidos na regulação de genes inflamatórios, como o *TNF α* , *IL6* e *IL1 β* (23,24). A ativação de vias alternativas do TLR4 também favorece a ativação das proteínas quinases ativadas por mitógenos (MAPKs), incluindo a cinase c-jun N-terminal kinase (JNK) (25).

O aumento da produção de citocinas pró-inflamatórias decorrente da ativação da via de sinalização do TLR4 amplifica os níveis intracelulares da *Supressor of cytokine signaling-3* (SOCS3) e da *Protein-tyrosine phosphatase 1B* (PTB1B), ambas supressoras da sinalização da leptina e da insulina no hipotálamo (26). Além disso, a ativação da proteína serina quinase I κ K e a ativação de JNK também se associa com o estado de resistência à insulina e leptina hipotalâmica por alterarem o padrão fisiológico de fosforilação das proteínas pertencentes às cascatas sinalizadoras destes hormônios. É importante notar que vias metabólicas e inflamatórias convergem em muitos pontos, e que sinais inflamatórios são antagonistas e dominantes sobre as variáveis fisiológicas coordenadas, dentre outros, pela insulina e pela leptina, incluindo a manutenção do peso, do gasto energético e do apetite.

O sistema de homeostase energética no controle do apetite

O apetite é regulado por um complexo circuito neural que, coletivamente, integra diversas variáveis fisiológicas representadas por nutrientes circulantes, hormônios e informações ascendentes do nervo vago. Os ramos do nervo vago e suas terminações sensoriais no trato gastrointestinal (TGI) detectam hormônios secretados pelas células enteroendócrinas do intestino envolvidos na saciedade do apetite, como a colecistocinina (CCK), peptídeo YY (PYY) e o *glucagon-like peptide 1* (GLP-1) e também pela detecção sensorial da distensão mecânica do TGI, o que ocorre após o consumo alimentar (27). Estes sinais são transmitidos ao tronco encefálico através de fibras aferentes do nervo vago, que por sua vez realizam conexões glutamatérgicas com neurônios localizados no núcleo do trato solitário (NTS) (27,28). Uma vez ativados, os neurônios do NTS modulam, por meio de projeções, a atividade de neurônios no

núcleo parabraquial (PBN), núcleo dorsal motor do vago (DMV), hipotálamo, entre outros (28) (Figura 1).

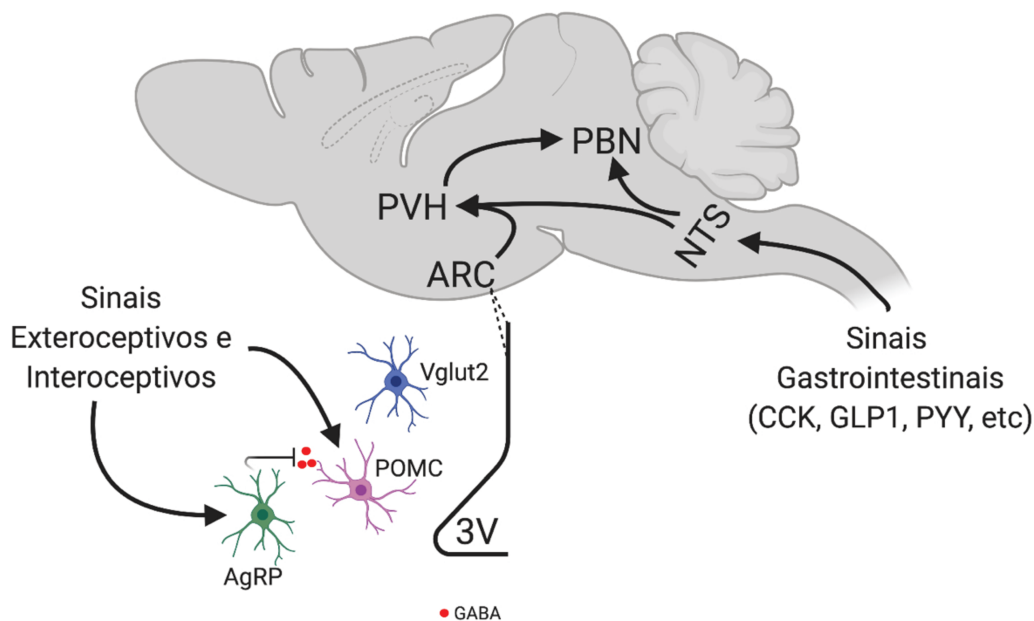


Figura 1. Neurônios do núcleo arqueado do hipotálamo e outros núcleos envolvidos no controle do apetite. Neurônios do NTS recebem sinais ascendentes provenientes dos hormônios produzidos e secretados pelo TGI e controlam a saciedade através de projeções eferentes nos neurônios do PVH e PBN. A atividade dos neurônios do ARC pode ser modulada por sinais exteroceptivos (visão e odor) e interoceptivos. Neurônios AgRP estimulam o apetite, em parte, via inibição GABAérgica de neurônios POMC e estes estimulam a saciedade com menor latência em relação aos neurônios Vglut2. PVH, *paraventricular hypothalamus*; PBN, *parabrachial nucleus*; AgRP, *agouti-related peptide*; POMC, *proopiomelanocortin*; Vglut2, *vesicular glutamate transporter 2*; CCK; *colecistokinin*; GLP1, *glucagon-like peptide 1*; PYY, *peptide YY*; 3V; *3rd ventricle*, GABA, *gamma-Aminobutyric acid*.

Nos últimos cinco anos, houve grande avanço na caracterização anatômica, genética e neuroquímica dos neurônios do NTS e do nervo vago. Neurônios do nervo vago com terminações sensoriais na mucosa do TGI são especializados na detecção química de hormônios secretados pelas células enteroendócrinas e expressam *Vip* e *Gpr65*, ao passo que aqueles cujas terminações sensoriais estão localizadas na camada muscular e nas terminações laminares intraganglionares são especializados na detecção de estímulos mecânicos, como na distensão do TGI, e expressam *Oxtr* e *Glp1r* (29). No NTS, neurônios que expressam CCK são rapidamente ativados após o consumo alimentar e suprimem o apetite através da ativação de neurônios que expressam *calcitonin gene-related peptide* (CGRP) no PBN e neurônios que expressam *melanocortin-4 receptor* (MC4R) no núcleo paraventricular do hipotálamo (PVH) (30–

32). Neurônios do NTS também secretam neuromoduladores como o GLP-1, que por sua vez promove saciedade através da ativação de neurônios no PVH (33).

Além dos sinais gastrointestinais, o sistema de homeostase energética também compreende sinais relativos ao estoque energético provenientes do TAB. Como tecido endócrino, o TAB produz e secreta diversas adipocinas com múltiplas funções e a leptina é o mediador humoral mais estudado e talvez o mais importante na regulação do apetite. A leptina é produzida e secretada pelos adipócitos e funciona como um eficiente sinal aferente de *feedback* negativo na manutenção da massa de TAB, isto é, reduz o apetite quando há aumento na massa de TAB e vice-versa (34). A sinalização da leptina é mediada pelo seu receptor (LepRb), pertencente à classe I dos receptores de citocinas, e sinaliza via JAK2-Stat3 (34). Embora não exclusivamente, a leptina inibe o apetite e aumenta o gasto energético através da modulação da atividade de neurônios hipotalâmicos presentes no ARC (35,36).

O hipotálamo como centralizador de sinais interoceptivos e exteroceptivos

Ao hipotálamo são atribuídas muitas funções neuroendócrinas envolvidas no controle do metabolismo, da reprodução, do crescimento, entre outros. Diversas populações neuronais que residem nos vários núcleos do hipotálamo apresentam conectividade entre si e com outras regiões do cérebro contribuindo para o fino controle de suas funções. O desenvolvimento e a aplicação de técnicas de sequenciamento de RNA *single-cell* e a manipulação genética neurônio-específica tem contribuído para avanços na caracterização fenotípica e funcional dos neurônios do hipotálamo, permitindo que se defina com precisão como o hipotálamo participa da regulação homeostática do organismo.

O sistema melanocortina, compreendido pelos neurônios que co-expressam *agouti-related peptide* (AgRP)/*neuropeptide Y* (NPY)/GABA - aqui referidos apenas como AgRP- e neurônios que expressam Proopiomelanocortina (POMC), integra hormônios periféricos e nutrientes para orquestrar a ingestão alimentar e a homeostase energética. A sinalização anorexigênica dos neurônios POMC envolve a ativação do MC4R no PVH através do *α-melanocyte stimulating hormone* (α MSH), um peptídeo derivado de múltiplas clivagens proteolíticas de POMC (37). Por outro lado, neurônios AgRP estimulam o apetite através de sua função antagônica ao MC4R e da sinalização

inibitória via NPY e GABA em neurônios anorexigênicos que expressam MC4R no PVH e nos neurônios POMC (38).

A regulação hormonal dos neurônios POMC e AgRP depende do estado energético do organismo. Em jejum, a grelina ativa os neurônios AgRP através do seu receptor (GHSR) e induz hiperfagia fisiológica (39). No estado pós-prandial, a leptina inibe os neurônios AgRP e ativa os neurônios POMC. Nos últimos três anos, alguns estudos revisitaram a sinalização da leptina nestes neurônios e revelaram resultados controversos. Estudos iniciais com deleção pré-natal do *LepRb* em neurônios POMC demonstram que a sinalização da leptina nestes neurônios seria primordial para o controle da ingestão alimentar e massa corporal (40). No entanto, outro estudo revelou que a deleção pós-natal do *LepRb* em neurônios POMC não provoca alterações na ingestão alimentar e na massa corporal, e estaria associada apenas a um desbalanço na homeostase glicêmica (41). Mais recentemente, outro estudo demonstrou que a deleção do *LepRb* em neurônios AgRP provoca obesidade, hiperfagia e diabetes severa, sugerindo que a leptina suprime o apetite através dos neurônios AgRP e não dos neurônios POMC (42). Finalmente, um estudo demonstrou que os efeitos anorexigênicos da leptina são mediados por neurônios GABAérgicos do ARC e que camundongos *ob/ob*, que apresentam deficiência genética na produção de leptina, normalizaram a ingestão alimentar após o tratamento com leptina mesmo na ausência de neurônios AgRP, deletados geneticamente (43). Baseado nas atuais evidências, compreende-se que a sinalização da leptina em neurônios POMC está envolvida com o controle glicêmico periférico e também com a ativação do sistema simpático e aumento do gasto energético (36). Em relação aos neurônios-alvo para supressão do apetite mediado pela leptina, o debate continua em aberto.

O desenvolvimento de técnicas de ativação e inibição artificial de neurônios ofereceram uma prova de conceito e acrescentaram novas informações a respeito das características biofísicas e sinápticas dos neurônios do sistema melanocortina. A ativação optogenética dos neurônios AgRP demonstrou sua capacidade de estimular o apetite em um período extremamente curto de tempo, ao passo que o efeito na redução do apetite após a ativação optogenética de neurônios POMC foi consumado apenas após alguns minutos (44). O contraste nestes períodos de latência neuronal

revelou a existência de uma população glutamatérgica no ARC com função anorexigênica, que rapidamente inibe o apetite quando optogeneticamente estimulada (45). Em consonância com o α MSH, estes neurônios glutamatérgicos potencializam a ativação dos neurônios MC4R do PVH (45).

A neurociência foi revolucionada também com a utilização de indicadores de cálcio geneticamente codificados em neurônios de interesse. Desta forma, o potencial de ação e o *input* sináptico podem ser avaliados e até mensurados através do monitoramento das alterações de cálcio intracelular em neurônios específicos. A aplicação desta técnica para analisar a dinâmica de cálcio em neurônios POMC e AgRP revolucionou profundamente os conceitos de neurônios homeostáticos atribuídos a estes. Isto porque foi demonstrado que neurônios POMC e AgRP podem ser rapidamente modulados por fatores exteroceptivos, como cheiro e visualização de alimentos (46). Camundongos em jejum, por exemplo, apresentaram rápida redução na atividade de neurônios em AgRP após visualizar ração e, interessantemente, a redução na atividade destes neurônios foi ainda maior quando houve a apresentação de um alimento com maior densidade calórica (47–49). Esta e outras características observadas nestes estudos demonstram que estes neurônios do ARC podem sofrer regulação antecipatória, na qual se processa e calcula a necessidade, a densidade energética e a palatabilidade do alimento antes mesmo de ele ser consumido, com o objetivo de acoplar o consumo e a demanda energética da maneira mais eficiente possível.

Inflamação hipotalâmica e disfunção de neurônios POMC na obesidade

Em decorrência dos mecanismos evolutivos e de sobrevivência, nosso cérebro foi programado para a busca por alimentos com maior densidade energética. No entanto, a abundância na oferta e consumo de alimentos processados e ultra-processados no mundo moderno exacerbaram o problema da obesidade que, em parte, está atrelada à disfunção e ao dano estrutural de neurônios hipotalâmicos envolvidos no controle do apetite e do gasto energético.

Alguns trabalhos recentes têm demonstrado que o consumo de dietas hiperlipídicas (HFD) pode dessensibilizar neurônios controladores do apetite aos sinais

gerados por alimentos menos calóricos (50, 51). O que se observa nesses estudos é que animais inicialmente alimentados com HFD apresentam maior necessidade de consumo calórico proveniente da ração padrão para se aliviar a valência negativa associada à fome, isto é, a prévia exposição à HFD parece alterar o limiar de saciedade dos animais através de mecanismos homeostáticos e hedônicos. Análises longitudinais da atividade de neurônios AgRP evidenciaram também que o consumo de HFD atenua as respostas destes neurônios aos estímulos exteroceptivos (50), discutidos no tópico anterior, e até mesmo à infusão de nutrientes intragástricos (51). O prejuízo na detecção sensorial e interoceptiva dos alimentos pode, ainda, ser acentuado com os danos funcionais e pela resposta anômala de neurônios POMC após o consumo crônico de HFD.

Estudos prévios do nosso e de outros laboratórios identificaram maior suscetibilidade à apoptose em neurônios POMC em relação aos neurônios AgRP, o que repercute diretamente no prejuízo das sinalizações anorexigênicas (52–55). Alguns estudos indicam que o estresse mitocondrial em neurônios POMC pode estar associado com sua disfunção em camundongos obesos. Yi e colaboradores demonstraram que células da microglia ativadas no ARC em decorrência do consumo de HFD, produzem e secretam TNF- α , que por sua vez estimula a fusão e o estresse mitocondrial em neurônios POMC (56). Nesse contexto, o consumo de HFD também provoca a perda do contato entre mitocôndria e retículo endoplasmático via redução de mitofusina-2, tal alteração na comunicação entre as duas organelas reduz a capacidade destes neurônios em responder adequadamente às flutuações na disponibilidade de nutrientes (57). Além disto, a produção de α MSH após a maturação e o processamento do neuropeptídeo POMC depende da homeostase do retículo endoplasmático e distúrbios neste sistema podem desencadear hiperfagia e obesidade (58).

A sensibilidade à glicose em neurônios POMC é crucial para o correto funcionamento do sistema melanocortina. A despolarização destes neurônios mediada por glicose envolve a inibição de canais de potássio ATP-dependentes e a geração de espécies reativas de oxigênio (EROs) (59). Dados obtidos em camundongos obesos demonstraram que os mecanismos supracitados são afetados pelo aumento dos níveis

de UCP2 (60), que por sua vez promove o desacoplamento da cascata de fosforilação oxidativa e a redução de EROs (61,62). Tomadas em conjunto, estas alterações interferem na capacidade dos neurônios POMC responderem adequadamente à presença de glicose, o que ocorre, em última análise, em condições pós-prandiais.

A proteína TRIL e o receptor nuclear PPAR δ como potenciais alvos terapêuticos

A sinalização do receptor TLR4 no sistema nervoso central requer uma proteína acessória denominada *TLR4-interactor with Leucine-rich repeats* (TRIL). Esta proteína acessória apresenta um domínio rico em leucina, com 13 repetições; um domínio fibronectina e uma região transmembrana uni-passo. Sua função no cérebro ainda não foi completamente esclarecida, ao que parece atua como proteína de intersecção entre o LPS e o TLR4, semelhantemente ao CD14. No entanto, a proteína CD14 é altamente expressa em células da microglia, mas pouco expressa em astrócitos e neurônios. Interessantemente, existem variações nos padrões de expressão gênica de TRIL em subpopulações de neurônios, com alta prevalência em neurônios POMC e baixa em AARP.

O receptor nuclear *peroxisome proliferator-activated receptor β/δ* (PPAR δ) é a isoforma da família dos PPARs mais expressa no sistema nervoso central, particularmente no hipotálamo, e os efeitos da sua ativação neste tecido são completamente desconhecidos. Ácidos graxos saturados e insaturados são ligantes naturais do PPAR δ em tecidos metabolicamente ativos e sua ativação está relacionada com o aumento da expressão de genes envolvidos no metabolismo oxidativo, sobretudo, dos ácidos graxos. Interessantemente, camundongos *ob/ob*, cuja obesidade e hiperfagia severa estão atrelados à deficiência genética na produção de leptina, apresentam expressão de PPAR δ anormalmente elevada no hipotálamo. Além disso, os neurônios POMC destes animais são menos sensíveis à glicose e este fenômeno parece estar associado à UCP2, cujo controle transcricional ocorre, pelo menos em parte, pelo PPAR δ .

Ainda não existem evidências mecanísticas que expliquem a maior labilidade de neurônios POMC dentro do contexto da inflamação hipotalâmica induzida por HFD. Assim, nesta Tese, avaliamos inicialmente o envolvimento da proteína *TLR4-interactor with Leucine-rich repeats* (TRIL) na inflamação hipotalâmica induzida por dieta e na apoptose de neurônios POMC. Em seguida, investigamos o possível envolvimento do PPAR δ como mediador da dessensibilização de neurônios POMC à glicose e à leptina em modelo animal alimentado com HFD (Figura 2).

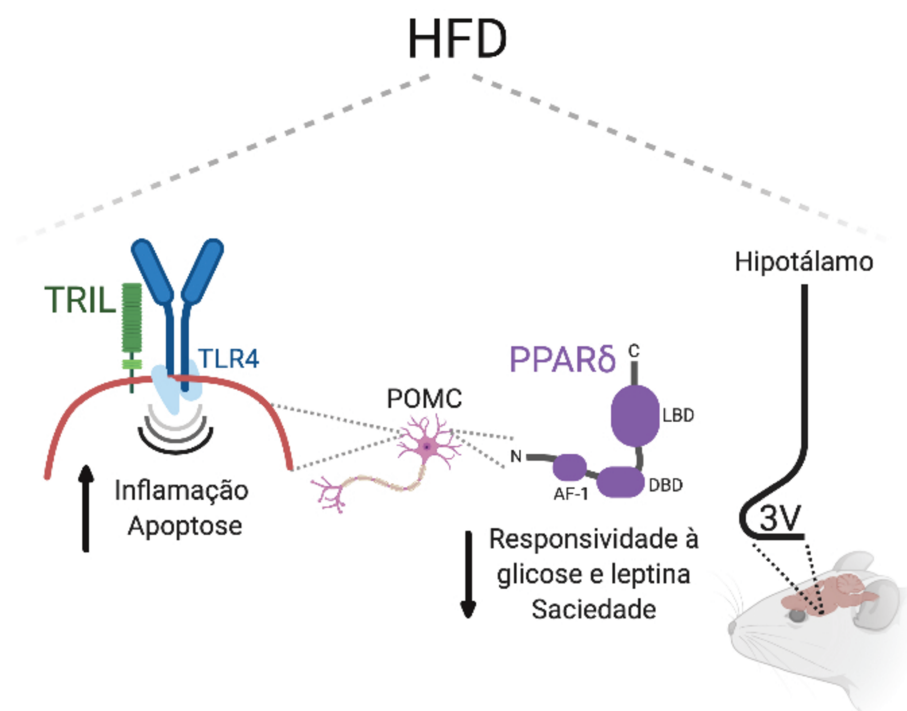


Figura 2. Hipótese dos mecanismos celulares envolvidos na disfunção dos neurônios POMC. Neurônios POMC do hipotálamo de camundongos com obesidade induzida por HFD apresentam resposta anômala aos sinais interoceptivos, tais alterações podem estar atreladas à inflamação induzida por HFD e por mecanismos de dessensibilização neuronal. AF-1, *activation function-1*; DBD, *DNA-binding domain*; LBD; *ligand-binding domain*.

CAPÍTULO 1: Artigo 1**TLR4-interactor with leucine-rich repeats (TRIL) is involved in diet-induced hypothalamic inflammation**

Alexandre Moura-Assis¹, Pedro A. Nogueira¹, Jose C. de-Lima-Junior¹, Fernando M. Simabuco², Joana M. Gaspar¹, Jose Donato Jr³, Licio A. Velloso^{1,4}

¹Laboratory of Cell Signalling-Obesity and Comorbidities Research Center, University of Campinas, Campinas, Brazil

²Multidisciplinary Laboratory of Food and Health (LABMAS), School of Applied Sciences (FCA), University of Campinas (UNICAMP), Limeira, São Paulo, Brazil.

³Department of Physiology and Biophysics, Institute of Biomedical Sciences, University of Sao Paulo, Sao Paulo, Brazil

⁴National Institute of Science and Technology on Neuroimmunomodulation

Corresponding Author:

Lício A. Velloso

Laboratory of Cell Signaling, Obesity and Comorbidities Research Center

University of Campinas, Campinas, SP, Brazil

Email: lavelloso@unicamp.br

Declaration of competing interest. The authors declare that they have no known competing financial interests or personal relationships that could have appeared to influence the works reported in this study.

ABSTRACT

Background/objectives: Obesity and high-fat diet (HFD) consumption result in hypothalamic inflammation and metabolic dysfunction. While the TLR4 activation by dietary fats partially mediates neuronal and glial inflammation, the role of its accessory proteins in the diet-induced hypothalamic inflammation remains unknown. Here, the TLR4-interactor with leucine-rich repeats (Tril) was explored as a potential candidate for mediating the harmful effects of HFD consumption in the hypothalamus and in proopiomelanocortin (Pomc) neurons.

Methods: The expression and modulation of Tril in the hypothalamus were characterized in HFD-fed mice. Metabolic phenotyping, leptin signaling and immunohistochemical analyses were performed on mice with shRNA-based knockdown of Tril in the arcuate nucleus (ARC) and in Pomc neurons.

Results: The knockdown of Tril in the ARC resulted in reduced hypothalamic inflammation, increased whole-body energy expenditure, increased systemic glucose tolerance and protection against diet-induced obesity. The Pomc-specific knockdown of Tril resulted in decreased body fat, decreased white adipose tissue inflammation and a trend toward increased leptin signaling in Pomc neurons.

Conclusion: Tril was identified as a new component of the complex mechanisms that promote hypothalamic dysfunction in experimental obesity and its inhibition in the hypothalamus may represent a novel target for obesity treatment.

Key words: Obesity, Hypothalamus, Inflammation, Metabolic Dysfunction.

ABBREVIATIONS:

AAV, adeno-associated virus

AgRP, agouti-related protein

ARC, arcuate nucleus

DIO, diet-induced obesity

HFD, high fat diet

iBAT, interscapular brown adipose tissue

ipGTT, intraperitoneal glucose tolerance test

ipITT, intraperitoneal insulin tolerance test

MSH, melanocyte-stimulating hormone

Myd88, myeloid differentiation primary response gene 88

POMC, proopiomelanocortin-expressing

TLR4, toll-like receptor 4

Tril, TLR4-interactor with leucine-rich repeats

UCP1, uncoupling protein 1

INTRODUCTION

The hypothalamus is a key brain region involved in the regulation of food intake and systemic homeostasis. In diet-induced obesity (DIO), a chronic and low-grade proinflammatory response in the arcuate nucleus (ARC) of the hypothalamus impairs the neuronal control of energy balance (1, 2). Thus, to understand how such inflammation develops in the hypothalamus is pivotal in determining obesity treatment.

Saturated fatty acids from hypercaloric diets can serve as ligands for the toll-like receptor-4 (TLR4) (3) and genetic mouse models lacking either TLR4 (4) or its downstream accessory protein myeloid differentiation primary response gene 88 (MyD88) (5) are protected from DIO and hypothalamic inflammation. Despite progress towards characterization of TLR4 signaling, the role of other critical components of TLR4 signaling in the hypothalamus remain poorly understood.

The TLR4-interactor with leucine-rich repeats (Tril) is a single transmembrane spanning 89 kDa protein that contains 13 leucine-rich repeats and is highly expressed in the brain (6). It plays an important role mediating TLR4 signal transduction, and whole-body Tril knockout results in defective inflammatory cytokine production in response to LPS and *E. coli*, particularly in the central nervous system (CNS) (7). A previous study has shown an enrichment of Tril in proopiomelanocortin-expressing (POMC) neurons (8), a leptin-responsive and appetite-suppressant group of hypothalamic neurons largely affected by obesity (9-12). Here, we hypothesized that Tril might be involved in diet-induced hypothalamic inflammation and in the regulation of POMC neurons. We show that knockdown of hypothalamic Tril protects mice from diet-induced body mass gain and systemic glucose intolerance.

MATERIAL AND METHODS

Animal models. Six-week old, male, Swiss and C57BL/6J mice were obtained from the University of Campinas experimental animal breeding facility. AgRP-IRES-Cre mice (#012899, *Agrptm1(cre)Lowl/J*, Jackson Laboratories) were crossed with the Cre-inducible tdTomato reporter mouse (#007909, B6;129S6-Gt(ROSA)26Sortm9(CAG-tdTomato)Hze/J, Jackson Laboratories), and POMC-Cre (#005965, Jackson

Laboratories) were used in Cre-dependent rAAV experiments or crossed with Cre-inducible GFP-reporter mice (#004178, The Jackson Laboratory) to determine the colocalization of Tril with fluorescently labeled AgRP and POMC neurons, respectively. Mice were housed individually at 22°C ($\pm 1^\circ\text{C}$) using a 12 h light/12 h dark cycle. All mice had ad libitum access to chow (3.7 kcal g⁻¹) or a HFD (60% kcal from fat, 5.1 kcal g⁻¹) and water (macronutrient composition of diets is presented in Supplementary Table 1). For refeeding experiments, mice were deprived of the respective diets for 12 hours during the dark cycle and thereafter the hypothalamus was harvested 1, 3, 6, 12 and 24h after refeeding; these experiments were performed after a five-day washout period to eliminate the novelty and the initial overfeeding associated with HFD introduction. All experiments were approved by the Ethics Committee at the University of Campinas (#4069-1 and #4985-1).

Respirometry. To determine O₂ consumption, CO₂ production and energy expenditure, mice were acclimatized for 48 h in an open circuit calorimeter system, the LE 405 Gas Analyzer (Panlab – Harvard Apparatus, Holliston, MA, USA). Thereafter, data were recorded for 24 h. Results are presented as the average of light and dark cycles. Analysis of covariance (ANCOVA) was used for the comparison of energy expenditure and body mass in mice.

Glucose and insulin tolerance tests. Following 6 h of fasting, mice received intraperitoneal (ip) injections with solutions containing glucose (2.0 g/kg body weight) or insulin (1.5 IU/kg body weight) and then blood samples were collected for ip-glucose tolerance test (ipGTT) or ip-insulin tolerance test (ipITT), respectively. Glucose concentrations were measured in tail blood using a portable glucose meter (Optium Xceed, Abbott) at 0, 15, 30, 60 and 120 minutes after glucose administration or 0, 5, 10, 15, 20, 25 and 30 minutes after insulin administration.

Assessment of body composition. To determine total body fat and lean mass, time-domain nuclear magnetic resonance (TD-NMR) was applied using the LF50 body composition mice analyzer (Bruker, Germany). Measurements were performed on the last day of the experiment.

Thermal images. The estimated iBAT temperatures were determined using an infrared (IR) camera (FLIR T450sc, FLIR systems, Inc. Wilsonville, USA) and analyzed with FLIR-Tools software.

Tissue collection and histology. C57BL/6J, AgRP tdTomato and POMC-GFP mice were deeply anesthetized with ketamine (100 mg/kg) and xylazine (10 mg/kg) and submitted to transcardiac perfusion with 0.9% saline followed by 4% paraformaldehyde (PFA). Brains were removed, postfixed 24 h in 4% PFA solution and then transferred to a solution containing 20% sucrose in 0.1 M PBS (pH 7.4) for 12 h. Perfused brains were frozen at -30°C and sectioned on a cryostat at a thickness of 30 µm. For immunohistochemistry, free-floating sections were washed three times for 10 minutes with 0.1 M PBS. Next, sections were blocked in 5% donkey serum and 0.2% Triton X-100 in 0.1 M PBS for 1 h at room temperature, followed by incubation in goat anti-TRIL primary antibody (sc-24489, Santa Cruz Biotechnology, Santa Cruz, CA, USA), rabbit anti-IBA1 (Wako Chemicals, #019-19741), rabbit anti-cleaved caspase-3 (Cell Signaling, #9661S), rabbit anti-POMC (Phoenix Pharmaceuticals, #H-029-30), sheep anti-αMSH (Chemicon, #AB5087) and rabbit anti-AgRP (Phoenix Pharmaceuticals, #H-003-53) for 24 h. The sections were then washed three times in 0.1 M PBS and incubated for 2 h at room temperature in donkey anti-goat AlexaFluor⁵⁴⁶ (1:500, Invitrogen, #A-11056), donkey anti-goat FITC (1:500, Santa Cruz, sc-2025), donkey anti-rabbit FITC (1:500, Abcam, ab6798), donkey anti-rabbit IgG AlexaFluor⁵⁹⁴ (1:500, Jackson Immuno Research, #711-585-152) and donkey anti-sheep AlexaFluor⁴⁸⁸ (1:500, Jackson Immuno Research, #713-545-003) conjugated secondary antibodies. Thereafter, the sections were mounted onto slides, and the nuclei were labeled with TOPRO (Life Technologies, T3605). The sections were analyzed with a LEICA TCS SP5 II confocal laser-scanning microscope (Leica Microsystems, Wetzlar, Germany).

Multiplex fluorescent in situ hybridization (FISH). Brains from C57BL/6J mice were quickly harvested and frozen in OCT at -20°C and stored at -80°C. The slides containing a 15-µm-thick brain sections were processed for multiplex FISH using the RNAscope system (ACDBio) and probes for the following mRNA: Tril (C-1), Pomc (C-2) and AgRP (C-3). The pretreatment was performed by sequential incubations of slides in 4% PFA, 50% EtOH, 70% EtOH and 100% EtOH at room temperature. Probe hybridization was

achieved by incubation of 30 μ l mRNA target probes for 2h at 40°C using a HyBez oven. The signal was then amplified by subsequent incubation of Amp-1, Amp-2 and Amp-3 for 30, 30 and 15 minutes, respectively, at 40°C using a HyBez oven. Each incubation step was followed by RNAscope washing buffer washes. The slides were coverslipped and mounted using DAPI Fluoromount-G (SouthernBiotech). Slides were visualized with an inverted Zeiss LSM 780 laser scanning confocal microscope using a x20 lens.

pSTAT3 staining. Mice were submitted to 12 h of fasting and then received ip injections with mouse leptin (5 mg/kg body weight, Calbiochem, Billerica, MA, USA). After 1 h, mice were submitted to transcardiac perfusion with 0.9% saline followed by 4% PFA. After sectioning on a microtome, the brain sections were rinsed in 0.02 M KPBS (pH 7.4), followed by pretreatment in a water solution containing 1% hydrogen peroxide and 1% sodium hydroxide for 20 minutes. After extensive washings in 0.02 M KPBS, the sections were incubated in 0.3% glycine for 10 minutes and then 0.03% lauryl sulfate for 10 minutes. Thereafter, the sections were blocked in 3% normal donkey serum for 1 h, followed by incubation in rabbit anti-pSTAT3^{Tyr705} (1:1000, Cell Signaling, #91315) for 48 h. For the immunofluorescence reactions, sections were rinsed in KPBS and incubated for 120 minutes in Fab fragment donkey anti-rabbit AlexaFluor⁴⁸⁸ (1:500, Jackson Immuno Research, #711-547-003). Thereafter, sections were washed three times in 5% formalin for 10 minutes and then washed three times in 0.02 M KPBS for 5 minutes. Sections were then incubated with POMC antibody (1:1000, Phoenix Pharmaceuticals, #H-029-30) overnight at room temperature. After washing in 0.1 M PBS, the sections were incubated for 30 minutes with the secondary antibody AlexaFluor⁵⁹⁴ (1:500, Jackson Immuno Research, #711-585-152) diluted in 0.02 M KPBS. After three washes in 0.02 M KPBS for 10 minutes, the sections were mounted onto gelatin-coated slides and coverslipped with Fluoromount G (Electron Microscopic Sciences, Hatfield, PA, USA). The percentage of pSTAT3-positive POMC neurons was determined in blind counting by three distinct researchers using hemisections of the middle ARC from four animals for statistical comparison. The sections were processed simultaneously under identical conditions and analyzed with the same microscope set-up.

Liver histological analysis. Fragments of left lobe were collected and fixed in 10% buffered formalin, embedded in paraffin and stained with hematoxylin and eosin (H&E, Merck, USA), and analyzed and photographed using a light microscope (Axio Observer D1, Zeiss, USA).

Lentiviral clones. Three different shRNA clones targeting Tril (Sigma-Aldrich, St Louis, MO, USA) and scramble lentiviral particles were used for the overall knockdown experiments (13). For arcuate nucleus (Arc) bilateral lentiviral delivery, 8–12 week old male C57BL/6J mice were anesthetized with ketamine (100 mg/kg body weight) and xylazine (10 mg/kg body weight) intraperitoneally, and the stereotaxic surgery was carried out using a stereotaxic frame (Stoelting Apparatus, Wood Dale, IL, USA) set at AP -1.7 mm, ML \pm 0.3 mm and DV -5.6 mm coordinates from Bregma.

Cre-dependent recombinant adeno-associated viral (rAAV) vectors. With regard to the POMC-specific knockdown of Tril, referred to here as POMC rAAV^{miTRIL}, a TRIL-based miRNA construct was constructed by modifying the Cre-dependent AAV-FLEX-EGFP-mir30 (Scn9a) (Addgene plasmid # 79672) (14, 15). Briefly, the plasmid was modified by replacing the self-complementary sequences of Tril shRNA, using EcoRI and XhoI. All miR sequences were preserved. The sequence used was the following, where complementary sequences are underlined:

5'CGAGGCAGTAGGCACCCAGTATCTTACTGTGTTATTTACA
TCTGTGGCTTCACTAAAATAACACAGTAAGATACTGGCGCTCACTGTCAACAGCAATATACCTT-
3'. The rAAV particles were produced in the LNBio (Brazilian Biosciences National Laboratory) facility and titrated using an Addgene protocol by qPCR (16). Briefly, purified AAV particles were treated with DNase by incubation for 30 min at 37°C. A standard curve was generated using the AAV-FLEX-EGFP-mir30 (TRIL) plasmid serial diluted. SYBR Green quantitative PCR (qPCR) was performed using the primers: fwd ITR primer 5'-GGAACCCCTAGTGATGGAGTT-3' and rev ITR primer 5'-CGGCCTCAGTGAGCGA-3'. The Cre-dependent bilateral injections of the rAAV vectors in the Arc were performed in POMC-Cre mice at the following stereotaxic coordinates: AP -1.7 mm, ML \pm 0.3 mm and DV -5.6 mm from Bregma. All AAVs were allowed 2 weeks for expression before experiments were initiated.

Gene expression analysis. Total RNA was extracted from the hypothalamus, inguinal and epididymal white adipose tissue, brown adipose tissue and liver using TRIzol reagent (Invitrogen). cDNA synthesis was performed using 2 µg of total RNA. The PCR containing 25 ng of reverse-transcribed RNA was performed using the ABI Prism 7500 sequence detection system (Applied Biosystems). For RT-PCR calculation, the delta CT was used, and the relative gene expression was normalized to that of GAPDH in all samples. In the figures 1E, 1F and 1G the mRNA expression of *Tril* in mice fed on HFD was also normalized for the respective control group of mice fed on chow. The primers used were *Tril* (Mm01330899_s1), *Ucp1* (Mm01244861_m1), *PGC1α* (Mm01188700_m1), *Zic1* (Mm00656094_m1), *LHX8* (Mm00802919_m1), *Tfam* (Mm00447485_m1), *PPARγ* (Mm01184322_m1), *Scd1* (Mm00772290_m1), *Srebf1* (Mm01138344_m1), *Cd36* (Mm01135198_m1), *Tnfa* (Mm00443258_m1), *F4/80* (Mm00802529_m1), *Il1-β* (Mm00434228_m1), *Nlrp3* (Mm00840904_m1), *Hsp90* (Mm00441926_m1), *Hspa5* (Mm00517691_m1), *Caspase-3* (Mm01195085_m1), *Pomc* (Mm00435874_m1), *AgRP* (Mm00475829_g1), *Mch* (Mm01242886_g1), *Tmem26* (Mm01173641_m1), *Th* (Mm00447557_m1), *Ccl2* (Mm99999056_m1) and *Tbx1* (Mm00448949_m1).

Western blotting. Hypothalamic specimens were homogenized in solubilization buffer (1% Triton X-100, 100 mM Tris (pH 7.4), 100 mM sodium 22 pyrophosphate, 100 mM 4 sodium fluoride, 10 mM EDTA, 10 mM sodium vanadate, 2 mM 23 PMSF and 0.1 mg/mL 5 aprotinin). A total of 100 µg of protein per sample were separated by sodium dodecyl sulfate-polyacrylamide gel electrophoresis (SDS-PAGE), transferred to nitrocellulose membranes and blocked in 3% BSA solution in TBST for 2 h. After a washing step, the membranes were blotted with goat-anti TRIL antibody (sc-24489, Santa Cruz Biotechnology, Santa Cruz, CA, USA), and α-tubulin (Sigma-Aldrich, T5168) was used as loading control. Specific bands were labeled by chemiluminescence and were quantified by optical densitometry after exposure to Image Quant LAS4000 (GE Healthcare, Life Sciences).

Statistical analysis. Results are presented as mean ± standard error of the mean (SEM). Statistical comparisons between different times of refeeding and controls were performed using analysis of variance (ANOVA), followed by Tukey's post hoc test.

Student's t tests were applied for comparisons between scramble and KD^{TRIL} in experiments with lentiviral clones or POMC Cre^{miNonTarget} and POMC Cre^{miTRIL} in experiments with Cre-dependent rAAV.

RESULTS

Hypothalamic Tril expression is increased in diet-induced obesity. *Tril* mRNA expression was detected in 44% of POMC neurons and only 25% of AgRP neurons (Fig. 1A); the major *Tril* overlap with POMC neurons was further confirmed in hypothalamic slices from POMC-GFP mice (Suppl. Fig. 1A) in comparison with AgRP-tdTomato mice (Suppl. Fig. 1B). *Tril* was also detected in some Iba1-expressing cells (Suppl. Fig. 1C). In outbred obesity-prone Swiss mice (Fig. 1C), the hypothalamic (Fig. 1D) but not hippocampal (Fig. 1E) expression of *Tril* underwent increase one and two weeks after the introduction of a HFD. This was accompanied, in the first week, by the increased expression of hypothalamic *Tlr4* (Fig. 1F). In isogenic C57BL/6J mice, the hypothalamic expression of *Tril* was increased after refeeding in mice fed a HFD (Fig. 1G) but not in mice fed a standard chow (Fig. 1H).

Inhibition of hypothalamic Tril protects from diet-induced obesity. Three distinct lentiviral clones containing a shRNA to knockdown *Tril* were tested in the ARC and a scramble was used as a negative, non-silencing control (Fig. 2A, 2B and Suppl. Fig. 2); the lentivirus clone #3 (sequence depicted in Fig. 2A and *Tril* protein inhibition in Figure 2B;) generated a significant *Tril* knockdown. The protocol (using lentivirus #3) was designed to evaluate whether the knockdown of hypothalamic *Tril* could prevent the effect of a HFD on metabolic parameters, since the introduction of a HFD occurred after the injection of the lentivirus particles (Fig. 2C). The inhibition of hypothalamic *Tril* resulted in the reduction of transcript expression of hypothalamic *Il1 β* , *Nlrp3* and *Hspa5* (Fig. 2D); no changes were detected in baseline expression of transcripts encoding for *Pomc*, *Agrp* and *Mch* (Fig. 2E). The inhibition of hypothalamic *Tril* resulted in reduced body mass gain (Fig. 2F) and no change in caloric intake (Fig. 2G and 2H); in addition, inhibition of hypothalamic *Tril* resulted in reduced absolute (Fig. 2I) and relative (Fig. 2J) epididymal white adipose tissue mass.

Inhibition of hypothalamic Tril improves systemic glucose tolerance. In mice under hypothalamic inhibition of *Tril* and fed a HFD (as depicted in the experimental protocol

in Fig. 2C), there was a trend in the increase in whole body energy expenditure (Fig. 3A–3C). This was accompanied by reduced absolute (Fig. 3D) and relative (Fig. 3E) mass of the interscapular brown adipose tissue (iBAT) but no changes in the temperature (Fig. 3F–3H) of iBAT and expression of iBAT transcripts encoding proteins involved in thermogenesis (Fig. 3I). Moreover, the inhibition of hypothalamic *Tril* improved systemic glucose tolerance (Fig. 3J and 3K), promoted a trend to increase systemic insulin sensitivity (Fig. 3L) and reduced liver steatosis (Fig. 3M), which was accompanied by reduced hepatic expression of transcripts encoding for *Scd1* and *CD36* (Fig. 3N).

POMC-specific knockdown of Tril reduces body adiposity and increases hypothalamic responsiveness to leptin. A Cre-dependent AAV was designed to selectively knockdown *Tril* in POMC neurons of the ARC (Fig. 4A and 4B). Since the introduction of a HFD occurred after the injection of rAAV, this protocol was designed to evaluate whether the knockdown of *Tril* in POMC neurons could prevent the effect of a HFD on metabolic parameters (Fig. 4C). This approach resulted in a trend to overcome HFD-induced body mass gain (Fig. 4D and 4E) and a significant reduction of fat (Fig. 4F) but not lean mass (Fig. 4G). In addition, there were trends to reduce absolute (Fig. 4H) and relative (Fig. 4I) epididymal fat mass and significant reductions of epididymal adipose tissue expression of the inflammatory transcripts *Il1b* and *Tnf α* (Fig. 4J). The knockdown of *Tril* in POMC neurons resulted in a trend to reduce cumulative food intake throughout the experimental period (Fig. 5A) and a significant reduction of food intake acutely after a period of prolonged fasting (Fig. 5B). This was accompanied by increased leptin-induced activation of STAT3 in POMC neurons (Fig. 5C and 5E) but not in the retrochiasmatic hypothalamus (Fig. 5D). Inhibiting *Tril* in POMC neurons promoted no modification in the density of α -MSH (Fig. 5F, upper panels and Fig. 5G) and AgRP (Fig. 5F, lower panels and Fig. 5H) projections to the paraventricular hypothalamus.

POMC-specific knockdown of Tril increases the thermogenic gene expression in brown adipose tissue. No changes in whole body energy expenditure were observed after POMC-specific knockdown of *Tril* either in mice fed a chow (Fig. 6A–6C) or in mice fed a HFD (Fig. 6D–6F). There was a trend to reduce absolute brown adipose tissue (Fig.

6G) but not relative mass (Fig. 6H). Brown adipose tissue temperature was not modified (Fig. 6I–6J), but the expression of the thermogenic genes *Lhx8* and *Zic1* were increased in mice under the inhibition of Tril in POMC neurons (Fig. 6L). In addition, the inhibition of Tril in POMC neurons led to lower fasting blood glucose (Fig. 6M) but no change in whole body glucose tolerance (Fig. 6N).

Inhibition of Tril in POMC neurons cannot revert the diet-induced obesity phenotype but increases the expression of thermogenic genes in brown adipose tissue. In all preceding experiments, the inhibition of Tril either in the ARC or specifically in POMC neurons occurred two weeks before the introduction of a HFD; thus, the approaches aimed at preventing the harmful effects of the diet. In order to test the hypothesis that inhibition of Tril in POMC neurons could revert the metabolically adverse effects of long-term consumption of a HFD, mice were fed a HFD for 14 weeks and then injected with rAAV shTril. After 2 weeks of recovery, mice were maintained for another 8 weeks on the HFD and metabolic parameters were evaluated (Suppl. Fig. 3A). As depicted in Suppl. Fig. 3B and 3C, the inhibition of Tril in POMC neurons could neither revert obesity nor change caloric intake in this group of mice. In addition, there were no changes in epididymal fat mass (Suppl. Fig. 3D and 3E), brown adipose tissue mass (Suppl. Fig. 3F and 3G) and brown adipose tissue temperature (Suppl. Fig. 3H–3J). Nevertheless, in mice submitted to the inhibition of Tril in POMC neurons, there was a trend to increase brown adipose tissue expression of *Ucp1* and a significant increase in the expression of *Tmem26* (Suppl. Fig. 3K).

Inhibition of Tril in POMC neurons of obese mice did not change the number of POMC neurons in the arcuate nucleus. In experimental obesity, there is increased apoptosis of neurons in the ARC, and this predominantly affects the number of POMC neurons (9, 17, 18). In obese mice submitted to the protocol of inhibition of Tril in POMC neurons (Fig. 7A), there were neither changes in the number of POMC neurons (Fig. 8A and 8B) nor in the cellular expression of cleaved caspase-3 (Fig. 8C and 8D).

DISCUSSION

The stability of body mass depends on the functional and structural fitness of ARC neurons, as demonstrated by a number of different experimental approaches (19-22). Many advancements have been made towards the molecular programs involved in the obesity-associated hypothalamic inflammation and how the neuronal control of energy balance is affected during the course of HFD feeding (3, 18, 23, 24).

In DIO, POMC neurons are affected at the functional and structural levels by distinct but integrated mechanisms (2, 3, 5, 18, 25-27). The core mechanism behind DIO-associated POMC abnormalities is inflammation (28-32), and its drivers include the activation of RNA stress granules (33, 34), endoplasmic reticulum stress (2, 3, 26), PKC θ (27) and TLR4 (3, 35). The long-term persistence of hypothalamic inflammation, as it occurs when mice are fed a HFD for longer than 8 weeks, leads to a progressive and potentially irreversible deterioration of the melanocortin system (9, 17, 30, 36-38). Interestingly, despite the fact that POMC and AgRP neurons share anatomical space, and thus, are potentially exposed to similar harmful factors, POMC undergoes more dramatic changes in response to DIO (9, 17, 18), raising the possibility that POMC-specific factors could be involved in this increased sensitivity to the diet.

Using a POMC-specific transcriptomics (8), we identified Tril, a TLR4-associated membrane protein previously shown to mediate the inflammatory response to LPS in the brain (6). Our analysis of *in situ* mRNA expression revealed that Tril is present in 44% of POMC-expressing neurons and 25% of AgRP-expressing neurons in the ARC. We also employed POMC and AgRP reporter mice to anatomically define the expression of Tril in the hypothalamus and confirmed that Tril is mostly expressed in POMC neurons (8). In addition, as it could be expected for a TLR4-associated protein, Tril was detected in microglia (39). It has been recently shown that dietary excess facilitates the infiltration of bone-marrow-derived myeloid cells into the ARC and the activation of resident microglia, leading to an inflammatory responsiveness and neuronal and metabolic dysfunction (40, 41). Using two distinct mouse strains, we showed that hypothalamic Tril is regulated by the consumption of a HFD, as other inflammatory proteins involved in the development of hypothalamic abnormalities in DIO (2, 3, 18, 40, 42).

In order to explore the potential involvement of hypothalamic Tril in the development of HFD-associated obese and metabolic phenotypes, we used two distinct approaches. First, we employed a lentivirus encoding a shRNA to selectively knockdown Tril in a non-cell-specific fashion in the arcuate nucleus (13). Second, we employed Cre-dependent adeno-associated viral vector to specifically inhibit Tril in POMC-expressing neurons (43). When either inhibition was performed in mice fed chow, there were virtually no changes in the phenotype. Conversely, when either inhibition was performed in mice fed a HFD, there were considerable beneficial changes in the obese and metabolic phenotypes. The different outcomes obtained in mice fed the distinct diets support the potential involvement of Tril in the diet-induced inflammatory response.

The action of Tril is similar to CD14 (serving as an accessory molecule that facilitates the binding of LPS to TLR4), mediating at least part of the inflammatory response triggered in this context (7). Studies have previously shown that Tril is expressed in glial cells (6, 7). However, as first shown by Henry and coworkers using RNA sequencing of hypothalamic neurons (8) and now, confirmed in this study, Tril is also expressed in POMC neurons. One important aspect of TLR4-associated protein expression in the hypothalamus is that, whether CD14 is expressed in glial cells, it is not expressed in POMC neurons (44); thus, in this particular cell population, Tril may be essential for the activation of TLR4.

The arcuate nucleus non-restricted and POMC-restricted Tril inhibitions generated similar but not completely overlapping phenotypes. Identity was found for reduction of body adiposity, increased whole body energy expenditure and reduction of BAT mass. In addition, there was a significant reduction of body mass gain in arcuate nucleus non-restricted Tril inhibition and trend for reduction in POMC-restricted Tril inhibition. As Tril is also expressed in glial cells (6, 7, 44), some of the effects obtained in the non-cell-specific inhibition might be related to the diet-induced activation of this protein in cells other than POMC cells. In other studies, inhibition of distinct components of the diet-induced responsive inflammatory machinery specifically in POMC neurons, such as Myd88, IKK/NFkB, HIF and TGF- β R (5, 33, 45, 46), resulted in beneficial changes in the metabolic phenotype placing POMC as a direct target for the

harmful effects of a HFD. Although recent data have shown that leptin signaling in POMC neurons is dispensable for body weight control, the deletion of leptin receptor (LepR) in POMC neurons leads to defective sympathetic innervation of adipose tissue and glucose homeostasis (47). Here, we showed that inhibition of Tril resulted in a trend to increase STAT3 phosphorylation, suggesting that preserved leptin signaling in POMC neurons could have a role in the improved fasting glucose and increased expression of thermogenic genes in iBAT of obese mice.

In the final part of the study, we asked if the POMC-specific inhibition of Tril was capable of reverting the effects of long-term DIO. For that, mice were fed a HFD for 14 weeks before the inhibition of Tril in POMC neurons—was undertaken. As previously shown, the metabolic outcomes of feeding mice a HFD for shorter than 8 weeks can be reverted by returning mice to chow; however, longer periods on a HFD lead to irreversible metabolic outcomes (38). In concert with human obesity, studies show that the longer patients remain obese, the more severe the clinical outcomes and the more resilient the obese phenotype is, irrespective of the therapeutic approach employed (48, 49). Here, the inhibition of Tril in POMC neurons in long-term obese mice resulted in no change in body mass, adiposity and food intake. There was only a trend to increase Ucp1 and a significant increase in Tmem26 in BAT, suggesting that, despite the lack of effect on the obese phenotype, the inhibition of Tril in long-term obese mice may retain its thermogenic-inducing effect (50). In addition, the inhibition of Tril in POMC neurons in long-term obese mice was sufficient neither to change the number of arcuate nucleus POMC neurons nor the expression of cleaved-caspase 3.

In conclusion, Tril is predominantly expressed in hypothalamic POMC neuron and emerges as a new component of the complex mechanisms that promote hypothalamic dysfunction in experimental obesity. Pharmacological approaches aimed at inhibiting Tril in the hypothalamus could provide advance in the treatment of obesity.

Relevant conflicts of interests:/financial disclosures

The authors declare that no conflicts of interests exist.

Funding agencies

LAV, São Paulo Research Foundation (FAPESP – 2013/07607-8). FMS, São Paulo Research Foundation (FAPESP – 2018/14818-9). JDJr, São Paulo Research Foundation (FAPESP – 2017/02983-2). Conselho Nacional de Desenvolvimento Científico e Tecnológico, INCT-Neuroimmunomodulation. Coordenadoria de Aperfeiçoamento de Pessoal de Nível Superior.

Author's contribution statement

AM-A and LAV conceptualized and designed the experiments; AM-A, performed the majority of the experiments; PAN, JCLJr and JMG contributed to mouse experiments and analytical methods; FMS designed, cloned and titrated the Cre-dependent rAAV; JDJr contributed to histological analyzes and provided POMC-GFP, AgRP tdTomato and POMC Cre mice; AM-A and LAV discussed and organized results; AM-A and LAV wrote the paper; LAV was also responsible for funding acquisition. All authors contributed to the editing and discussion of the manuscript.

Acknowledgment

Alexandre Moura-Assis received financial support from the São Paulo Research Foundation (FAPESP #2016/01245-5 and #2019/129690-2). Pedro A. Nogueira received financial support from Coordenadoria de Aperfeiçoamento de Pessoal de Nível Superior through the graduate Course in Cellular and Structural Biology, Insitute of Biology, University of Campinas. The authors thank Erika Roman, Joseane Morari, Marcio Cruz and Gerson Ferraz for laboratory management.

REFERENCES

1. Posey KA, Clegg DJ, Printz RL, Byun J, Morton GJ, Vivekanandan-Giri A, et al. Hypothalamic proinflammatory lipid accumulation, inflammation, and insulin resistance in rats fed a high-fat diet. *Am J Physiol Endocrinol Metab*. 2009;296(5):E1003-12.
2. Zhang X, Zhang G, Zhang H, Karin M, Bai H, Cai D. Hypothalamic IKKbeta/NF-kappaB and ER stress link overnutrition to energy imbalance and obesity. *Cell*. 2008;135(1):61-73.
3. Milanski M, Degasperi G, Coope A, Morari J, Denis R, Cintra DE, et al. Saturated fatty acids produce an inflammatory response predominantly through the activation of TLR4 signaling in hypothalamus: implications for the pathogenesis of obesity. *J Neurosci*. 2009;29(2):359-70.
4. Zhao Y, Li G, Li Y, Wang Y, Liu Z. Knockdown of Tlr4 in the Arcuate Nucleus Improves Obesity Related Metabolic Disorders. *Sci Rep*. 2017;7(1):7441.
5. Kleinridders A, Schenten D, Konner AC, Belgardt BF, Mauer J, Okamura T, et al. MyD88 signaling in the CNS is required for development of fatty acid-induced leptin resistance and diet-induced obesity. *Cell Metab*. 2009;10(4):249-59.
6. Carpenter S, Carlson T, Dellacasagrande J, Garcia A, Gibbons S, Hertzog P, et al. TRIL, a functional component of the TLR4 signaling complex, highly expressed in brain. *J Immunol*. 2009;183(6):3989-95.
7. Wochal P, Rathinam VA, Dunne A, Carlson T, Kuang W, Seidl KJ, et al. TRIL is involved in cytokine production in the brain following Escherichia coli infection. *J Immunol*. 2014;193(4):1911-9.
8. Henry FE, Sugino K, Tozer A, Branco T, Sternson SM. Cell type-specific transcriptomics of hypothalamic energy-sensing neuron responses to weight-loss. *Elife*. 2015;4.
9. Yi CX, Walter M, Gao Y, Pitra S, Legutko B, Kalin S, et al. TNFalpha drives mitochondrial stress in POMC neurons in obesity. *Nat Commun*. 2017;8:15143.

10. Kim GH, Shi G, Somlo DR, Haataja L, Song S, Long Q, et al. Hypothalamic ER-associated degradation regulates POMC maturation, feeding, and age-associated obesity. *J Clin Invest*. 2018;128(3):1125-40.
11. Williams KW, Liu T, Kong X, Fukuda M, Deng Y, Berglund ED, et al. Xbp1s in Pomc neurons connects ER stress with energy balance and glucose homeostasis. *Cell Metab*. 2014;20(3):471-82.
12. Souza GF, Solon C, Nascimento LF, De-Lima-Junior JC, Nogueira G, Moura R, et al. Defective regulation of POMC precedes hypothalamic inflammation in diet-induced obesity. *Sci Rep*. 2016;6:29290.
13. Kanungo J. Puromycin-resistant lentiviral control shRNA vector, pLKO.1 induces unexpected cellular differentiation of P19 embryonic stem cells. *Biochem Biophys Res Commun*. 2017;486(2):481-5.
14. Branco T, Tozer A, Magnus CJ, Sugino K, Tanaka S, Lee AK, et al. Near-Perfect Synaptic Integration by Nav1.7 in Hypothalamic Neurons Regulates Body Weight. *Cell*. 2016;165(7):1749-61.
15. Tavares MR, Lemes SF, Fante T, Saenz de Miera Patin C, Pavan ICB, Bezerra RMN, et al. Modulation of hypothalamic S6K1 and S6K2 alters feeding behavior and systemic glucose metabolism. *J Endocrinol*. 2019.
16. Aurnhammer C, Haase M, Muether N, Hausl M, Rauschhuber C, Huber I, et al. Universal real-time PCR for the detection and quantification of adeno-associated virus serotype 2-derived inverted terminal repeat sequences. *Hum Gene Ther Methods*. 2012;23(1):18-28.
17. Moraes JC, Coope A, Morari J, Cintra DE, Roman EA, Pauli JR, et al. High-fat diet induces apoptosis of hypothalamic neurons. *PLoS One*. 2009;4(4):e5045.
18. Thaler JP, Yi CX, Schur EA, Guyenet SJ, Hwang BH, Dietrich MO, et al. Obesity is associated with hypothalamic injury in rodents and humans. *J Clin Invest*. 2012;122(1):153-62.

19. Bumaschny VF, Yamashita M, Casas-Cordero R, Otero-Corchon V, de Souza FS, Rubinstein M, et al. Obesity-programmed mice are rescued by early genetic intervention. *J Clin Invest.* 2012;122(11):4203-12.
20. Lam DD, Attard CA, Mercer AJ, Myers MG, Jr., Rubinstein M, Low MJ. Conditional expression of *Pomc* in the *Lepr*-positive subpopulation of POMC neurons is sufficient for normal energy homeostasis and metabolism. *Endocrinology.* 2015;156(4):1292-302.
21. Chhabra KH, Adams JM, Jones GL, Yamashita M, Schlapschy M, Skerra A, et al. Reprogramming the body weight set point by a reciprocal interaction of hypothalamic leptin sensitivity and *Pomc* gene expression reverts extreme obesity. *Mol Metab.* 2016;5(10):869-81.
22. Balthasar N, Coppari R, McMinn J, Liu SM, Lee CE, Tang V, et al. Leptin receptor signaling in POMC neurons is required for normal body weight homeostasis. *Neuron.* 2004;42(6):983-91.
23. Valdearcos M, Robblee MM, Benjamin DI, Nomura DK, Xu AW, Koliwad SK. Microglia dictate the impact of saturated fat consumption on hypothalamic inflammation and neuronal function. *Cell Rep.* 2014;9(6):2124-38.
24. Horvath TL, Sarman B, Garcia-Caceres C, Enriori PJ, Sotonyi P, Shanabrough M, et al. Synaptic input organization of the melanocortin system predicts diet-induced hypothalamic reactive gliosis and obesity. *Proc Natl Acad Sci U S A.* 2010;107(33):14875-80.
25. De Souza CT, Araujo EP, Bordin S, Ashimine R, Zollner RL, Boschero AC, et al. Consumption of a fat-rich diet activates a proinflammatory response and induces insulin resistance in the hypothalamus. *Endocrinology.* 2005;146(10):4192-9.
26. Ozcan L, Ergin AS, Lu A, Chung J, Sarkar S, Nie D, et al. Endoplasmic reticulum stress plays a central role in development of leptin resistance. *Cell Metab.* 2009;9(1):35-51.
27. Benoit SC, Kemp CJ, Elias CF, Abplanalp W, Herman JP, Migrenne S, et al. Palmitic acid mediates hypothalamic insulin resistance by altering PKC- θ subcellular localization in rodents. *J Clin Invest.* 2009;119(9):2577-89.

28. Cavadas C, Avelaira CA, Souza GF, Velloso LA. The pathophysiology of defective proteostasis in the hypothalamus - from obesity to ageing. *Nat Rev Endocrinol.* 2016;12(12):723-33.
29. Cai D, Khor S. "Hypothalamic Microinflammation" Paradigm in Aging and Metabolic Diseases. *Cell Metab.* 2019;30(1):19-35.
30. Thaler JP, Guyenet SJ, Dorfman MD, Wisse BE, Schwartz MW. Hypothalamic inflammation: marker or mechanism of obesity pathogenesis? *Diabetes.* 2013;62(8):2629-34.
31. Velloso LA, Schwartz MW. Altered hypothalamic function in diet-induced obesity. *Int J Obes (Lond).* 2011;35(12):1455-65.
32. Jais A, Bruning JC. Hypothalamic inflammation in obesity and metabolic disease. *J Clin Invest.* 2017;127(1):24-32.
33. Yan J, Zhang H, Yin Y, Li J, Tang Y, Purkayastha S, et al. Obesity- and aging-induced excess of central transforming growth factor-beta potentiates diabetic development via an RNA stress response. *Nat Med.* 2014;20(9):1001-8.
34. Araujo EP, de Souza CT, Velloso LA. Atypical transforming growth factor-beta signaling in the hypothalamus is linked to diabetes. *Nat Med.* 2014;20(9):985-7.
35. Milanski M, Arruda AP, Coope A, Ignacio-Souza LM, Nunez CE, Roman EA, et al. Inhibition of hypothalamic inflammation reverses diet-induced insulin resistance in the liver. *Diabetes.* 2012;61(6):1455-62.
36. Kim JD, Yoon NA, Jin S, Diano S. Microglial UCP2 Mediates Inflammation and Obesity Induced by High-Fat Feeding. *Cell Metab.* 2019.
37. Schneeberger M, Dietrich MO, Sebastian D, Imbernon M, Castano C, Garcia A, et al. Mitofusin 2 in POMC neurons connects ER stress with leptin resistance and energy imbalance. *Cell.* 2013;155(1):172-87.
38. Ignacio-Souza LM, Bombassaro B, Pascoal LB, Portovedo MA, Razolli DS, Coope A, et al. Defective regulation of the ubiquitin/proteasome system in the hypothalamus of obese male mice. *Endocrinology.* 2014;155(8):2831-44.

39. Jia H, Ma H, Li Z, Chen F, Fang B, Cao X, et al. Downregulation of LncRNA TUG1 Inhibited TLR4 Signaling Pathway-Mediated Inflammatory Damage After Spinal Cord Ischemia Reperfusion in Rats via Suppressing TRIL Expression. *J Neuropathol Exp Neurol.* 2019;78(3):268-82.
40. Morari J, Anhe GF, Nascimento LF, de Moura RF, Razolli D, Solon C, et al. Fractalkine (CX3CL1) is involved in the early activation of hypothalamic inflammation in experimental obesity. *Diabetes.* 2014;63(11):3770-84.
41. Valdearcos M, Douglass JD, Robblee MM, Dorfman MD, Stifler DR, Bennett ML, et al. Microglial Inflammatory Signaling Orchestrates the Hypothalamic Immune Response to Dietary Excess and Mediates Obesity Susceptibility. *Cell Metab.* 2017;26(1):185-97 e3.
42. Carraro RS, Souza GF, Solon C, Razolli DS, Chausse B, Barbizan R, et al. Hypothalamic mitochondrial abnormalities occur downstream of inflammation in diet-induced obesity. *Mol Cell Endocrinol.* 2018;460:238-45.
43. Quaresma PGF, Teixeira PDS, Furigo IC, Wasinski F, Couto GC, Frazao R, et al. Growth hormone/STAT5 signaling in proopiomelanocortin neurons regulates glucoprivic hyperphagia. *Mol Cell Endocrinol.* 2019;498:110574.
44. Campbell JN, Macosko EZ, Fenselau H, Pers TH, Lyubetskaya A, Tenen D, et al. A molecular census of arcuate hypothalamus and median eminence cell types. *Nat Neurosci.* 2017;20(3):484-96.
45. Purkayastha S, Zhang G, Cai D. Uncoupling the mechanisms of obesity and hypertension by targeting hypothalamic IKK-beta and NF-kappaB. *Nat Med.* 2011;17(7):883-7.
46. Zhang H, Zhang G, Gonzalez FJ, Park SM, Cai D. Hypoxia-inducible factor directs POMC gene to mediate hypothalamic glucose sensing and energy balance regulation. *PLoS Biol.* 2011;9(7):e1001112.
47. Friedman JM. Leptin and the endocrine control of energy balance. *Nat Metab.* 2019;1(8):754-64.

48. Ohlsson C, Bygdell M, Sonden A, Rosengren A, Kindblom JM. Association between excessive BMI increase during puberty and risk of cardiovascular mortality in adult men: a population-based cohort study. *Lancet Diabetes Endocrinol.* 2016;4(12):1017-24.
49. Hales CM, Fryar CD, Carroll MD, Freedman DS, Ogden CL. Trends in Obesity and Severe Obesity Prevalence in US Youth and Adults by Sex and Age, 2007-2008 to 2015-2016. *JAMA.* 2018;319(16):1723-5.
50. Walden TB, Hansen IR, Timmons JA, Cannon B, Nedergaard J. Recruited vs. nonrecruited molecular signatures of brown, "brite," and white adipose tissues. *Am J Physiol Endocrinol Metab.* 2012;302(1):E19-31.

FIGURES

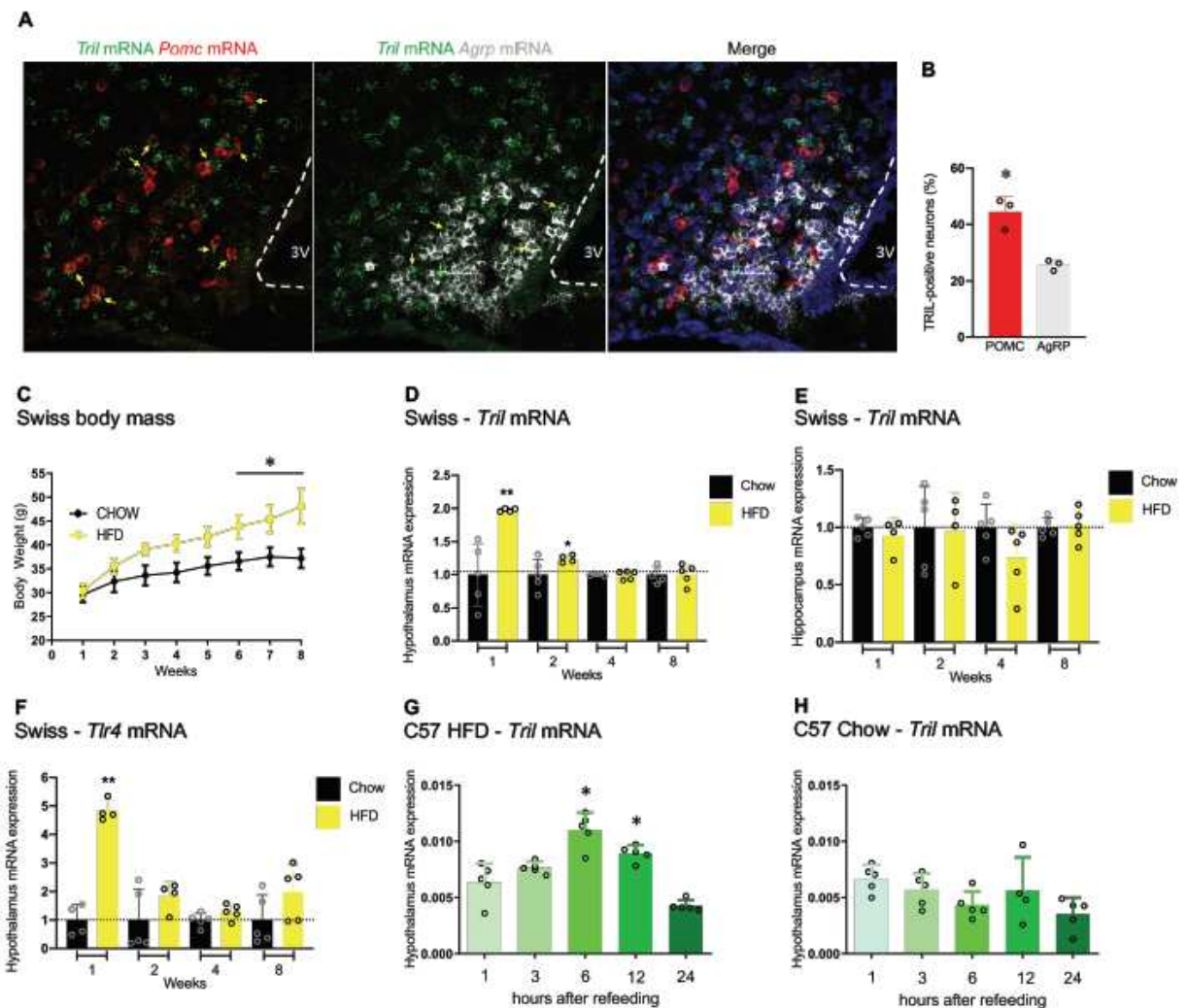


Figure 1. The impact of a high-fat diet on the expression of *Tril*. The hypothalamic *Tril* mRNA was analyzed in POMC and AgRP neurons using fluorescent in situ hybridization (A) and the overlap with POMC and AgRP neurons was quantified (B). In C-F, Swiss mice were fed chow or a high-fat diet (HFD) for 1 to 8 weeks; body mass is shown in C; transcript expressions of *Tril* (D, hypothalamus; E, hippocampus) and *Tlr4* (F, hypothalamus) in mice fed a HFD are plotted as normalized for the respective expressions in mice fed chow. C57BL/6J mice fed a HFD (G) or chow (H) were submitted to an overnight fast and hypothalami were extracted after 1, 6, 12 or 24 h of refeeding for determination of *Tril* mRNA expression. In A, images are representative of three independent samples. In C-F, n=4-5; *p<0.05 and **p<0.01 vs. respective control (chow). In G and H, n=5; *p<0.05 vs. 1 h.

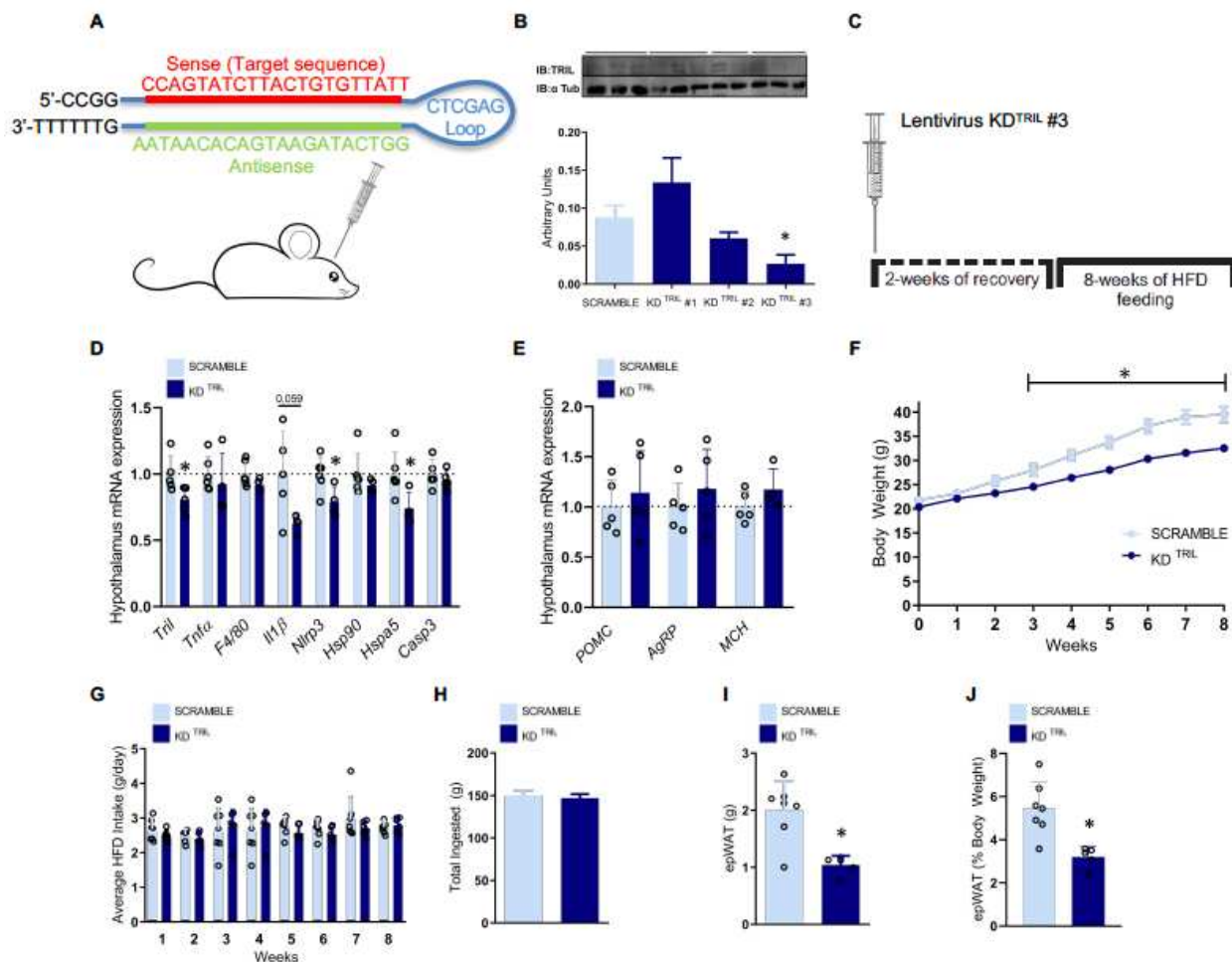


Figure 2. The inhibition of hypothalamic Tril affects body mass and adiposity.

C57BL/6J mice were submitted to an injection into the arcuate nucleus of a lentivirus carrying a scramble or one out of three different shRNA sequences for targeting Tril (KD^{TRIL}#1, KD^{TRIL}#2 or KD^{TRIL}#3) (A and B); immunoblot of hypothalamic extracts was employed to determine Tril expression in each experimental group (B); the sequence of the selected inhibitory sequence, KD^{TRIL}#3, is depicted in A. The protocol employed in the experiments is depicted in C. The hypothalamic transcript expression of inflammatory and apoptotic genes (D) and neurotransmitter genes (E) was determined at the end of the experimental period. Body mass (F) and food intake (G and H) were determined during the experimental period. Total (I) and relative (J) epididymal fat mass were determined at the end of the experimental period. In B, n=4; in D–J, n=5–7. In all experiments *p<0.05 vs. scramble. epWAT, epididymal white adipose tissue; HFD, high-fat diet; KD, knockdown.

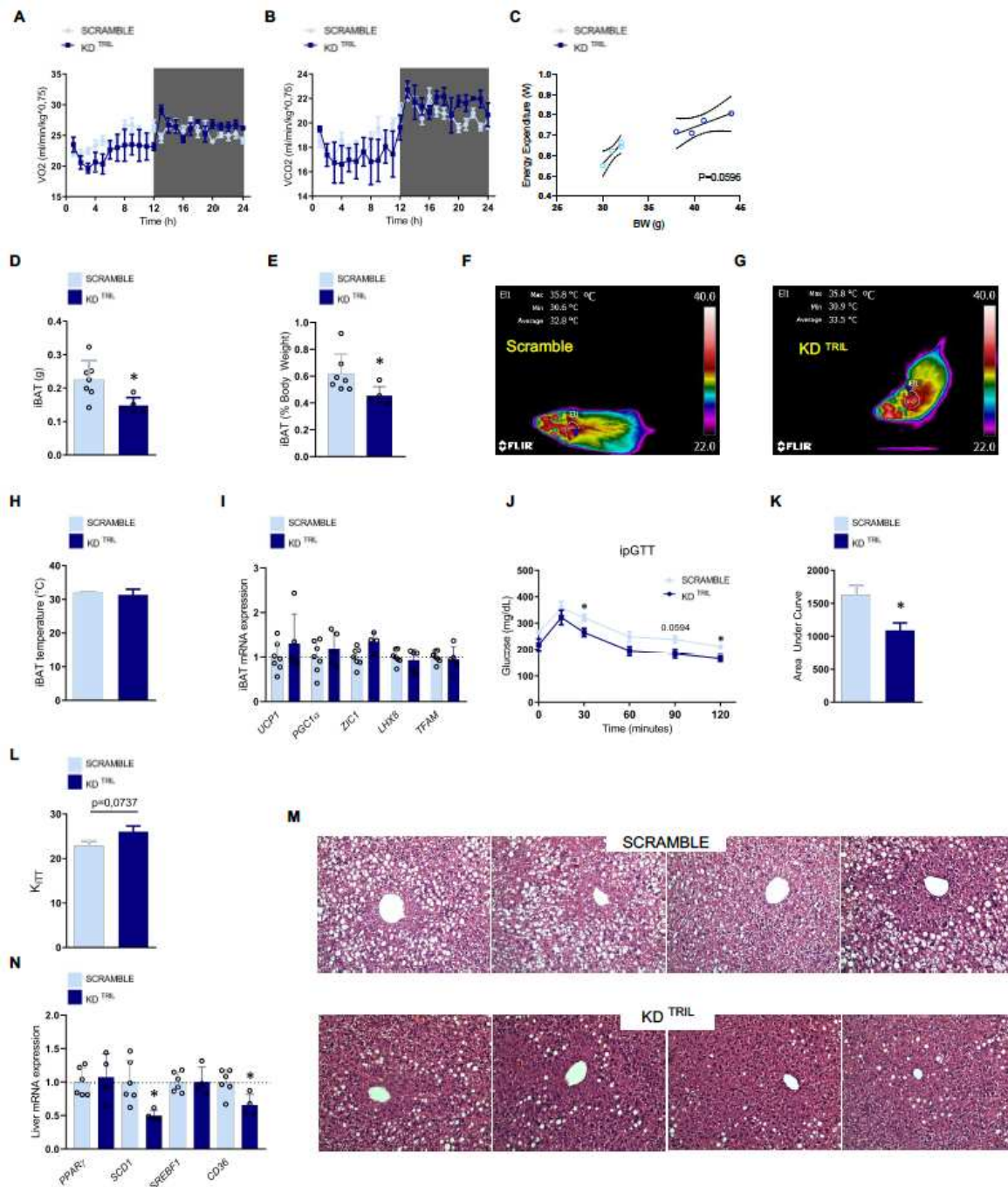


Figure 3. The inhibition of hypothalamic Tril affects energy expenditure and systemic metabolic parameters. C57BL/6J mice were submitted to an injection into the arcuate nucleus of a lentivirus carrying a scramble or a shRNA sequence (sequence KD^{TRIL}#3) employing the same experimental protocol as depicted in Fig. 2C. At the end of the experimental period, mice were submitted to determination of O₂ consumption (A), CO₂ production (B), energy expenditure (C), determination of interscapular brown adipose tissue total (D) and relative (E) mass, determination of interscapular temperature (F–H), determination of interscapular brown adipose transcript expression

of thermogenic genes (I), determination of whole-body glucose tolerance by means of an intraperitoneal glucose tolerance test (J), area under the curve of blood glucose levels (K) and determination of whole body insulin sensitivity by means of an insulin tolerance test (L, constant of blood glucose decay during the insulin tolerance test). The liver was extracted for histological examination (M) and also for determination of transcript expression of genes involved in lipogenesis or lipid uptake (N). In A–C, n=4 and in D–N, n=5–7; *p<0.05 vs. scramble. In M, images are representative of four independent experiments. EE, energy expenditure; iBAT, interscapular brown adipose tissue; ipGTT, intraperitoneal glucose tolerance test; Kitt, constant of blood glucose decay during the insulin tolerance test.

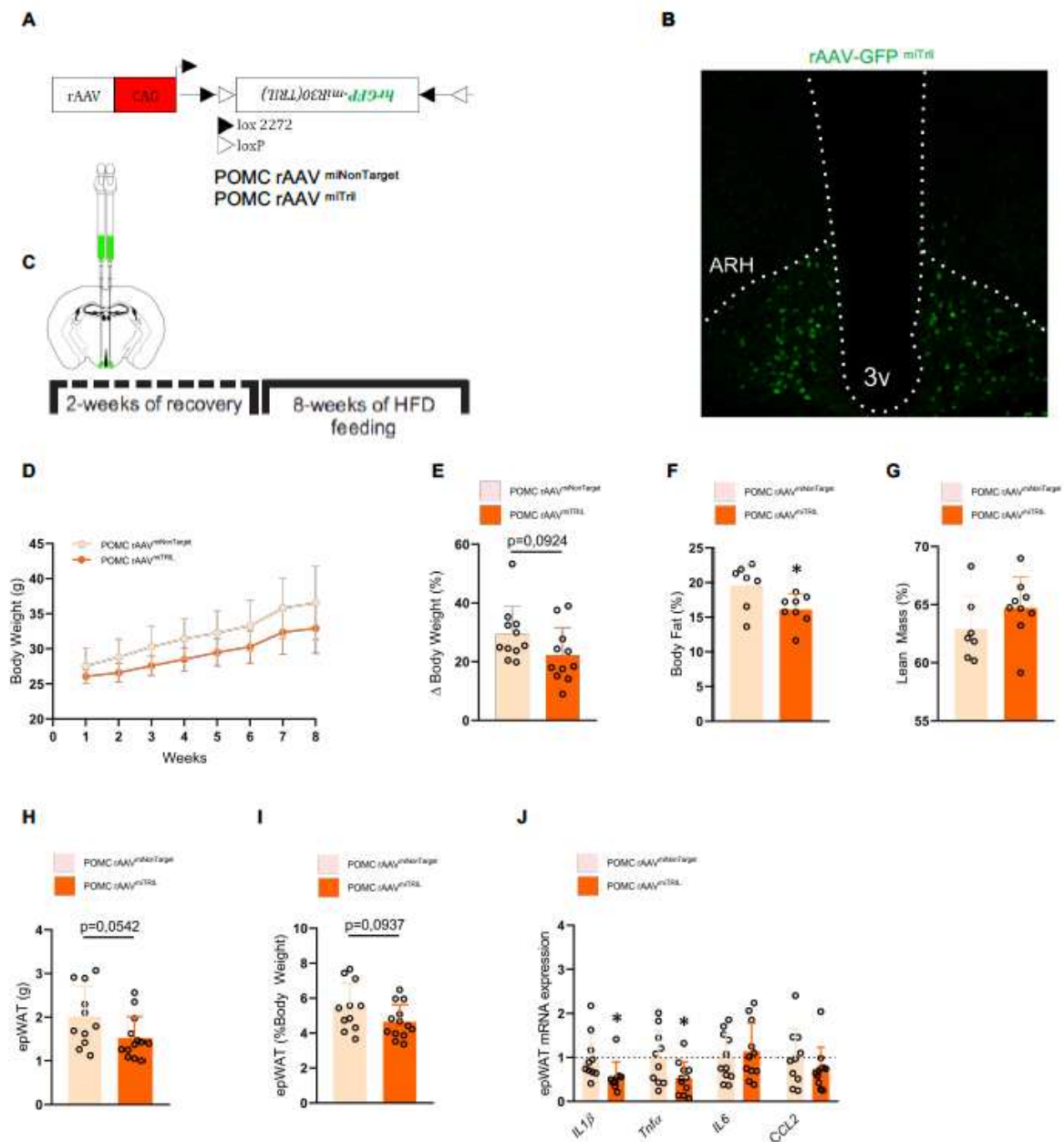


Figure 4. POMC-specific knockdown of *Tril* reduces body fat. POMC-Cre mice were submitted to an intracerebroventricular injection with Cre-dependent AAV-FLEX-EGFP-mir30(TRIL) carrying either a non-target sequence (rAAVmiNonTarget) or a *Tril* targeting sequence (rAAVmiTRIL) (A). GFP fluorescence exclusively in the ARC after bilateral infusions of AAV-FLEX-EGFP-mir30(TRIL) into the hypothalamus of *Pomc*-Cre mice (B). The protocol employed in the experiments is depicted in C. Body mass (D and E) was determined throughout the experimental period. Relative fat (F) and lean (G) mass as well as the absolute (H) and relative (I) epididymal fat mass were determined at the end of the experimental period. The expressions of inflammatory genes were determined in the epididymal adipose tissue at the end of the experimental period (J). In D–J, n=6–14; *p<0.05 vs. miNonTarget.

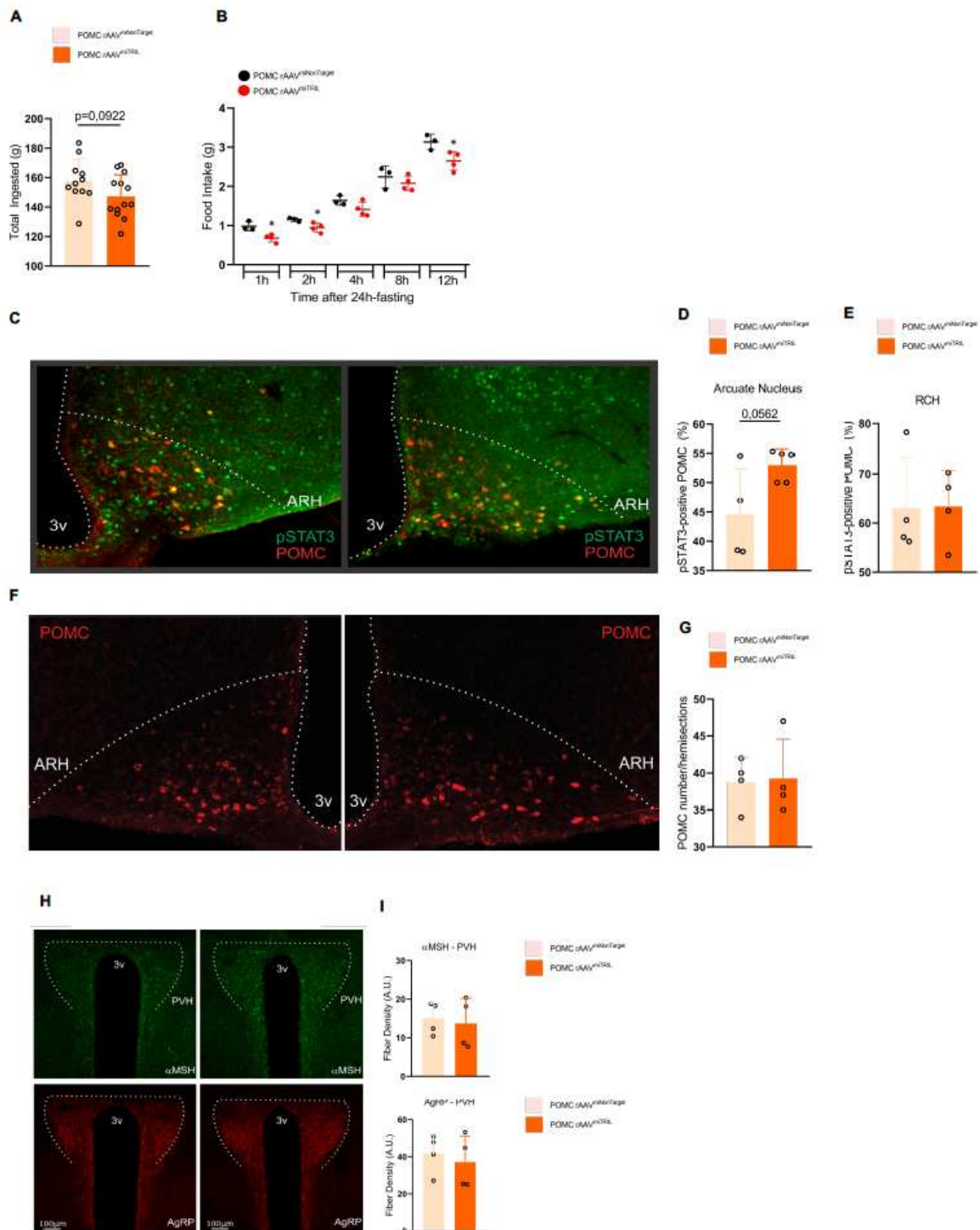


Figure 5. Inhibition of Tril in POMC neurons improves leptin sensitivity. POMC-Cre mice were submitted to an intracerebroventricular injection with Cre-dependent AAV-FLEX-EGFP-mir30 carrying either a non-target sequence (rAAVmiNonTarget) or a Tril targeting sequence (rAAVmiTRIL) and then submitted to the same protocol as in Fig. 4C. The cumulative consumption of diet was determined throughout the experimental period (A). At the end of the experimental period, mice were submitted to a

determination of spontaneous food intake after a period of 24 h fasting (B). Leptin-induced phosphorylation of STAT3 was determined by calculating the proportion of phospho-STAT3 per POMC-positive cells in the arcuate nucleus (D) and retrochiasmatic hypothalamus (E) employing immunofluorescence staining; an illustrative image obtained from the mediobasal hypothalamus is depicted in C. No difference was observed in the number of POMC neurons in the ARC (F and G). Immunofluorescence staining was employed to determine the density of α -MSH (H, upper panels and I) and AgRP (H, lower panels and I) fiber projections to the paraventricular hypothalamus. In A, n=11–13; in B–H, n=4–5; *p<0.05 vs. miNonTarget.

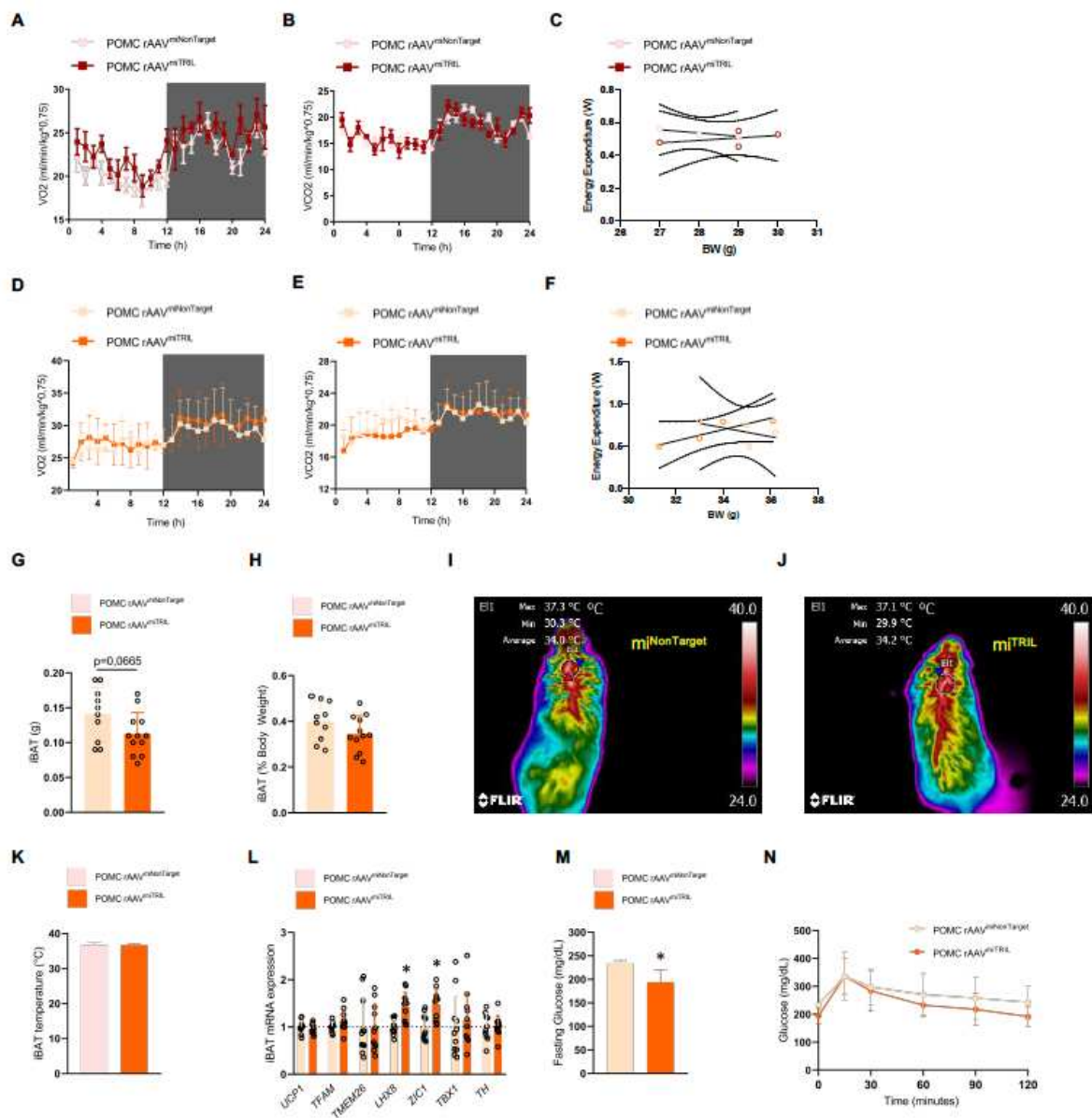
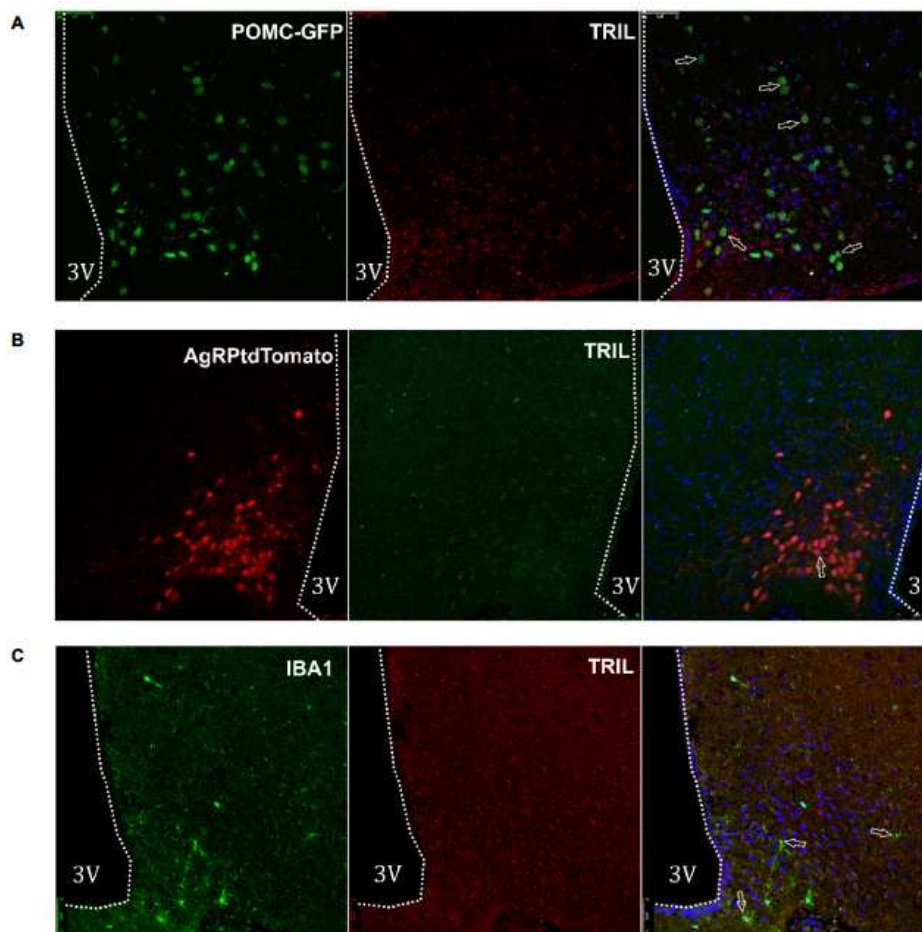


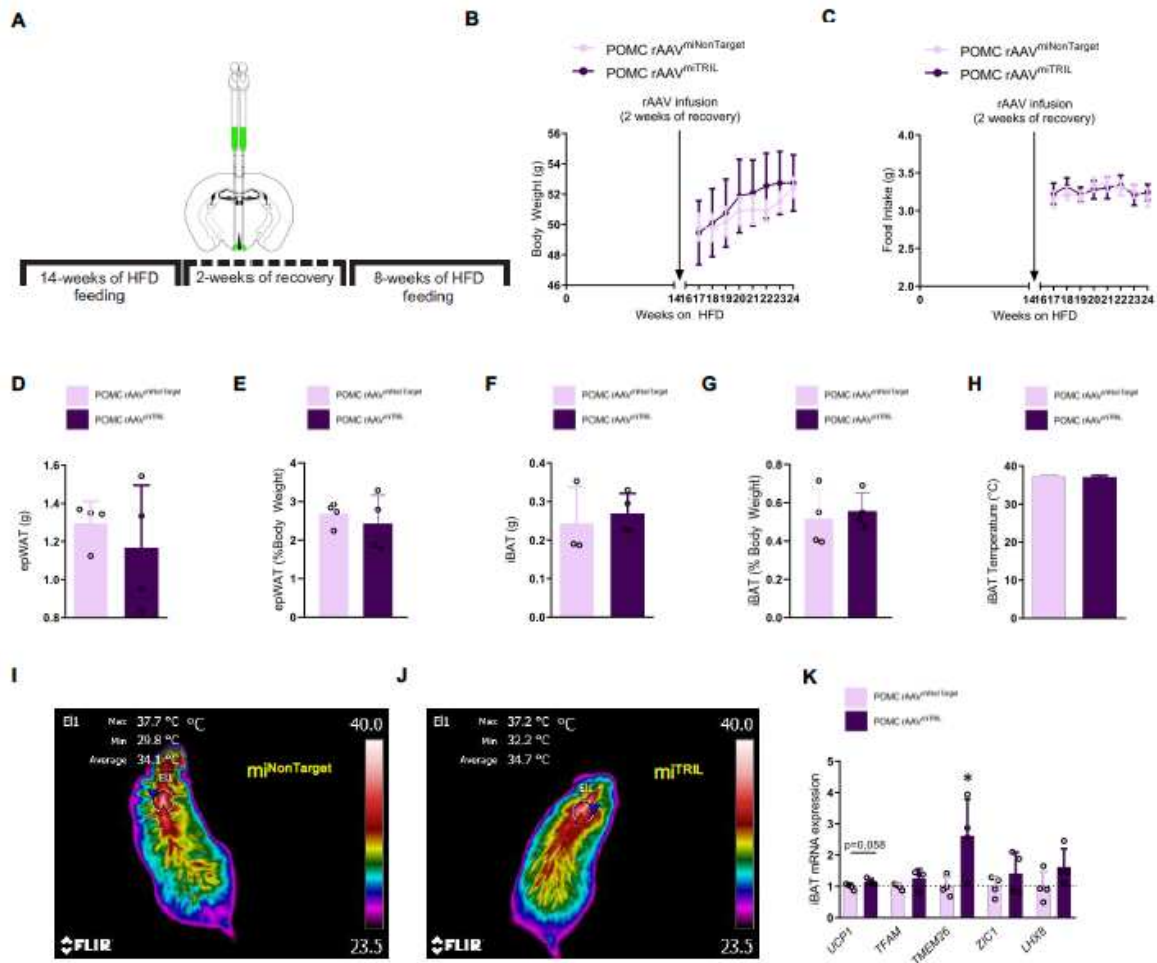
Figure 6. Inhibition of Tril in POMC neurons increases energy expenditure. In A–C, POMC-Cre mice were submitted to an intracerebroventricular injection with Cre-dependent AAV-FLEX-EGFP-mir30 carrying either a non-target sequence (rAAVmiNonTarget) or a Tril targeting sequence (rAAVmiTRIL) and allowed 2 weeks for recovery, followed by another 2 weeks fed on chow; at the end of the experimental period, mice were submitted to determination of O_2 consumption (A), CO_2 production (B) and energy expenditure (C). In D–N, POMC-Cre mice were submitted to an intracerebroventricular injection with Cre-dependent AAV-FLEX-EGFP-mir30 carrying either a non-target sequence (rAAVmiNonTarget) or a Tril targeting sequence (rAAVmiTRIL) and then submitted to the same protocol as in Fig. 4C. At the end of the experimental period, mice were submitted to determination of O_2 consumption (D),

CO₂ production (E), energy expenditure (F), determination of interscapular brown adipose tissue total (G) and relative (H) mass, determination of interscapular temperature (I-K) and determination of interscapular brown adipose transcript expression of thermogenic genes (L). In addition, blood glucose levels were determined in fasting mice (M) and whole-body glucose tolerance was determined by means of an intraperitoneal glucose tolerance test (N). In A–F, n=3-4; in G-N, n=12–14. In all, *p<0.05 vs. miNonTarget.

SUPPLEMENTARY FIGURES

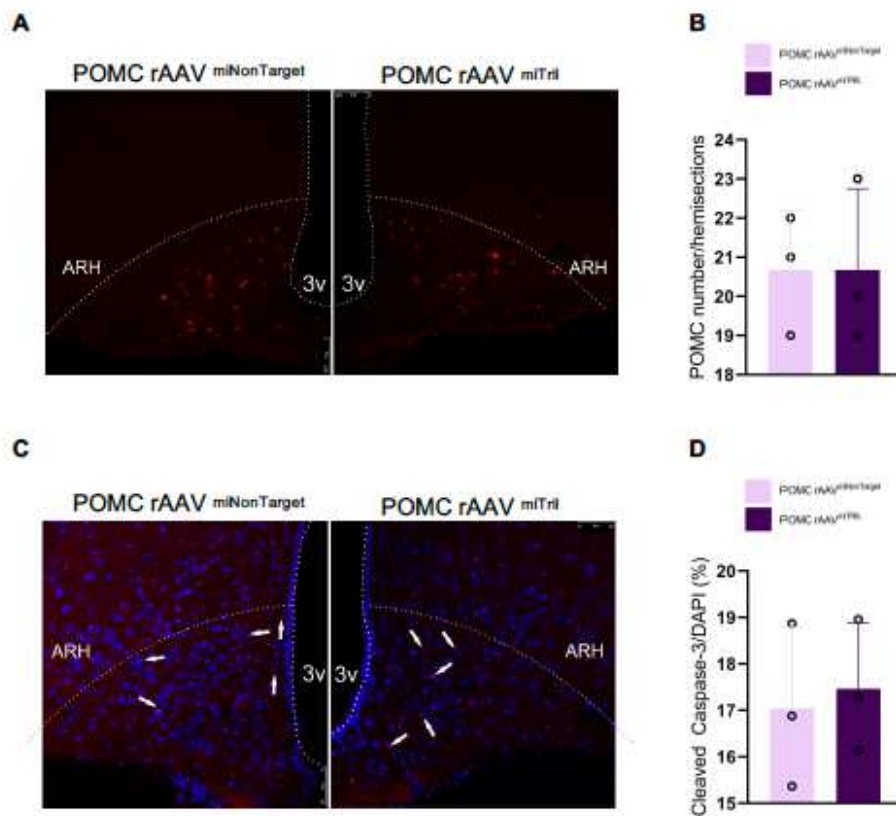


Supplementary Figure 1. Neuronal distribution of Tril in the ARC. The hypothalamic expression of Tril was determined using immunofluorescence staining in sections obtained from chow fed POMC-GFP (A), AgRPtdTomato (B) and C57BL/6J (C) mice; in A and B, POMC and AgRP neurons were detected as expressing the respective endogenous fluorescent peptides, whereas in C, Iba1-expressing cells were detected using a specific antibody. In A–C, Tril was detected using a specific antibody; the arrows indicate cells co-expressing target peptides.



Supplementary Figure 2. Inhibition of Tril in POMC neurons in mice submitted to long-term feeding on a high-fat diet fails to revert the obese phenotype. POMC-Cre mice were fed for 14 weeks on a high-fat diet and then submitted to an intracerebroventricular injection with Cre-dependent AAV-FLEX-EGFP-mir30 carrying either a non-target sequence (rAAVmiNonTarget) or a Tril targeting sequence (rAAVmiTRIL); after 2 weeks of recovery, mice were fed a high-fat diet for another 8 weeks (experimental protocol depicted in A). Body mass (B) and food intake (C) were recorded throughout the experimental period. Relative fat (F) and lean (G) mass as well as the absolute (H) and relative (I) epididymal fat mass were determined at the end of the experimental period. Absolute (D) and relative (E) epididymal fat mass as well as absolute (F) and relative (G) interscapular brown adipose tissue mass were

determined at the end of the experimental period. The interscapular temperature (H–J) and the determination of interscapular brown adipose transcript expression of thermogenic genes were determined at the end of the experimental period. In all experiments, n=4–5; *p<0.05 vs. miNonTarget.



Supplementary Figure 3. POMC-specific inhibition of Tril in mice submitted to long-term feeding on a high-fat diet do not prevent loss of POMC neurons. POMC-Cre mice were fed a high-fat diet for 14 weeks and then submitted to an intracerebroventricular injection with Cre-dependent AAV-FLEX-EGFP-mir30 carrying either a non-target sequence (rAAVmiNonTarget) or a Tril targeting sequence (rAAVmiTRIL); after 2 weeks of recovery, mice were fed a high-fat diet for another 8 weeks (according to the protocol depicted in Fig. 7A). Immunofluorescence staining was employed to determine the number of cells expressing POMC (A and B) and cleaved caspase-3 (C and D). In all experiments, n=3. In C, arrows depict cells expressing cleaved caspase-3.

CAPÍTULO 2: ARTIGO 2**POMC-specific deletion of PPAR δ attenuates diet-induced obesity and systemic glucose intolerance**

Alexandre Moura-Assis^{1,2}, Jeffrey M. Friedman^{2,3}, Licio A. Velloso¹

¹Laboratory of Cell Signalling-Obesity and Comorbidities Research Center, University of Campinas, Campinas, Brazil

²Laboratory of Molecular Genetics, The Rockefeller University, New York, USA.

³ Howard Hughes Medical Institute

Corresponding Author:

Lício A. Velloso

Laboratory of Cell Signaling, Obesity and Comorbidities Research Center

University of Campinas, Campinas, SP, Brazil

Email: lavelloso@unicamp.br

Declaration of competing interest. The authors declare that they have no known competing financial interests or personal relationships that could have appeared to influence the works reported in this study.

ABSTRACT

PPAR δ is a fatty acid sensor, ligand-binding nuclear receptor that regulates the expression of many genes involved in lipid and glucose metabolism. In order to understand how chronic overnutrition and obesity affect POMC-expressing neurons and promote metabolic dysfunction, we determined the metabolic outcomes of modulating hypothalamic PPAR δ . To assess the role of PPAR δ in a monogenic model of obesity, we pharmacologically activated central PPAR δ in ob/ob mice. Chronic intracerebroventricular administration of PPAR δ agonist, GW501615, was not sufficient to modify the anti-obesity effects of leptin in ob/ob mice. Next, we designed an AAV carrying a sgRNA targeting PPAR δ (gPPAR δ) and an AAV carrying a Cre-dependent mCherry as control to inject in the hypothalamic arcuate nucleus of POMC-Cre::LSL-Cas9 mice. In a cohort of mice fed on high-fat diet (HFD) for twelve weeks, we observed an initial reduction in caloric intake in POMC-specific PPAR δ deleted group. This was accompanied by a significant decrease in fat mass and improved glucose tolerance. Deletion of PPAR δ was not sufficient to modify POMC-specific leptin and glucose responsiveness. In addition, deletion of PPAR δ was not sufficient to change systemic energy homeostasis. Thus, hypothalamic PPAR δ is involved in the regulation of systemic glucose tolerance and body composition. We conclude that PPAR δ expression in POMC neurons emerges as a new player in the complex hypothalamic system that regulates systemic energy homeostasis.

Key words: obesity, leptin, glucose, hypothalamus

INTRODUCTION

Peroxisome proliferator-activated receptor (PPAR) β/δ (herein referred as PPAR δ) belongs to the nuclear receptor PPAR family that are ligand-activated transcription factors involved in the regulation of metabolism, immune response and growth (1,2). In contrast with the extensively studied PPAR α and PPAR γ isoforms, the functions of PPAR δ remain largely unknown (2). However, clinical data showing that certain PPAR δ gene polymorphisms are associated with increased risk for cardiovascular and metabolic diseases (3,4); and the beneficial effects of the synthetic PPAR δ agonist (GW501516) reducing liver fat content, blood triglycerides and LDL, and mitigating insulin resistance (5), strongly support its important role in whole body metabolism.

PPAR δ is the predominant PPAR isoform in the brain (6,7) and its expression is particularly high in the hypothalamic nuclei involved in the regulation of feeding and energy homeostasis (8). In leptin-deficient *ob/ob* mice, the hypothalamic expression of PPAR δ is increased (9); whereas mice with neuronal deletion of PPAR δ display increase fat mass, hyperleptinemia and abnormal responses to fast and feeding (7).

Single-cell RNA sequencing data revealed that POMC neurons are among the cell types expressing PPAR δ in the arcuate nucleus of the hypothalamus (https://singlecell.broadinstitute.org/single_cell/study/SCP97/a-molecular-census-of-arcuate-hypothalamus-and-median-eminence-cell-types#study-visualize). POMC neurons play a pivotal role in whole body energy homeostasis by providing anorexigenic signals in response to systemic hormonal and nutrient cues that indicate the energy stores of the body (10). In diet-induced obesity, the activity of POMC neurons is impaired resulting in the abnormal regulation of caloric intake and energy expenditure (11,12). Here, we hypothesized that PPAR δ expression in POMC neurons is involved on its dysfunction in experimental obesity. We show that POMC-specific deletion of PPAR δ reduces fat mass and improves the glucose homeostasis in obese mice.

METHODS

Experimental animals. All experimental procedures were approved by the Institutional Animal Care and Use Committee at the Rockefeller University. Mice were housed in a 12 h light/dark cycle at 22°-24°C with *ad libitum* access to water and food, in exception when specified in the text. WT male C57BL/6J mice (000664, Jackson Laboratory), *ob/ob* female (B6.Cg-Lepob/J; 000632, Jackson Laboratory; or bred in-house) POMC-Cre (Tg(Pomc1-cre)^{16Lowl/J}; 005965, Jackson Laboratory) and Rosa26-Cas9 knock-in (Gt(ROSA)^{26Sortm1.1(CAG-cas9*,-EGFP)Fezh/J}; 024858, Jackson Laboratory) were employed in this study. For diet-induced obesity studies, mice were fed on a 60% HFD (D12492, Research Diets). Following stereotaxic injections for AAV expression, mice were individually housed, and body weight and food intake were measured twice a week and body composition was measured using NMR imaging (EchoMRI).

Metabolic measurements. Metabolic phenotyping of mice was performed using an automated home cage phenotyping system (TSE-Systems). Mice were acclimated for 48 h in the metabolic cages prior to the measurements of metabolic parameters. A climate-controlled chamber was used and set at 22°C for four days and at 6°C for 36 h to analyze cold-induced thermogenesis. The locomotor activity was recorded as beam breaks and the distance/velocity detected by automated lasers into the cages.

PPAR δ deletion in Pomc neurons. A Cre-dependent AAV viral vector was constructed based on AAV-U6-LepRgRNA-EF1a-DIO-mCherry-WPRE-pA plasmid (13) (kindly provided by Dong Kong, Tufts University). The sgRNAPPAR δ was designed using the CRISPR online tools (<https://portals.broadinstitute.org/gpp/public/analysis-tools/sgrna-design> and <http://chopchop.cbu.uib.no/>). The tcgagtatgagaagtgcgat sequence targeting the exon 5 of *ppar δ* gene, which encodes the DNA-binding domain, was complemented with a PAM sequence “cgg”,

Viruses and stereotaxic surgery. The AAV8-U6-sgRNAPPAR δ -EF1a-DIO-mCherry-WPRE-pA was generated and titrated (1.6×10^{13} GC/ml) by the Vector Biolabs services and an AAV5-EF1a-DIO-mCherry (1.8×10^{13} GC/ml) from UNC Vector Core was used as control. For AAV delivery into the ARC (AP: -1.7 mm, DV: -5.8 mm and ML: ± 0.3 mm), mice were anesthetized with isoflurane, using 3% for induction and 1.5-2% for anesthesia

maintenance. Thereafter, mice were placed in a stereotaxic frame (Kopft Instruments) and an eye ointment was applied to avoid eye drying. The hair was shaved and an incision above the head was made. A bilateral small hole was drilled and 300 nl of virus was injected in each side using a Hamilton syringe (26s/2"/2). For postoperative care, mice received an intraperitoneal injection of meloxicam (2 mg/kg) and were monitored daily for two weeks until full recovery. All stereotaxic injection sites were verified by mCherry immunohistochemistry and the 'missed' animals were excluded from data analyses.

PPAR δ agonist and leptin treatment. *ob/ob* mice were anesthetized with isoflurane and a cannula was implanted into the lateral ventricle (AP: -0.5 mm, DV: -2.5 mm and ML: \pm 1.3 mm). A mini-osmotic pump (model 2001, Alzet) was implanted subcutaneously via a catheter connected to the cannula for i.c.v. infusion, filled with GW501516 (Cayman Chemical). Another mini-osmotic pump (model 2001, Alzet) was also implanted subcutaneously, filled with recombinant leptin (R&D Systems).

Glucose tolerance test. Following 6h fasting, mice received intraperitoneal (ip) injection with solutions containing glucose (2.0 g/kg body weight) and then blood samples were collected for ip-glucose tolerance test (ipGTT). Glucose concentrations were measured in the tail blood using a portable glucose meter (Optium Xceed, Abbott) at 0, 15, 30, 60 and 120 minutes after glucose administration.

Perfusion and immunohistochemistry. Mice were submitted to lethal anesthesia with isoflurane and transcardially perfused with 0.1M PBS (pH7.4) followed by 4x PFA at 4°C. The brains were postfixed for 24 h in 4x PFA and then transferred to a solution containing 30% sucrose in 0.1 M PBS (pH 7.4). Perfused brains were frozen at -25°C and sectioned on a cryostat at a thickness of 30 μ m. For immunohistochemistry, free-floating sections were washed three times for 10 minutes with 0.1 M PBS. Next, sections were blocked in 3% BSA and 2% normal goat serum in 0.2% PBST (Triton X-100) for 1 h at room temperature, followed by incubation in PPAR δ antibody (Thermo Fisher Scientific, PA1823A), c-FOS antibody (Synaptic Systems 226 004) and mCherry antibody (Abcam, ab205402). For pSTAT3 staining, mice were submitted to 12 h fasting and then injected i.p. with recombinant leptin (3 mg/kg body weight). After 1 h, mice were submitted to lethal anesthesia and the brain harvested and sectioned as

mentioned previously. Brain sections were rinsed in 0.02 M KPBS (pH 7.4), followed by pretreatment in a water solution containing 1% hydrogen peroxide and 1% sodium hydroxide for 20 minutes. After extensive washings in 0.02 M KPBS, the sections were incubated in 0.3% glycine for 10 minutes and then 0.03% lauryl sulfate for 10 minutes. Thereafter, the sections were blocked in 3% normal goat serum for 1 h, followed by incubation in rabbit anti-pSTAT3 (1:1000, Cell Signaling, #9145S) for 48 h. For the immunofluorescence reactions, sections were rinsed in KPBS and incubated for 2 h in goat anti-rabbit AlexaFluor⁶⁴⁷ (1:500, Life Technologies #A21245), goat anti-ginea pig AlexaFluor⁶³³ (1:500, Life Technologies #A21105) and goat anti-chicken AlexaFluor⁵⁹⁴ (1:500, Life Technologies #A11042). Images were obtained using an Inverted LSM 780 laser scanning confocal microscope (20x objective, Zeiss). For cFOS and pSTAT3 counting, the Cell Counter plugin from ImageJ (NIH) was used.

Adipo-Clear. Inguinal white adipose tissue (WAT) specimens were collected after isoflurane anesthesia and intracardiac perfusion with 0.1M PBS. The samples were post-fixed in 4% PFA at 4°C for 24 h and washed in 20%, 40%, 60% and 80% methanol in B1N buffer (H₂O, 0.1% Triton X-100 and 0.3M glycine, pH 7), and 100% methanol for 1 h each and delipidated with 100% dichloromethane (Sigma-Aldrich) after an overnight incubation. After, samples were washed in 100% methanol; 80%, 60%, 40% and 20% methanol in B1N buffer for 1 h each and transferred to PTwH buffer (PBS, 0.1% Triton X-100, 0.05% Tween 20 and 2mg/ml heparin) for 1 h twice. The samples were incubated in primary antibody (TH; 1:400; AB152; Millipore) diluted in PTwH buffer for 4 days and washed in PTwH for 5 min, 10 min, 15 min, 30 min, 1 h, 2 h, 4 h and overnight. Then, the samples were incubated in secondary antibody (AlexaFluor⁶⁴⁷) in PTwH buffer for 4 days and washed in PTwH for 5 min, 10 min, 15 min, 30 min, 1 h, 2 h, 4 h and overnight. The samples were finally dehydrated in 25%, 50%, 75% methanol/H₂O and 100% methanol for 1 h each. For the clearing step, the samples were embedded overnight in dibenzyl ether (DBE, Sigma-Aldrich) and the whole-tissue imaged on a light-sheet microscope (Ultramicroscope II, LaVision Biotec) with 1.3x objective. For the 3D reconstruction the Imaris x64 software was used.

RESULTS

Pharmacological activation of hypothalamic PPAR δ does not impact body mass. Leptin-deficient *ob/ob* mice are massively obese and display remarkable POMC dysfunction (14). To evaluate if the central PPAR δ activation can abolish the appetite-suppressant effect of leptin, we co-administered a PPAR δ agonist, GW 501516, and recombinant leptin (Fig. 1A). During the seven-day experimental period following the osmotic pump implantation, there were body weight and food intake reductions in the leptin group; however, the central PPAR δ activation was not sufficient to promote changes in baseline and leptin-induced caloric intake and body mass (Fig. 1B-1C). The infusion of leptin at 150 ng/h results in blood leptin levels of approximately 5 ng/ml, which is similar to levels found in lean wild-type mice, and promotes consistent metabolic effects (15), such as increased thermogenesis and normalization of blood glucose levels (16,17). In our model, we observed similar reduction of fasting glucose levels both in the leptin-treated group and in the leptin plus GW501516 group. However, there were no changes in systemic glucose levels when GW501516 was administered alone (Fig. 1D)

POMC-specific knockdown of PPAR δ reduces body adiposity and attenuates glucose intolerance. The consumption of fat-rich diets affects hypothalamic POMC neurons at the functional and structural levels (12,18,19). To evaluate the role of PPAR δ in POMC neurons, we crossed the POMC-Cre mice with the LSL-Cas9 mice, inducing the expression of Cas9 endonuclease specifically in POMC neurons. Thereafter, we constructed an AAV carrying a single-guide RNA targeting the mouse *Ppar δ* locus (gPPAR δ) and a Cre-dependent mCherry reporter, indicating transduced POMC neurons (Fig. 2A). After confirming the deletion of PPAR δ expression in the transduced POMC neurons and validating the CRISPR-Cas9 approach (Fig. 2B), mice were fed for 12 weeks on HFD. Despite no change in the body mass (Fig. 2C), POMC-specific deletion of PPAR δ resulted in reduced fat mass (Fig. 2D) and increased lean mass (Fig. 2E). Food intake was significantly reduced during the early stages of HFD feeding (Fig. 2F); however, at the end of 12 weeks on HFD, the dark/light cycle feeding (Fig. 2G) and refeeding after 24 hours of fasting (Fig. 2H) were the same in both groups. In addition,

mice under POMC-specific PPAR δ deletion were more tolerant to glucose, as determined by the GTT (Fig. 2I-2J).

POMC-specific knockdown of PPAR δ does not change energy expenditure. Next, we aimed at investigating the metabolic effects of PPAR δ deletion in POMC neurons. For that, mice were evaluated at 22°C (Fig. 3) and at 6°C (Fig. 4). In neither scenario, there were differences in oxygen consumption (Fig. 3A and Fig. 4A), carbon dioxide production (Fig. 3C and Fig. 4C), energy expenditure (Fig. 3E and Fig. 4E) and locomotor activity (Fig. 3G and Fig. 4G). Furthermore, the knockdown of PPAR δ in POMC neurons was not sufficient to modify the sympathetic innervation of WAT, as determined using a whole-mount tissue clearing (Adipo-Clear) immunolabeling tyrosine hydroxylase to mark sympathetic nervous system neurons in the adipose tissue (Fig. 5A-5B).

POMC-specific knockdown of PPAR δ does not change arcuate nucleus POMC neuron response to glucose and leptin. Glucose uptake and intracellular ROS generation are crucial for POMC neuronal firing (20) and diet-induced obese mice present decreased levels of ROS in POMC neurons (9). In addition, obese mice have increased levels of UCP2, which mediates the mitochondrial proton leak, limiting ROS generation in POMC neurons (9). The UCP2 is, at least in part, transcriptionally regulated by PPAR δ (21). To test if the PPAR δ deletion would alter the glucose responsiveness in POMC neurons, we analyzed c-Fos expression in response to an intraperitoneal injection of glucose (Fig. 6A). As depicted in Fig. 6B-6C, the number of c-Fos-positive POMC neurons were similar between the groups. Furthermore, to analyze POMC responsiveness to leptin, we acutely stimulated mice with recombinant leptin (Fig. 6D) and determined pSTAT3 expression in POMC neurons. As shown in Fig. 6E-6F, deletion of PPAR δ was not sufficient to modify POMC responsiveness to leptin.

DISCUSSION

The aim of this study was to determine the potential involvement of hypothalamic, and particularly POMC-specific PPAR δ in whole body energy homeostasis. The rationale behind the study relied on the fact that PPAR δ is the most common PPAR isoform in the brain and particularly in the hypothalamus (6,22); and that neuronal

deletion of PPAR δ increases circulating leptin and susceptibility to diet-induced obesity (7).

In the first part of the study, we employed a pharmacological approach to activate PPAR δ using a synthetic agonist continuously injected in the central nervous system (CNS). The agonist, GW501516, is a small molecule developed using combinatorial chemistry with high affinity for PPAR δ ($K_i=1.1$ nM) (22). In other experimental studies, systemic GW501516 was shown to exert a number of metabolic effects, such as increasing reverse cholesterol transport (23), reducing body adiposity (24) and increasing fatty acid oxidation (25). However, the central effects of GW501516-mediated PPAR δ activation are poorly understood. Here, we used an osmotic pump attached to an i.c.v. catheter to activate central PPAR δ for seven days in leptin-deficient *ob/ob* mice. Despite the appropriate response to recombinant leptin administration, there were no changes in body mass, food intake and fasting glucose levels when mice were treated with GW501516. In the arcuate nucleus, POMC and AgRP neurons, which exert opposing functions in the control of body mass, sit side-by-side in a very small anatomical territory. As both cell types express PPAR δ (https://singlecell.broadinstitute.org/single_cell/study/SCP97/a-molecular-census-of-arcuate-hypothalamus-and-median-eminence-cell-types#study-visualize), the lack of effect resulting from the central infusion of GW501516 could be attributed to a combined action of the PPAR δ agonist in both cell types, resulting in neutrality.

Next, in order to determine the POMC-specific actions of PPAR δ we employed the CRISPR-Cas9 system to delete PPAR δ specifically in POMC neurons. POMC neurons were selected for the intervention because they respond both to hormonal and nutrient signals to promote systemic adaptations to fuel availability (10,26). Studies have shown that in experimental obesity, there is a defective function of POMC neurons, that occurs early after the introduction of a HFD, and leads to abnormal regulation of feeding and body mass (18). Moreover, POMC neurons play an important role in the regulation of systemic glucose tolerance, placing this neuronal cell-type in a pivotal position in the regulation of whole-body metabolism (27). The POMC-specific deletion of PPAR δ promoted a reduction of fat mass and increased lean mass, which resulted in no significant change in total body mass. This was accompanied by a

reduction of caloric intake in the initial period of HFD feeding. Experimental studies have shown that upon introduction of a HFD, rodents present a transient increase in caloric intake, which progressively returns to levels similar to control, implying that caloric intake-dependent energy imbalance is highest at the beginning of dietary intervention (18). In this context, the changes in body adiposity occurring in POMC-specific PPAR δ deletion could be attributed to a time-limited reduction in caloric intake. This was further supported by the fact that mice presented no change in energy expenditure under either room-temperature or cold-exposure conditions. Moreover, the POMC-specific PPAR δ deletion did not change the sympathetic innervation of white adipose tissue, suggesting that neither lipolysis nor browning was playing an important role as mediators of reduced adipose tissue mass in this model.

CONCLUSIONS

POMC-specific PPAR δ is involved in the regulation of body composition and systemic glucose tolerance. The POMC-specific deletion of PPAR δ results in a favorable change in body mass composition, increasing lean and reducing fat mass. In addition, mice under POMC-specific deletion of PPAR δ were more tolerant to glucose. Thus, POMC-PPAR δ emerges as a new player in the regulation of whole body metabolism.

FIGURES

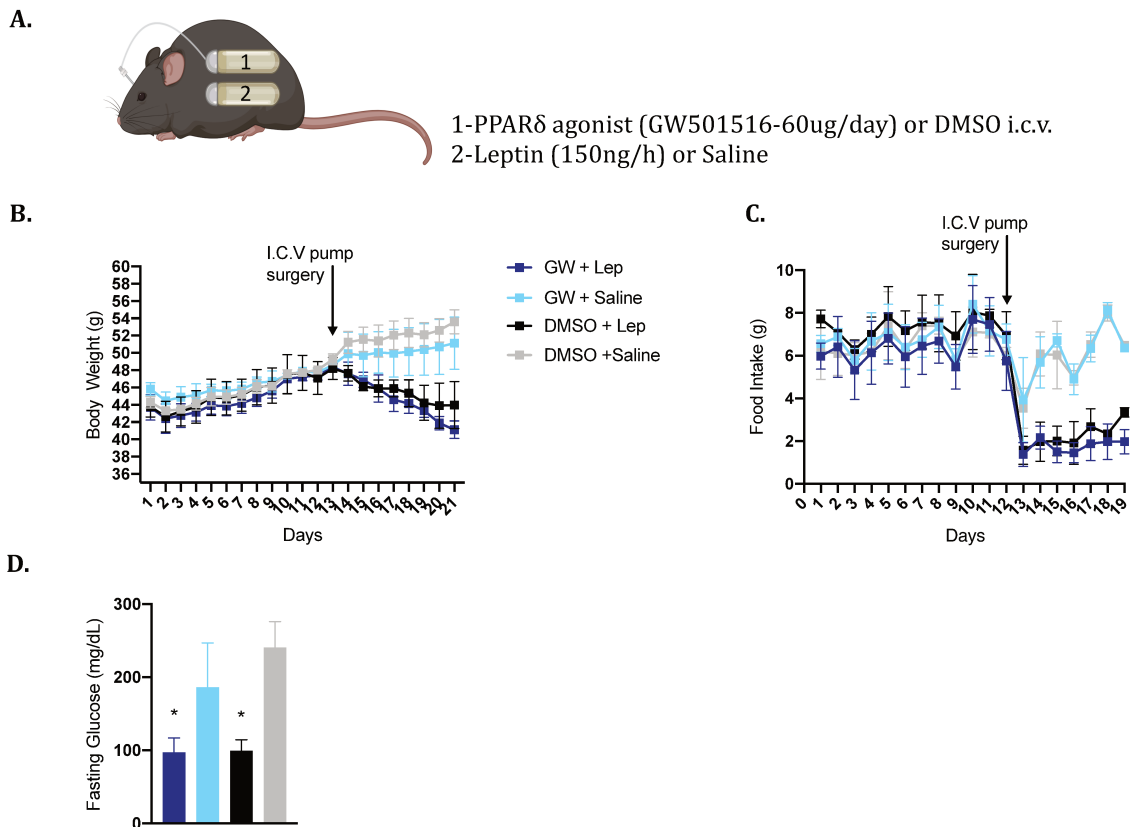


Figure 1. Central PPAR δ activation does not alter body weight and food intake of *ob/ob* mice. (A) Schematic of experimental strategy. *ob/ob* mice were implanted with osmotic pumps dispensing GW501516 (PPAR δ agonist) or DMSO (vehicle) directly into the lateral ventricle and subcutaneous leptin or saline. (B) Body weight of *ob/ob* mice before and after osmotic pumps implantation. (C) Daily food intake of *ob/ob* mice on chow diet. (D) After 7 days of treatment the glycemia was measured after an overnight fasting. N=4, *p<0.05 vs respective control (GW + Lep vs GW + Saline and DMSO + Lep vs DMSO + Saline). All error bars are \pm SEM.

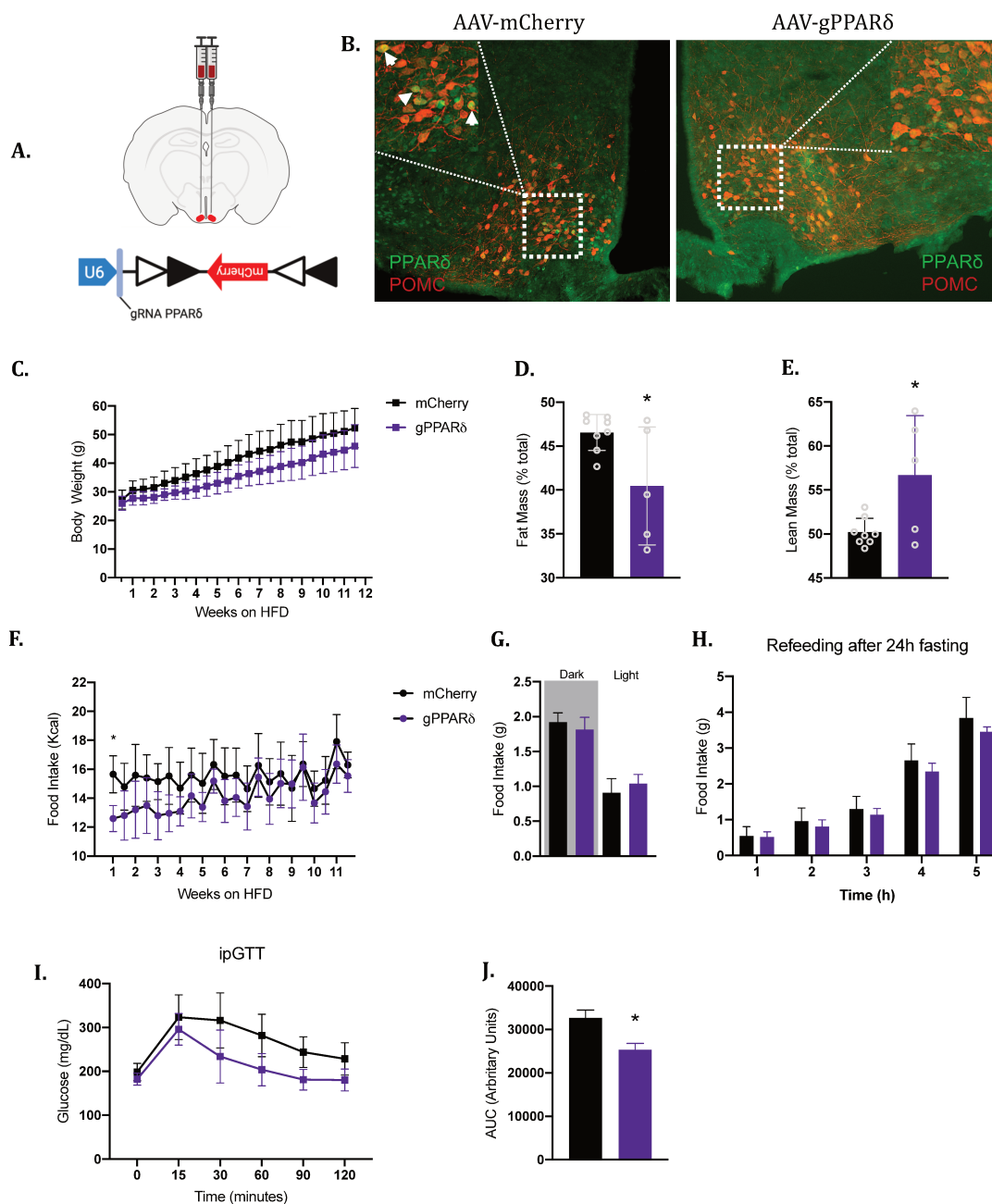
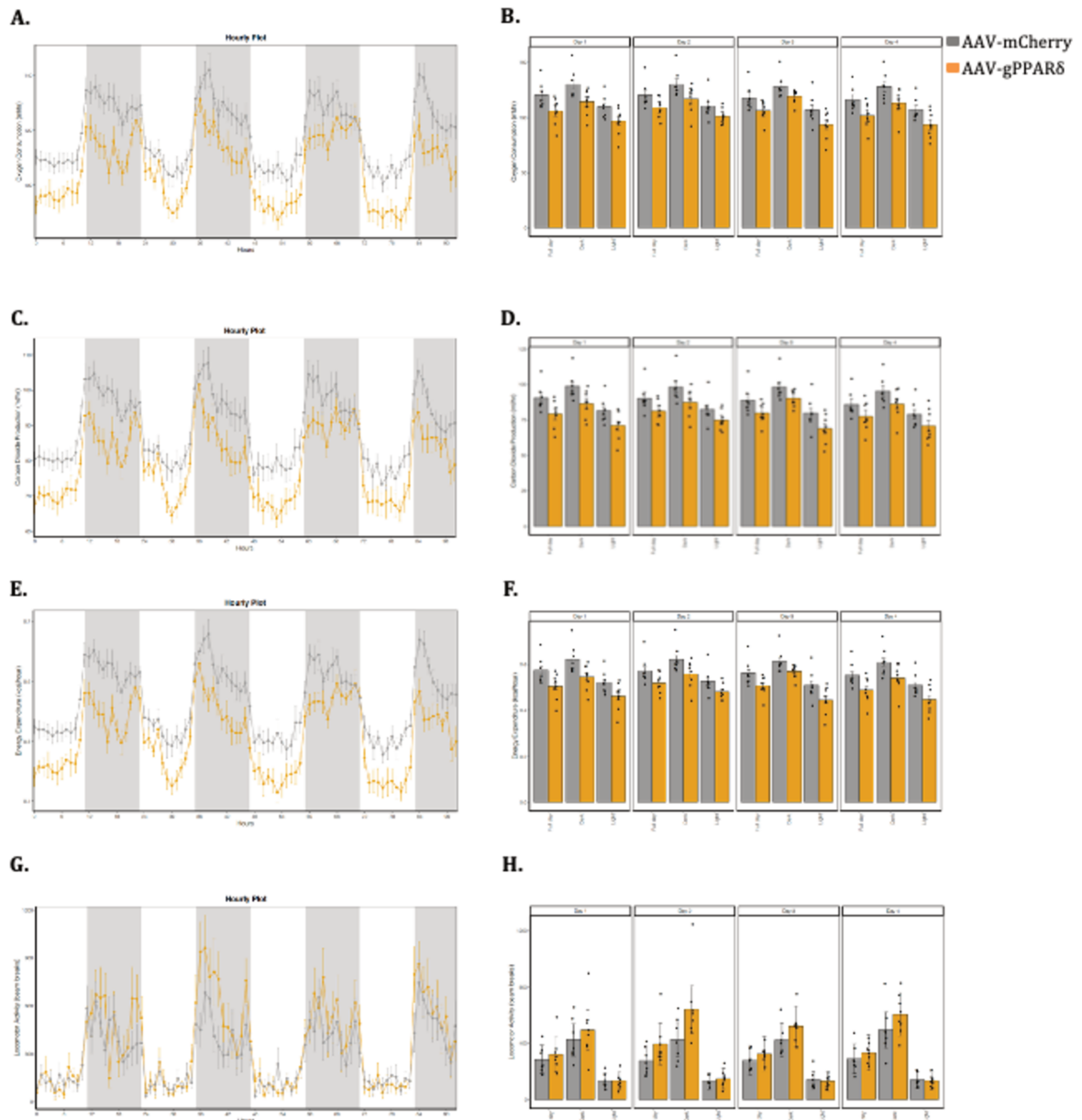


Figure 2. POMC-specific deletion of PPAR δ leads to discrete alterations on body composition and improves glucose homeostasis. (A) AAV-pU6-gRNAPPAR δ -EF1a-DIO-mCherry or AAV-DIO-mCherry was bilaterally injected into the ARC of POMC-cre::LSL-Cas9 mice. (B) Co-immunostaining of mCherry and PPAR δ . (C) Body weight. (D) Fat mass and (E) Lean mass. (F) Food intake of mice fed on HFD was measured twice a week. (G) 12 h feeding during the dark and light cycle. (H) Refeeding after 24 h of fasting. (D) Blood glucose levels after 6 h-fasting and (J) area under curve from blood glucose levels. N= 5-8, *p<0.05. ipGTT, intraperitoneal glucose tolerance test.



3. POMC-specific deletion of PPAR δ does not alter metabolic parameters at 22°C.

POMC-Cre::LSL-Cas9 mice submitted to an AAV injection into the ARC for PPAR δ deletion in POMC neurons and the respective control group were fed on HFD for 8 weeks. At the end of the experimental period mice were allocated into metabolic cages for metabolic phenotyping. (A) Real-time oxygen consumption and (B) quantification of oxygen consumption. (C) Real-time carbon dioxide production and (D) quantification of carbon dioxide production. (E) Real-time energy expenditure and (F) quantification of energy expenditure. (G) Real-time locomotor activity and (H) quantification of locomotor activity. N=7-8.

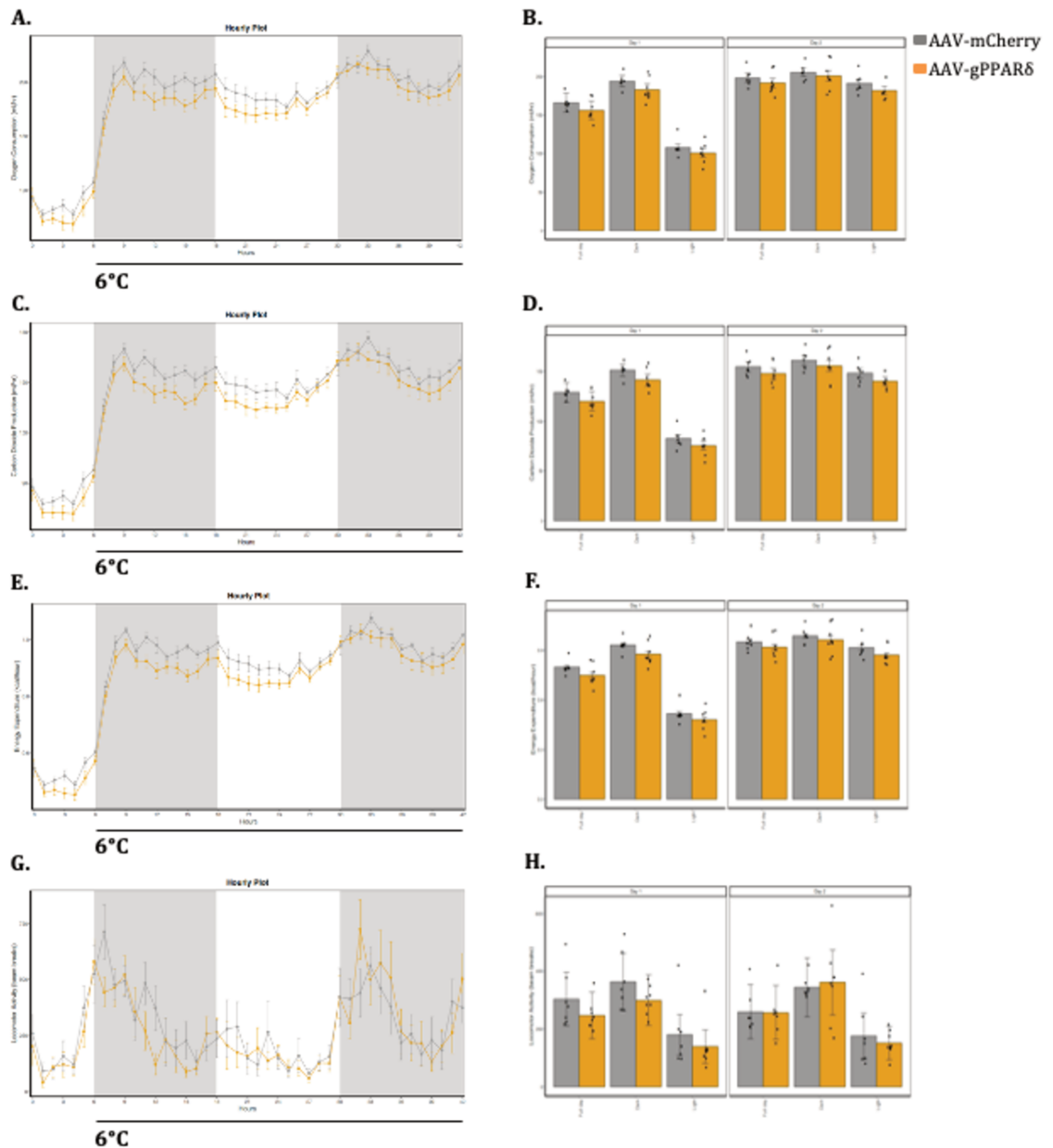


Figure 4. POMC-specific deletion of PPAR δ does not alter metabolic parameters at 6°C. POMC-Cre::LSL-Cas9 mice received an AAV injection into the ARC for PPAR δ deletion in POMC neurons and the respective control group were fed on HFD for 8 weeks. At the end of the experimental period mice were allocated into metabolic cages for metabolic phenotyping at 22°C and after 4 days, submitted to a cold-challenge experiment at 6°C for 36 h. (A) Real-time oxygen consumption and (B) quantification of oxygen consumption. (C) Real-time carbon dioxide production and (D) quantification of carbon dioxide production. (E) Real-time energy expenditure and (F) quantification of energy. (G) Real-time locomotor activity and (H) quantification of locomotor activity. N=7-8.

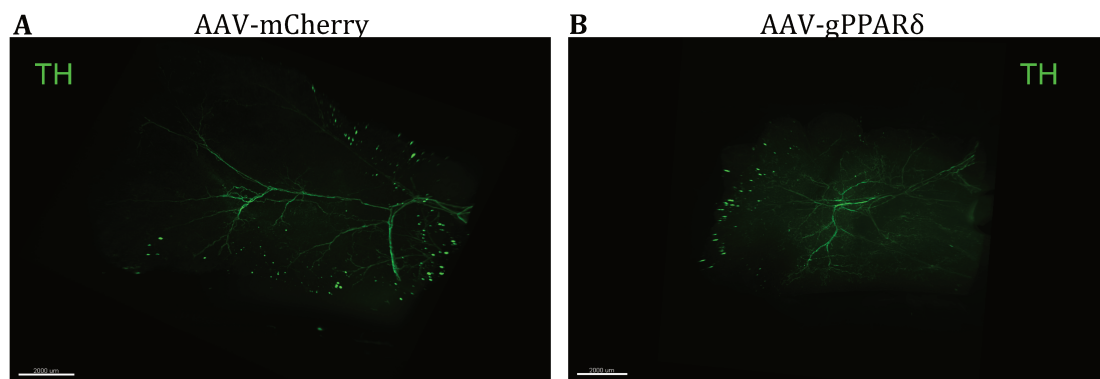


Figure 5. POMC-specific deletion of PPAR δ does not alter the sympathetic innervation of adipose tissue. TH immunolabeling in the epididymal fat depot from (A) control mice or (B) PPAR δ -deleted POMC neurons after 12 weeks on HFD. N=3. TH, tyrosine hydroxylase.

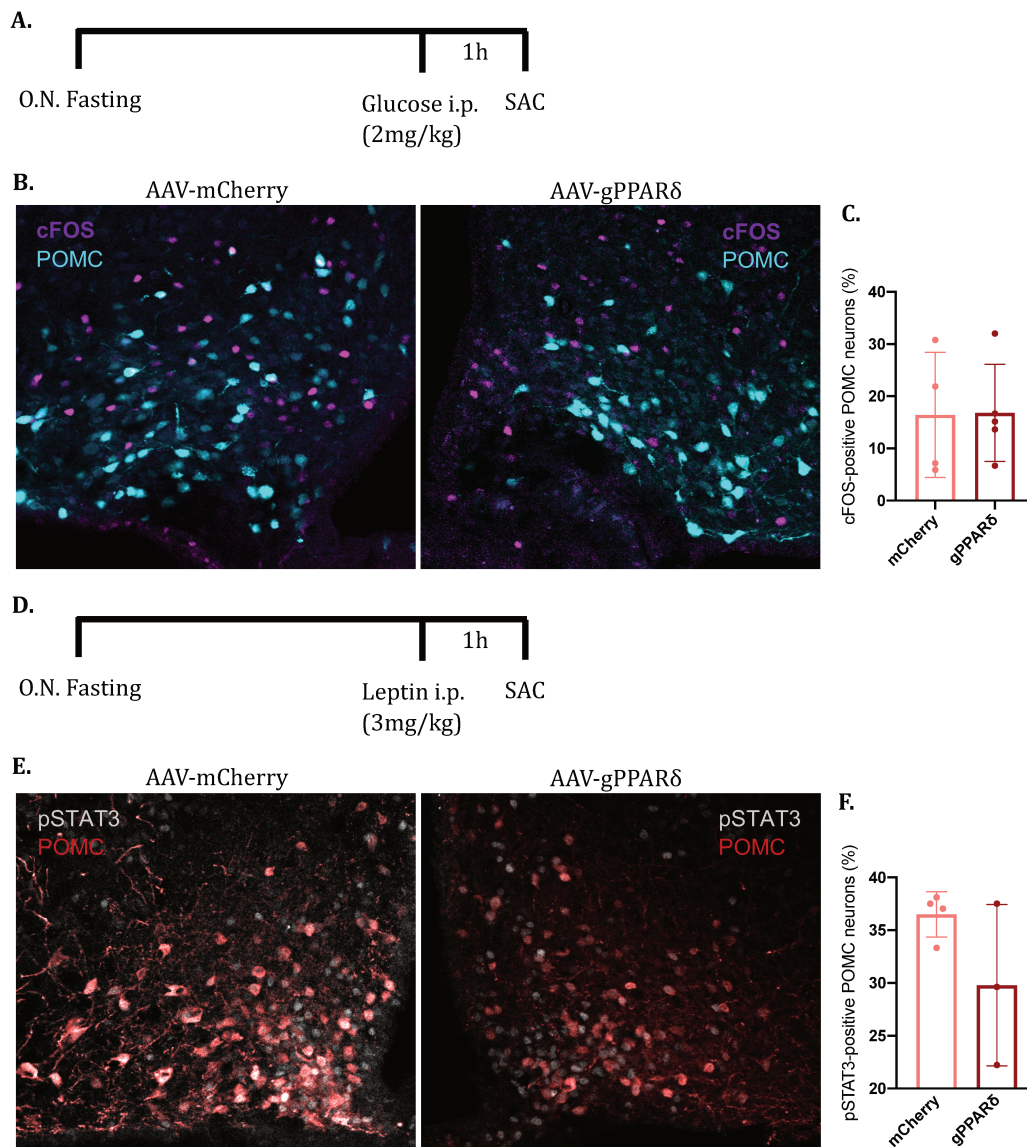


Figure 6. PPAR δ does not alter acute responses of POMC neurons to glucose and leptin. (A) Schematic of experimental strategy to assess glucose responsiveness. Representative confocal images of double labeling for (B) cFOS and POMC in the ARC of the hypothalamus of mice fed on HFD for 8 weeks and (C) the quantification of cFOS-positive POMC neurons in percentage. (D) Schematic of experimental strategy to assess leptin-associated signal in POMC neurons. (E) Representative confocal images of pSTAT3 expression in POMC neurons and (F) the quantification of pSTAT3-positive POMC neurons in percentage. N=3-4.

REFERENCES

1. Christofides A, Konstantinidou E, Jani C, Boussiotis VA. The role of peroxisome proliferator-activated receptors (PPAR) in immune responses. *Metabolism*. 2021;114.
2. Dubois V, Eeckhoutte J, Lefebvre P, Staels B. Distinct but complementary contributions of PPAR isotypes to energy homeostasis. *J Clin Invest*. 2017;127(4):1202–14.
3. Andrulionyte L, Peltola P, Chiasson JL, Laakso M. Single nucleotide polymorphisms of PPARD in combination with the Gly482Ser substitution of PGC-1A and the Pro12Ala substitution of PPARG2 predict the conversion from impaired glucose tolerance to type 2 diabetes: The STOP-NIDDM trial. *Diabetes*. 2006;55(7):2148–52.
4. Skogsberg J, Kannisto K, Cassel TN, Hamsten A, Eriksson P, Ehrenborg E. Evidence that peroxisome proliferator-activated receptor delta influences cholesterol metabolism in men. *Arterioscler Thromb Vasc Biol*. 2003;23(4):637–43.
5. Risérus U, Sprecher D, Johnson T, Olson E, Hirschberg S, Liu A, et al. Activation of peroxisome proliferator-activated receptor (PPAR) δ promotes reversal of multiple metabolic abnormalities, Reduces oxidative stress, and increases fatty acid oxidation in moderately obese men. *Diabetes*. 2008;57(2):332–9.
6. Moreno S, Farioli-vecchioli S, Cerù MP. Immunolocalization of peroxisome proliferator-activated receptors and retinoid X receptors in the adult rat CNS. *Neuroscience*. 2004;123(1):131–45.
7. Kocalis HE, Turney MK, Printz RL, Laryea GN, Muglia LJ, Davies SS, et al. Neuron-Specific Deletion of Peroxisome Proliferator- Activated Receptor Delta (PPAR d) in Mice Leads to Increased Susceptibility to Diet-Induced Obesity. 2012;7(8).
8. Warden A, Truitt J, Merriman M, Ponomareva O, Jameson K, Ferguson LB, et al. Localization of PPAR isotypes in the adult mouse and human brain. *Nat Publ Gr [Internet]*. 2016;(June):1–15.
9. Diano S, Liu Z, Jeong JK, Dietrich MO, Ruan H, Kim E, et al. Peroxisome proliferation – associated control of reactive oxygen species sets melanocortin

- tone and feeding in diet-induced obesity. 2011;17(9).
10. Rubinstein M, Low MJ. Molecular and functional genetics of the proopiomelanocortin gene, food intake regulation and obesity. *FEBS Lett.* 2017;591(17):2593–606.
 11. Moraes JC, Coope A, Morari J, Cintra DE, Roman E a., Pauli JR, et al. High-fat diet induces apoptosis of hypothalamic neurons. *PLoS One.* 2009;4(4).
 12. Yi CX, Walter M, Gao Y, Pitra S, Legutko B, Kälin S, et al. TNF α drives mitochondrial stress in POMC neurons in obesity. *Nat Commun.* 2017;8(May).
 13. Xu J, Bartolome CL, Low CS, Yi X, Chien CH, Wang P, et al. Genetic identification of leptin neural circuits in energy and glucose homeostases. *Nature.* 2018;556(7702):505–9.
 14. Friedman JM. Leptin and the endocrine control of energy balance. *Nat Metab.* 2019;1(8):754-64.
 15. Knight ZA, Hannan KS, Greenberg ML, Friedman JM. Hyperleptinemia is required for the development of leptin resistance. *PLoS One.* 2010;5(6):1–8.
 16. Zeng W, Pirzgalska RM, Pereira MMA, Kubasova N, Barateiro A, Seixas E, et al. Sympathetic Neuro-adipose Connections Mediate Leptin-Driven Lipolysis. *Cell* 2015;163(1):84–94.
 17. Wang P, Loh KH, Wu M, Morgan DA, Schneeberger M, Yu X, et al. A leptin–BDNF pathway regulating sympathetic innervation of adipose tissue. *Nature* . 2020;583(7818):839–44.
 18. Souza GFP, Solon C, Nascimento LF, Junior JCD-, Nogueira G, Moura R, et al. Defective regulation of POMC precedes hypothalamic inflammation in diet-induced obesity. *Sci Rep.* 2016;(October 2015):1–9.
 19. Parton LE, Ye CP, Coppari R, Enriori PJ, Choi B, Zhang C, et al. Glucose sensing by POMC neurons regulates glucose homeostasis and is impaired in obesity. 2007;449(September).
 20. Shadel GS, Horvath TL. Mitochondrial ROS Signaling in Organismal Homeostasis. *Cell.* 2015;163(3):560–9.
 21. Vázquez-carrera M. Unraveling the Effects of PPAR β / δ on Insulin Resistance and Cardiovascular Disease. *Trends Endocrinol Metab.* 2016;27(5):319–34.

22. Sznaidman ML, Haffner CD, Maloney PR, Fivush A, Chao E, Goreham D, et al. Novel selective small molecule agonists for peroxisome proliferator-activated receptor δ (PPAR δ) - Synthesis and biological activity. *Bioorganic Med Chem Lett*. 2003;13(9):1517–21.
23. Oliver WR, Shenk JL, Snaith MR, Russell CS, Plunket KD, Bodkin NL, et al. A selective peroxisome proliferator-activated receptor δ agonist promotes reverse cholesterol transport. *Proc Natl Acad Sci U S A*. 2001;98(9):5306–11.
24. Wang YX, Lee CH, Tjep S, Yu RT, Ham J, Kang H, et al. Peroxisome-proliferator-activated receptor δ activates fat metabolism to prevent obesity. *Cell*. 2003;113(2):159–70.
25. Tanaka T, Yamamoto J, Iwasaki S, Asaba H, Hamura H, Ikeda Y, et al. Activation of peroxisome proliferator-activated receptor δ induces fatty acid β -oxidation in skeletal muscle and attenuates metabolic syndrome. *Proc Natl Acad Sci U S A*. 2003;100(26):15924–9.
26. Toda C, Santoro A, Kim JD, Diano S. POMC Neurons: From Birth to Death. *Annu Rev Physiol*. 2017;79(1):209–36.
27. Berglund ED, Vianna CR, Donato J, Kim MH, Chuang JC, Lee CE, et al. Direct leptin action on POMC neurons regulates glucose homeostasis and hepatic insulin sensitivity in mice. *J Clin Invest*. 2012;122(3):1000–9.

CONCLUSÃO GERAL

Esta Tese caracterizou, de forma inédita, duas proteínas envolvidas na regulação de neurônios POMC no hipotálamo. Demonstramos que a proteína TRIL regula a resposta a estímulos inflamatórios e sua inibição em neurônios POMC reduz adiposidade e melhora a sensibilidade hipotalâmica à leptina. Demonstramos também que o receptor nuclear PPAR δ em neurônios POMC participa da regulação da tolerância sistêmica a glicose e da composição corporal. Assim, esta Tese promoveu avanço na caracterização mecanística da regulação hipotalâmica da homeostase energética e na fisiopatologia da obesidade induzida pelo consumo de dieta hiperlipídica.

REFERÊNCIAS

1. Bhupathiraju SN, Hu FB. Epidemiology of obesity and diabetes and their cardiovascular complications. *Circ Res*. 2016;118(11):1723–35.
2. Font-Burgada J, Sun B, Karin M. Obesity and Cancer: The Oil that Feeds the Flame. *Cell Metab* [Internet]. 2016;23(1):48–62.
3. Ortega FB, Lavie CJ, Blair SN. Obesity and cardiovascular disease. *Circ Res*. 2016;118(11):1752–70.
4. Blüher M. Metabolically healthy obesity. *Endocr Rev*. 2020;41(3):405–20.
5. Shulman GI. Ectopic Fat in Insulin Resistance, Dyslipidemia, and Cardiometabolic Disease. 2014;31:1131–41.
6. Blüher M. Obesity: global epidemiology and pathogenesis. *Nat Rev Endocrinol*. 2019;15(5):288–98.
7. Health Effects of Overweight and Obesity in 195 Countries over 25 Years. *N Engl J Med*. 2017;377(1):13–27.
8. IBGE IB de G e E. Pesquisa Nacional de Saúde [Internet]. 2020. 70 p. Available from: <https://biblioteca.ibge.gov.br/visualizacao/livros/liv101758.pdf>
9. Locke AE, Kahali B, Berndt SI, Justice AE, Pers TH, Day FR, et al. Genetic studies of body mass index yield new insights for obesity biology. *Nature*. 2015;518(7538):197–206.
10. Akiyama M, Okada Y, Kanai M, Takahashi A, Momozawa Y, Ikeda M, et al. Genome-wide association study identifies 112 new loci for body mass index in the Japanese population. *Nat Genet*. 2017;49(10):1458–67.
11. Speakman JR. Thrifty genes for obesity, an attractive but flawed idea, and an alternative perspective: The “drifty gene” hypothesis. *Int J Obes*. 2008;32(11):1611–7.
12. Hall KD, Guo J. Obesity Energetics: Body Weight Regulation and the Effects of Diet Composition. *Gastroenterology* [Internet]. 2017;152(7):1718-1727.e3. Available from: <http://dx.doi.org/10.1053/j.gastro.2017.01.052>
13. Hall KD. Did the Food Environment Cause the Obesity Epidemic? *Obesity*. 2018;26(1):11–3.
14. Hall KD, Guo J, Courville AB, Boring J, Brychta R, Chen KY, et al. Effect of a plant-based, low-fat diet versus an animal-based, ketogenic diet on ad libitum energy intake. *Nat Med* [Internet]. 2021;27(February). Available from: <http://dx.doi.org/10.1038/s41591-020-01209-1>
15. Kroemer G, López-Otín C, Madeo F, de Cabo R. Carbotoxicity—Noxious Effects of Carbohydrates. *Cell*. 2018;175(3):605–14.
16. Lottenberg AM, Afonso MDS, Lavrador MSF, Machado RM, Nakandakare ER. The role of dietary fatty acids in the pathology of metabolic syndrome. *J Nutr Biochem* [Internet]. 2012;23(9):1027–40.
17. Itani SI, Ruderman NB, Schmieder F, Boden G. Lipid-induced insulin resistance in human muscle is associated with changes in diacylglycerol, protein kinase C, and I κ B α . *Diabetes*. 2002;51(7):2005–11.
18. Valdearcos M, Robblee MM, Xu AW, Koliwad SK, Valdearcos M, Robblee MM, et al.

- Microglia Dictate the Impact of Saturated Fat Consumption on Hypothalamic Inflammation and Neuronal Function Article Microglia Dictate the Impact of Saturated Fat Consumption on Hypothalamic Inflammation and Neuronal Function. *CellReports* [Internet]. 2014;9(6):2124–38.
19. Robblee MM, Kim CC, Abate JP, Valdearcos M, Sandlund KLM, Shenoy MK, et al. Saturated Fatty Acids Engage an IRE1 α -Dependent Pathway to Activate the NLRP3 Inflammasome in Myeloid Cells. *Cell Rep* [Internet]. 2016;14(11):2611–23.
 20. Milanski M, Degasperi G, Coope A, Morari J, Denis R, Cintra DE, et al. Saturated fatty acids produce an inflammatory response predominantly through the activation of TLR4 signaling in hypothalamus: implications for the pathogenesis of obesity. *J Neurosci*. 2009;29(2):359–70.
 21. Shi H, Kokoeva M V, Inouye K, Tzameli I, Yin H, Flier JS. TLR4 links innate immunity and fatty acid – induced insulin resistance. *J Clin Invest*. 2006;116(11):3015–25.
 22. Hotamisligil G, Shargill N, Spiegelman B. Adipose Expression of Tumor Necrosis Factor α : Direct Role in Obesity-Linked Insulin Resistance. *Science* (80-) [Internet]. 1993;259(5091):87–91.
 23. Akira S, Takeda K, Kaisho T. Toll-like receptors : critical proteins linking innate and acquired immunity. *Nat Immunol*. 2001;2(8):675–80.
 24. Akira S. Toll-like receptor signaling. *J Biol Chem*. 2003;278(40):38105–8.
 25. Takeuchi O, Akira S. Pattern Recognition Receptors and Inflammation. *Cell* [Internet]. 2010;140(6):805–20.
 26. Velloso L a, Schwartz MW. Altered hypothalamic function in diet-induced obesity. *Int J Obes* [Internet]. 2011;35(12):1455–65.
 27. Gribble FM, Reimann F. Function and mechanisms of enteroendocrine cells and gut hormones in metabolism. *Nat Rev Endocrinol* [Internet]. 2019;15(4):226–37.
 28. Moura-assis A, Friedman JM, Velloso LA. Gut-to-brain signals in feeding control. 2021;1(November 2020):3–9.
 29. Bai L, Mesgarzadeh S, Ramesh KS, Zeng H, Krasnow MA, Knight ZA. Genetic Identification of Vagal Sensory Neurons That Article Genetic Identification of Vagal Sensory Neurons That Control Feeding. *Cell*. 2019;179(5):1129-1143.e23.
 30. Roman CW, Derkach VA, Palmiter RD. Genetically and functionally defined NTS to PBN brain circuits mediating anorexia. *Nat Commun*. 2016;7(May):1–11.
 31. Garfield AS, Shah BP, Madara JC, Burke LK, Patterson CM, Flak J, et al. A parabrachial-hypothalamic cholecystokinin neurocircuit controls counterregulatory responses to hypoglycemia. *Cell Metab* [Internet]. 2014;20(6):1030–7.
 32. Agostino GD, Lyons DJ, Cristiano C, Burke LK, Madara JC, Campbell JN, et al. Appetite controlled by a cholecystokinin nucleus of the solitary tract to hypothalamus neurocircuit. 2016;1–15.
 33. Gaykema RP, Newmyer BA, Ottolini M, Raje V, Warthen DM, Lambeth PS, et al. Activation of murine pre-proglucagon-producing neurons reduces food intake and body weight. *J Clin Invest*. 2017;127(3):1031–45.
 34. Friedman JM. Leptin and the endocrine control of energy balance. *Nat Metab*.

35. Zeng W, Pirzgalska RM, Pereira MM a, Martins GG, Friedman JM, Domingos Correspondence AI, et al. Sympathetic Neuro-adipose Connections Mediate Leptin-Driven Lipolysis Optogenetic activation of sympathetic fibers in fat drives lipolysis and fat mass reduction Sympathetic Neuro-adipose Connections Mediate Leptin-Driven Lipolysis. *Cell* [Internet]. 2015;163(1):84–94.
36. Wang P, Loh KH, Wu M, Morgan DA, Schneeberger M, Yu X, et al. A leptin–BDNF pathway regulating sympathetic innervation of adipose tissue. *Nature* [Internet]. 2020;583(7818):839–44.
37. Toda C, Santoro A, Kim JD, Diano S. POMC Neurons: From Birth to Death. *Annu Rev Physiol* [Internet]. 2017;79(1):209–36.
38. Andermann ML, Lowell BB. Toward a Wiring Diagram Understanding of Appetite Control. *Neuron* [Internet]. 2017;95(4):757–78.
39. Wang Q, Liu C, Uchida A, Chuang JC, Walker A, Liu T, et al. Arcuate AgRP neurons mediate orexigenic and glucoregulatory actions of ghrelin. *Mol Metab* [Internet]. 2014;3(1):64–72.
40. Balthasar N, Coppari R, Mcminn J, Liu SM, Lee CE, Tang V, et al. Leptin Receptor Signaling in POMC Neurons Is Required for Normal Body Weight Homeostasis. 2004;42:983–91.
41. Caron A, Lemko HMD, Castorena CM, Fujikawa T, Lee S, Lord CC, et al. POMC neurons expressing leptin receptors coordinate metabolic responses to fasting via suppression of leptin levels. *Elife*. 2018;7:1–18.
42. Xu J, Bartolome CL, Low CS, Yi X, Chien CH, Wang P, et al. Genetic identification of leptin neural circuits in energy and glucose homeostases. *Nature* [Internet]. 2018;556(7702):505–9.
43. Zhu C, Jiang Z, Xu Y, Cai ZL, Jiang Q, Xu Y, et al. Profound and redundant functions of arcuate neurons in obesity development. *Nat Metab*. 2020;2(8):763–74.
44. Aponte Y, Atasoy D, Sternson SM. AGRP neurons are sufficient to orchestrate feeding behavior rapidly and without training. *Nat Neurosci* [Internet]. 2011;14(3):351–5.
45. Fenselau H, Campbell JN, Verstegen AMJ, Madara JC, Xu J, Shah BP, et al. A rapidly acting glutamatergic ARC→PVH satiety circuit postsynaptically regulated by α -MSH. *Nat Neurosci*. 2017;20(1):42–51.
46. Chen Y, Knight ZA. Making sense of the sensory regulation of hunger neurons. 2016;38(4):316–24.
47. Chen Y, Lin YC, Kuo TW, Knight ZA. Sensory Detection of Food Rapidly Modulates Arcuate Feeding Circuits. *Cell*. 2015;160(5):829–41.
48. Betley JN, Xu S, Fang Z, Cao H, Gong R, Magnus CJ, et al. Neurons for hunger and thirst transmit a negative-valence teaching signal. 2015;
49. Mandelblat-Cerf Y, Ramesh RN, Burgess CR, Patella P, Yang Z, Lowell BB, et al. Arcuate hypothalamic AgRP and putative pomc neurons show opposite changes in spiking across multiple timescales. *Elife*. 2015;4(JULY 2015):1–25.
50. Mazzone CM, Liang-Guallpa J, Li C, Wolcott NS, Boone MH, Southern M, et al. High-fat food biases hypothalamic and mesolimbic expression of consummatory drives. *Nat Neurosci* [Internet]. 2020;9

51. Beutler LR, Corpuz T V., Ahn JS, Kosar S, Song W, Chen Y, et al. Obesity causes selective and long-lasting desensitization of AgRP neurons to dietary fat. *Elife*. 2020;9:1–21.
52. Nascimento LFR, Souza GFP, Signaling C, Biology C, Lav B, Signaling C. Omega-3 fatty acids induce neurogenesis of predominantly POMC- expressing cells in the hypothalamus. 2015;1–33.
53. Razolli DS, Moura-Assis A, Bombassaro B, Velloso LA. Hypothalamic neuronal cellular and subcellular abnormalities in experimental obesity. *Int J Obes [Internet]*. 2019;43(12):2361–9.
54. Moraes JC, Coope A, Morari J, Cintra DE, Roman E a., Pauli JR, et al. High-fat diet induces apoptosis of hypothalamic neurons. *PLoS One*. 2009;4(4).
55. Souza GFP, Solon C, Nascimento LF, Junior JCD-, Nogueira G, Moura R, et al. Defective regulation of POMC precedes hypothalamic inflammation in diet-induced obesity. *Nat Publ Gr [Internet]*. 2016;(October 2015):1–9.
56. Yi CX, Walter M, Gao Y, Pitra S, Legutko B, Kälin S, et al. TNF α drives mitochondrial stress in POMC neurons in obesity. *Nat Commun*. 2017;8(May).
57. Schneeberger M, Dietrich MO, Sebastia D, Garcia A, Esteban Y, Gonzalez-franquesa A, et al. Mitofusin 2 in POMC Neurons Connects ER Stress with Leptin Resistance and Energy Imbalance. 2012;
58. Kim GH, Shi G, Somlo DRM, Haataja L, Song S, Long Q, et al. Hypothalamic ER-associated degradation regulates POMC maturation, feeding, and age-associated obesity. *J Clin Invest*. 2018;128(3):1125–40.
59. Nasrallah CM, Horvath TL. Mitochondrial dynamics in the central regulation of metabolism. *Nat Rev Endocrinol [Internet]*. 2014;10(11):650–8.
60. Parton LE, Ye CP, Coppari R, Enriori PJ, Choi B, Zhang C, et al. Glucose sensing by POMC neurons regulates glucose homeostasis and is impaired in obesity. 2007;449(September).
61. Horvath TL, Andrews ZB, Diano S. Fuel utilization by hypothalamic neurons : roles for ROS. 2008;(December).
62. Long L, Toda C, Jeong JK, Horvath TL, Diano S. PPAR γ ablation sensitizes proopiomelanocortin neurons to leptin during high-fat feeding. *J Clin Invest [Internet]*. 2014;124(124(9)):1–11.

ANEXOS

Anexo 1. Autorização para transferência de OGM proveniente do Laboratório de Neuroanatomia do ICB/USP para o Laboratório de Sinalização Celular da FCM/UNICAMP



LABORATÓRIO DE SINALIZAÇÃO CELULAR

Centro de Pesquisa em Obesidade e Comorbidade
Rua: Carl von Lennéus s/nº
CEP 13083-864
Tel-(19)3521-0026
Lavelloso.unicamp@gmail.com

Cidade Universitária "Zeferino Vaz", 10 de Agosto de 2018.

Prof. Dr. Enrique Mario Boccardo Pirulivo
Presidente da CIBio
ICB/USP

Assunto: Transferência de OGM

Eu, **Lício Augusto Velloso** na qualidade de Pesquisador principal do projeto "Avaliação da proteína TRIL na inflamação e apoptose de neurônios POMC – CIBio/FCM003/2018", aprovado junto à CIBio da Faculdade de Ciências Médicas da UNICAMP, de **CQB número 072/98**, solicito a liberação dos animais geneticamente modificados (OGM) listados abaixo para sua utilização em nossas instalações em regime de contenção de acordo com as instruções da CTNBio.

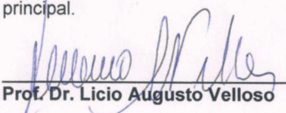
I-Tg POMC1-cre16Low/J
II-Agrp^{tm1(cre)Low/J}

20 animais de cada linhagem (I e II), sexo masculino, com 05 semanas de idade provenientes do Biotério do Laboratório de Neuroanatomia

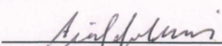
Este documento indica a ciência e autorização de ambas as CIBios para retirada dos OGMs citados que serão transferidos do ICB/USP, CQB0046/98 para a responsabilidade da CIBio da Faculdade de Ciências Médicas da UNICAMP, CQB 072/98, destinatária.

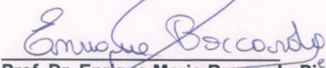
Assumo que o transporte será realizado de acordo com **Instrução normativa CTNBio número 4 de 19/12/1996 – item 6 e item 13**, e o sistema de contenção será cumprido dentro da **Instrução normativa CTNBio**.

Tenho consciência de que os animais só sairão do Biotério do Instituto de Ciências Biomédicas - USP em caixa, de polipropileno, identificados corretamente e transporte adequado e mediante a entrega deste documento devidamente assinado por ambas as CIBios envolvidas na transferência e pelo pesquisador principal.


Prof. Dr. Lício Augusto Velloso

Cientes,


Prof. Dr. Arjibal Vercesi
Presidente da CIBio/FCM-UNICAMP
CQB 0072/98


Prof. Dr. Enrique Mario Boccardo Pirulivo
Presidente da CIBio/ICB-USO
CQB 0046/98

Anexo 2. Certificado de aprovação do projeto pela Comissão de Ética no Uso de Animais (UNICAMP) - I



CEUA/UNICAMP

CERTIFICADO

Certificamos que a proposta intitulada Avaliação da proteína TRIL no hipotálamo de camundongos Swiss com obesidade induzida por dieta e seu efeito na inflamação e apoptose de neurônios POMC, registrada com o nº 4069-1(A), sob a responsabilidade de Prof. Dr. Lício Augusto Velloso / Alexandre Moura Assis, que envolve a produção, manutenção ou utilização de animais pertencentes ao filo *Chordata*, subfilo *Vertebrata* (exceto o homem) para fins de pesquisa científica (ou ensino), encontra-se de acordo com os preceitos da **LEI Nº 11.794, DE 8 DE OUTUBRO DE 2008**, que estabelece procedimentos para o uso científico de animais, do **DECRETO Nº 6.899, DE 15 DE JULHO DE 2009**, e com as normas editadas pelo **Conselho Nacional de Controle da Experimentação Animal (CONCEA)**, tendo sido aprovada pela **Comissão de Ética no Uso de Animais da Universidade Estadual de Campinas - CEUA/UNICAMP**, em reunião de 1º de agosto de 2016.

Finalidade:	() Ensino (X) Pesquisa Científica
Vigência do projeto:	05/09/2016-01/10/2019
Vigência da autorização para manipulação animal:	05/09/2016-01/10/2019
Espécie / linhagem/ raça:	Camundongo isogênico / C57BL/6
No. de animais:	728
Peso / Idade:	04 semanas / 20g
Sexo:	machos
Origem:	CEMIB/UNICAMP

A aprovação pela CEUA/UNICAMP não dispensa autorização prévia junto ao **IBAMA**, **SISBIO** ou **CIBio**.

Campinas, 1º de agosto de 2016.

Profa. Dra. Liana Maria Cardoso Verinaud
Presidente

Fátima Alonso
Secretária Executiva

IMPORTANTE: Pedimos atenção ao prazo para envio do relatório final de atividades referente a este protocolo: até 30 dias após o encerramento de sua vigência. O formulário encontra-se disponível na página da CEUA/UNICAMP, área do pesquisador responsável. A não apresentação de relatório no prazo estabelecido impedirá que novos protocolos sejam submetidos.

Anexo 3. Certificado de aprovação do projeto pela Comissão de Ética no Uso de Animais da UNICAMP - II



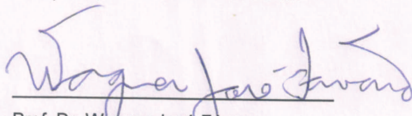
CERTIFICADO

Certificamos que a proposta intitulada **Avaliação da proteína TRIL na inflamação hipotalâmica em camundongos com obesidade induzida por dieta**, registrada com o nº **4985-1/2018**, sob a responsabilidade de **Prof. Dr. Lício Augusto Velloso e Alexandre Moura Assis**, que envolve a produção, manutenção ou utilização de animais pertencentes ao filo *Chordata*, subfilo *Vertebrata* (exceto o homem) para fins de pesquisa científica (ou ensino), encontra-se de acordo com os preceitos da **LEI Nº 11.794, DE 8 DE OUTUBRO DE 2008**, que estabelece procedimentos para o uso científico de animais, do **DECRETO Nº 6.899, DE 15 DE JULHO DE 2009**, e com as normas editadas pelo **Conselho Nacional de Controle da Experimentação Animal (CONCEA)**, tendo sido aprovada pela **Comissão de Ética no Uso de Animais da Universidade Estadual de Campinas - CEUA/UNICAMP**, em **26 de outubro de 2018**.

Finalidade:	() Ensino (X) Pesquisa Científica
Vigência do projeto:	10/09/2018-01/03/2020
Vigência da autorização para manipulação animal:	26/10/2018-01/03/2020
Espécie / linhagem/ raça:	Camundongo transgênico / Tg POMC1-cre16Low/J
No. de animais:	20
Idade/Peso:	04 semanas / 20g
Sexo:	machos
Espécie / linhagem/ raça:	Camundongo transgênico / Agrptm1(cre)Low/J
No. de animais:	20
Idade/Peso:	04 semanas / 20g
Sexo:	machos
Origem:	Biotério do Laboratório de Neuroanatomia, Localização Instituto de Ciências Biomédicas II - USP
Biotério onde serão mantidos os animais:	Biotério do Laboratório de Sinalização Celular, NMCE, FCM/UNICAMP

A aprovação pela CEUA/UNICAMP não dispensa autorização prévia junto ao **IBAMA**, **SISBIO** ou **CIBio** e é **restrita** a protocolos desenvolvidos em biotérios e laboratórios da Universidade Estadual de Campinas.

Campinas, 26 de outubro de 2018.


 Prof. Dr. Wagner José Favaro
 Presidente


 Fátima Alonso
 Secretária Executiva

IMPORTANTE: Pedimos atenção ao prazo para envio do relatório final de atividades referente a este protocolo: até 30 dias após o encerramento de sua vigência. O formulário encontra-se disponível na página da CEUA/UNICAMP, área do pesquisador responsável. A não apresentação de relatório no prazo estabelecido impedirá que novos protocolos sejam submetidos.

Anexo 4. Política editorial da American Physiology Society (APS), concedendo permissão aos autores para reprodução integral de seus artigos em suas teses e dissertações sem requisitar permissão.

Reuse by Authors of Their Work Published by APS

The APS Journals are copyrighted for the protection of authors and the Society. The Mandatory Submission Form serves as the Society's official copyright transfer form. Author's rights to reuse their APS-published work are described below:

Republication in New Works	Authors may republish parts of their final-published work (e.g., figures, tables), without charge and without requesting permission, provided that full citation of the source is given in the new work.
Meeting Presentations and Conferences	Authors may use their work (in whole or in part) for presentations (e.g., at meetings and conferences). These presentations may be reproduced on any type of media in materials arising from the meeting or conference such as the proceedings of a meeting or conference. A copyright fee will apply if there is a charge to the user or if the materials arising are directly or indirectly commercially supported ¹ . Full citation is required.
Theses and Dissertations	Authors may reproduce whole published articles in dissertations and post to thesis repositories without charge and without requesting permission. Full citation is required.

Anexo 5. Artigo de revisão publicado como parte das atividades desenvolvidas na UNICAMP e na Rockefeller University durante o doutorado.

Am J Physiol Endocrinol Metab 320: E326–E332, 2021.
First published December 7, 2020; doi:10.1152/ajp-endo.00388.2020



AMERICAN JOURNAL OF PHYSIOLOGY
**ENDOCRINOLOGY
AND METABOLISM.**

MINI-REVIEW

Gut-to-brain signals in feeding control

Alexandre Moura-Assis,^{1,2} Jeffrey M. Friedman,^{2,3} and Ucio A. Velloso¹

¹Laboratory of Cell Signaling, Obesity and Comorbidity Research Center, State University of Campinas, Campinas, Brazil;

²Laboratory of Molecular Genetics, The Rockefeller University, New York, New York; and ³Howard Hughes Medical Institute, New York, New York

Abstract

Interoceptive signals from gut and adipose tissue and sensory cues from the environment are integrated by hubs in the brain to regulate feeding behavior and maintain homeostatic control of body weight. In vivo neural recordings have revealed that these signals control the activity of multiple layers of hunger neurons and eating is not only the result of feedback correction to a set point, but can also be under the influence of anticipatory regulations. A series of recent technical developments have revealed how peripheral and sensory signals, in particular, from the gut are conveyed to the brain to integrate neural circuits. Here, we describe the mechanisms involved in gastrointestinal stimulation by nutrients and how these signals act on the hindbrain to generate motivated behaviors. We also consider the organization of multidirectional intra- and extrahypothalamic circuits and how this has created a framework for understanding neural control of feeding.

feeding; gut-to-brain; hypothalamus

INTRODUCTION

Gut vagal terminals act as polymodal sensors of gastrointestinal (GI) content responding to stimuli, such as stretching, osmolarity, pH, and nutrients, and connecting with the brain in order to elicit energy homeostatic responses (1, 2). Vagal afferent nerve terminals are anatomically distributed in different layers of the GI tract, as shown in Fig. 1. Intraganglionic luminal endings (IGLEs) act as mechanoreceptors, sensing GI stretching, whereas vagal mucosal endings can sense chemical stimuli. A large heterogeneous group of nerve terminals also express receptors for enteroendocrine hormones and their activation, in part by mechanosensing, generates signals that can regulate food intake (3). These diverse afferent signals are processed by the nodose ganglia (NG) that contains the cell bodies of ~2,300 neurons (4) comprising the vagal afferent system and conveys the chemical and mechanical information from the GI tract (and other organs) to the nucleus of the solitary tract (NTS) and area postrema (AP) in the hindbrain. NTS neurons integrate the information and in turn excite other hindbrain regions, such as the parabrachial nucleus (PBN), which in turn project broadly to higher centers in the brain.

Recent studies have also reshaped our understanding about the roles of hypothalamic neurons, revealing that they function primarily as interoceptive sensors of hormone levels that reflect the milieu interne that can be further modulated by sensory cues that modulate their firing (5). The identification of these novel intra- and extrahypothalamic populations has elucidated how the central nervous system adjusts food

consumption and energy expenditure to maintain energy homeostasis.

In this mini-review, we describe recent advances obtained from mouse studies in the characterization of GI-brain connections involved in the regulation of appetite and also the neuronal networks integrating hypothalamic and extrahypothalamic signals.

THE ASCENDING PATHWAY FOR FEEDING CONTROL

The enteroendocrine cells in the gut are equipped with an array of nutrient, chemical, and mechanical sensors and influence food digestion and appetite by releasing a plethora of hormones (6). A new identified class of epithelial cells in the colon and small intestine, termed neuropod cells, release glutamate in response to a sugar stimulus and synapse with vagal neurons, suggesting a new mechanism by which a luminal stimulus is rapidly conveyed to the brain (7).

Recent genetic mapping, anatomical tracing, and optogenetic activation of different nodes of afferent vagal neurons have defined their neurochemical phenotypes and effects on feeding behavior. The role of *Gpr65*- and *Glipr*-expressing vagal neurons was extensively explored after the identification of G protein-coupled receptors (GPCRs) in distinct vagal afferents. The *Gpr65*-expressing vagal neurons were found in mucosal-ending terminals, mainly in duodenal villi, and *Glipr*-expressing afferents were identified in IGLEs in the stomach muscle. Interestingly, in vivo calcium image (GCaMP3) in nodose ganglia of the respective *Cre*-knockin

Correspondence: A. Moura-Assis (amoura@odrive/ro.unicamp.br).

Submitted 29 July 2020 / Revised 9 November 2020 / Accepted 23 November 2020

E326

0193-1849/21 Copyright © 2021 the American Physiological Society

<http://www.ajpendo.org>

Downloaded from journals.physiology.org/journal/ajpendo at Yale Univ (130.132.173.180) on February 5, 2021.

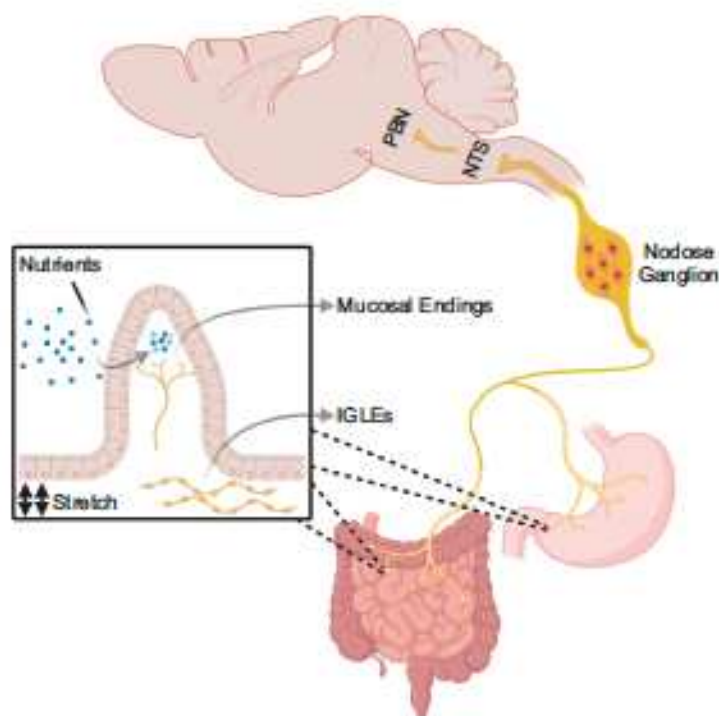


Figure 1. Vagal afferent neurons. The gastrointestinal tract is densely innervated by the vagus nerve and its mucosal endings acts as chemosensory terminals detecting nutrients and hormones, whereas the IGLEs are anatomically concentrated in muscle layers and detect gastrointestinal stretch. The cell bodies of the afferent fibers are located in the nodose ganglion and the signals from their terminals are relayed to the NTS. The PBN, in turn, receives ascending inputs from the NTS and coordinates meal termination. IGLEs, intraganglionic laminar endings; NTS, nucleus tractus solitarius; PBN, parabrachial nucleus.

mice showed that GPR65 neurons are responsive to nutrients in the intestinal lumen whereas GLP1R neurons in nodose respond to gastrointestinal distension but not to GLP1 (8).

A recent study evaluated the putative appetite-suppressant role of afferent vagal neurons. The genetic characterization of vagal sensory neurons as revealed by single-cell RNA sequence (sc-RNAseq) of GI-targeted afferent neurons identified 12 clusters; eight of them expressing unique markers: *Oxtr*⁺, *Olf78*⁺, *Npasla*⁺, *Sst*⁺, *Calca*⁺, *Vip*⁺/*Utsb2b*⁺, *Prom1*⁺, and *Edn3*⁺. However, considering that the vagus nerve innervates most organs in the thoracic and abdominal cavities, it is worth mentioning that none of these unique genetic markers have been confirmed to exclusively innervate the gut. Following a GI tract-nodose ganglia neuronal retrograde tracing, the authors identified *Vip*⁺- and *Gpr65*⁺-expressing neurons in mucosal-endings and *Oxtr*⁺- and *Glp1r*⁺-expressing neurons in IGLEs. Surprisingly, only IGLE-targeted neurons (*Oxtr*⁺ and *Glp1r*⁺) inhibited food intake after optogenetic (ChR2) and chemogenetic (hM3D) activation; however, these findings do not rule out the role of chemosensing on feeding control. Mechanosensing signaling triggered by *Oxtr*⁺-expressing vagal neurons activated tyrosine hydroxylase (*Th*)-expressing neurons in the NTS, calcitonin (*Calc*)-expressing neurons localized in the external lateral parabrachial nucleus (PBNel), and another neuronal population in the dorsal lateral parabrachial nucleus (PBNdl) (9). In addition, signaling by mechanosensing vagal afferents to the hindbrain through the nodose ganglion also led to the identification of neurons in the PBN that express

prodynorphin (PBN^{dyn}) that are responsive to liquid and solid food consumption (10). Two-photon calcium imaging demonstrated rapid and reversible activation of PBN^{dyn} neurons upon gastric distension with an appetite-suppressing effect after chemogenetic activation of PBN^{dyn} neurons, suggesting that these neurons might be components of a rapid anorexigenic feedback response to avoid overconsumption. Interestingly, the synaptic inputs shown by tracing experiments demonstrated connections between NTS regions that receive oral and oropharyngeal sensory information and, consistently, the PBN^{dyn} neurons were rapidly activated by tongue and esophagus sensation from a gavage needle (10). The cocaine- and amphetamine-regulated transcript (CART), which is co-released with pro-opiomelanocortin (POMC) in neurons in the arcuate nucleus (ARC) of the hypothalamus, also plays a role in the gut-brain axis (11). The NG, in particular the right NG, expresses CART peptide and its release into the NTS is necessary to inhibit food intake (11).

Gut-innervating sensory vagal afferents have also been implicated as having roles in the transmission of reward signals to the brain. Han et al. (12) have shown that the selective activation of the right NG, but not the left NG, produced reward-like behaviors. Because the right NG neurons do not project directly to the substantia nigra (SNc), which in turn release dopamine onto dorsal striatum (DS) neurons producing behavioral reinforcement, the authors found that the increased dopamine release in the DS after optogenetic activation of the right NG is mediated by the circuit NTS-PBNdl-

SNe (12). Interestingly, another work has recently shown that vagal sensory neurons are responsive to intestinal sugar and are implicated in the development of preference for sugar. The activation of vagal sensory neurons by sugar is dependent on the sodium-glucose-linked transporter-1 (SGLT1) expressed in enterocytes and endocrine cells in the gut, as its pharmacological inhibition abrogated the vagal activation (13).

As a gateway for ascending information from the GI tract, the NTS is at the intersection of the central nervous system and digestive system and its activity is controlled by a number of different neuropeptides and neuromodulators. Feeding results in rapid activation of cholecystoldin (Cck)-expressing neurons in NTS (NTS^{CCK}) (14). NTS^{CCK} circuit mapping showed that calcitonin gene-related peptide (CGRP)-expressing neurons in the lateral parabrachial nucleus (LPBN^{CGRP}) (14) and melanocortin-4 receptor (MC4R)-expressing neurons in the paraventricular hypothalamus (PVH) (14) are potential downstream mediators of the anorexigenic effects of NTS^{CCK} activation. It was recently shown that calcitonin receptor-expressing neurons in NTS (NTS^{CalcR}) (15), which do not overlap with NTS^{CCK}, mediates nonaversive suppression of food intake, as mice consumed more of the flavor paired with the activation of NTS^{CalcR} in a two-flavor preference assay. The NTS^{CalcR} suppress food intake via projections to a PBN node yet to be identified but do not project to LPBN^{CGRP}, which mediates feeding aversion in response to GI malaise (15). The visceral malaise is also associated with increased levels of growth differentiation factor 15 (GDF15), a potent anorectic factor implicated in the cancer-associated cachexia (16, 17). Recent studies have reported that the anorectic effects of GDF15 are mediated through GDNF-family receptor- α -like (GFRAL), which is expressed exclusively in the AP and NTS (18–20). Further neurochemical characterization of GFRAL expression has demonstrated that the majority of GFRAL neurons are CCK-positive and the deletion of CCK in the AP and NTS significantly reduces the anorectic effects of GDF15 (21). Interestingly, the administration of recombinant GDF15 results in an aversive response pattern to flavored food (22).

Because many of the identified NTS neuronal types comprise of key circuits for satiation, some antiobesity drugs may influence feeding through this node. In concert, it was recently shown that the antiobesity effects of lorcaserin depends, at least partially, on a subset of pro-opiomelanocortin (POMC) neurons in the NTS that also express the 5-hydroxytryptamine 2C receptor (5-HT_{2C}R) (11). The GLP1R is also a target for obesity treatment and GLP1R agonists, such as the liraglutide, reduce appetite. In the NTS, a portion of GLP1R-expressing neurons also express γ -aminobutyric acid (GABA), and the chemogenetic silencing of GABAergic neurons in the NTS reduces the appetite-suppressant effect of liraglutide (23). To analyze the endogenous effects of GLP-1 in the NTS, Cheng et al. (24) ablated the proglucagon (Ppg), whose selective cleavage gives rise to GLP-1, in leptin receptor (LepR)- and Ppg-expressing neurons in the NTS. Although the Ppg deletion in both populations did not alter body weight and food intake, Cheng et al. (24) found that the chemogenetic activation of LepR- and Ppg-expressing neurons reduced the food intake.

In contrast to the most NTS neurons described so far that convey satiety, tyrosine hydroxylase (Th)- and epinephrine-

expressing NTS populations (NTSTH and NTS^E, respectively) with appetite-stimulant properties were recently identified (25, 26). The NTSTH neurons densely project to the ARC and drives agouti-related peptide (AgRP) neural activation through direct norepinephrine (NE) signaling; the NTS^E, in turn, coexpress the orexigenic neuropeptide Y (NPY) and its chemogenetic activation stimulates feeding (25, 26).

AgRP-expressing neurons in the hypothalamus potently induce feeding when stimulated and are key neurons in the regulation of energy balance (27, 28). For many years, AgRP neurons were exclusively considered to function as long-term homeostatic neurons. However, measurements of AgRP neuron dynamics in awake, behaving mice demonstrated that sensory cues, such as sight and smell of food, can rapidly inhibit these neurons (29, 30). Caged food presentation induces rapid and transient AgRP neuron inhibition in fasted mice, but if the food is subsequently consumed the inhibition is sustained, pointing to a key role for signals from the GI tract in the rapid control of AgRP neurons. Consistent with this, it was shown that intragastric infusion of calorie-containing nutrients promote persistent AgRP inhibition (31, 32). Moreover, intragastric infusion of water or consumption of a calorie-free gel resulted in only a small reduction in AgRP neuron activity (31, 32). Consistent with the known role of IGLs, mechanoreceptors sensing GI distention, chemogenetic activation of *Oxtr*⁺-expressing neurons in IGLs, and *Gpr*⁺ with a lesser magnitude also inhibited AgRP neurons (9). Also consistent with this, the *Oxtr*⁺ IGL is specifically expressed in the intestine and a calorie-free volumetric load in the intestine, but not in the stomach, sustained AgRP neuron inhibition (9).

Gut microbiota landscape is yet another factor affecting the gut-brain axis (33). Studies with germ-free rodents have that shown elevated levels of PYY and enteroglucagon (34) and the metabolites generated by enzymatic processing of nutrients, such as the short-chain fatty acids produced by the microbiota, can stimulate GLP1 release from L cells, suggesting that the gut bacteria participate in endocrine physiology (35). In addition to controlling metabolites, the microbiota is also able to produce signaling molecules with putative functions on feeding control. The *Escherichia coli*, for instance, produces a caseinolytic peptidase B protein homologue (ClpB), an α MSH-like peptide, whose plasma levels are associated with increased POMC neuronal activation (36).

NOVEL INTRA- AND EXTRAHYPOTHALAMIC CIRCUIT NODES IN FEEDING CONTROL

The sustained feeding behavior seen after activating AgRP neurons is quenched by sensory cues, raising the possibility that sustained hunger is mediated by another long-lasting neuropeptide. The AgRP neurons also release NPY and GABA, and the contribution of each of these neuromodulators to sustained hunger signal was recently assessed. AgRP neurons were optogenetically activated in animals in which GABA or NPY signaling was ablated by a cell-specific knockout for 15 min and food intake was subsequently measured (37). Mice lacking NPY presented a time-locked feeding and less drive for food-seeking upon stimulation, establishing

NPY as the neuromodulator responsible for the sustained hunger and motivated behaviors produced by AgRP neuronal activation (37). In addition, the activation of AgRP neurons induces peripheral insulin resistance and this effect is also NPY dependent (38).

AgRP- and POMC-expressing neurons project to the PVH, leading to increased and decreased food intake, respectively. Optogenetic activation of AgRP terminals in the PVH rapidly stimulate food intake through the inhibitory and fast-acting transmitters GABA and NPY (39). Conversely, the slow-acting, PVH^{MC4R} agonist, α MSH (cleaved from POMC) decreases food intake but only after hours (40). Thus, it was further hypothesized that there is another unknown fast-acting satiety neuron in the ARC. A group of glutamatergic neurons (ARC^{VGLUT2}) was recently identified as the source of excitatory input onto PVH neurons, and they were shown to rapidly induce satiety (41). Moreover, there is plasticity of glutamatergic transmission to PVH^{MC4R} and this is potentiated by α MSH. ChR2-assisted circuit mapping (CRACM) demonstrated that ARC^{VGLUT2} neurons receive light-evoked inhibitory postsynaptic currents (IPSCs) from ARC^{AgRP} neurons. Thus, ARC^{VGLUT2} neurons are inhibited by GABAergic projections from ARC^{AgRP} neurons under fasting conditions (41).

The PVH^{MC4R} is an important downstream effector site for ARC neurons and a critical node for satiety signaling. However, PVH^{MC4R} does not account for all satiety-related signaling of PVH neurons, as demonstrated by the comparison between the chemogenetic activation of single-minded-1-expressing neurons in PVH (PVH^{SM1}), which is expressed by most PVH neurons, and the chemogenetic activation of PVH^{MC4R} neurons on food intake. It was recently shown that the chemogenetic activation of glucagon-like peptide 1-expressing neurons in PVH (PVH^{GLP1R}) acutely suppress food intake and their silencing induced body weight gain and hyperphagia (42). Nevertheless, the significant overlap between PVH^{MC4R} and PVH^{GLP1R} neurons rules out the possibility that the putative PVH^{SM1}-positive/PVH^{MC4R}-negative neurons are this satiety-inducing population. The investigation of a prodynorphin-expressing neuron in PVH (PVH^{PDYN}),

which does not overlap with PVH^{MC4R}, led to the identification of this putative PVH^{SM1}-positive appetite-suppressing population, as their silencing also triggered obesity and hyperphagia (43). Anterograde viral tracing demonstrated that PVH^{PDYN} project to the central compartment of the lateral parabrachial nucleus (cLPBN) and prelocus coeruleus (pLC), but PVH^{PDYN} make glutamatergic synapses onto neurons in the pLC but not the cLPBN. Finally, the authors found that PVH^{PDYN} neurons receive GABAergic input from ARC^{AgRP} neurons, as demonstrated by light-evoked IPSCs (43).

In contrast to the short-term and gut-derived signals to the brain, leptin secretion by adipose tissue acts as long-term afferent signal to modulate food intake and body weight by controlling the activity of ARC, and other, neurons (44). Previous reports have indicated that leptin receptor-expressing (LepR) ARC^{POMC} neurons are important for feeding and body weight regulation. However, LepR deletion in ARC^{POMC} of adult mice does not affect body weight and food intake (45). Rather, leptin signaling in ARC^{POMC} is required for the regulation of glucose homeostasis independent of its effect on energy balance (45). A recent work demonstrated that CRISPR-mediated deletion of LepR in ARC^{AgRP} induced severe obesity, diabetes, and food intake, suggesting that leptin largely suppresses appetite by targeting ARC^{AgRP} and not ARC^{POMC} neurons (46). This work has now been challenged by a recent finding showing that the antiobesity effects of leptin are mediated by GABA-positive neurons in the ARC and its chronic activation induces massive obesity (47). The authors also observed that leptin administration in ARC^{AgRP}-ablated *ob/ob* mice is sufficient to normalize the body weight. Interestingly, the chronic chemogenetic activation of ARC^{AgRP} neurons increases feeding initially and induces significant weight gain, however the food intake and body weight return to baseline after 7 and 60 days, respectively (48). Taken together, the aforementioned studies highlight the complexity of hypothalamic circuits involved in the energy homeostasis.

Whereas increased leptin levels inhibit the food intake, a fall in leptin levels disinhibits ARC neurons and stimulate appetite. This hormonal programming to conserve fuel

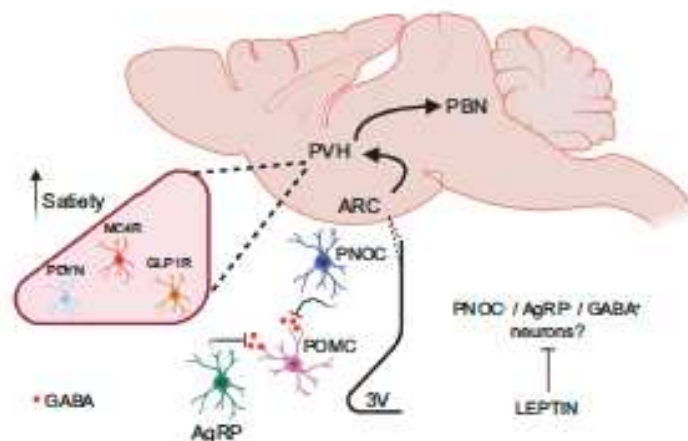


Figure 2. Novel ARC and PVH neurons. POMC-expressing neurons are activated by short-term HFD feeding and, in concert with AgRP neurons, inhibit POMC neurons through GABAergic projections. Recent studies suggest a distinct GABAergic neuronal population as the primary effector of leptin signaling in the ARC. The ARC neurons project to and target PVH neurons to control feeding. GLP1R, MC4R, and PDYN are expressed in different neurons in PVH and their activation induce satiety through different efferent circuitry in PBN. AgRP, agouti-related peptide; ARC, arcuate nucleus; GABA, gamma-aminobutyric acid; GLP1R, glucagonlike peptide-1 receptor; MC4R, melanocortin-4 receptor; PBN, parabrachial nucleus; PDYN, prodynorphin; POMC, pro-opiomelanocortin; PVH, paraventricular nucleus; 3V, third ventricle.

stores was recently extended by a recent work demonstrating that food-restricted mice display increased serum concentration of growth-hormone (GH) and the activation of its receptor (GHR) in ARC^{AgRP} induces metabolic responses consistent with energy conservation, such as reduction in energy expenditure and increased food intake (49).

Another novel GABAergic neuronal population regulating food intake was recently identified in the ARC. Prepro-nociceptin-expressing neurons (ARC^{PNO}) are distinct from ARC^{AgRP} and ARC^{POMC} and are glucose-excited (50). ARC^{PNO} project locally to the ARC and further assessment of its innervations identified an inhibitory connectivity onto ARC^{POMC} neurons. The optogenetic activation of ARC^{PNO} neurons promotes feeding but does not trigger acute effects on glucose homeostasis or insulin sensitivity. Interestingly, the *Pnoc* gene was one of the most enriched transcripts in the hypothalamus in mice fed an acute high-fat diet (HFD), indicating that PNO-expressing neurons may have a role in the overconsumption of mice fed a HFD (Fig. 2) (50). A recent report demonstrated that ARC^{AgRP} neurons receive input from a separate population of nociceptin-expressing neurons in the anterior bed nuclei of the stria terminalis (aBNST) (51). Moreover, the ablation of nociceptin-expressing neurons in aBNST increased body weight and food intake, suggesting a putative role of these neurons in energy homeostasis by controlling ARC^{AgRP} neurons activity (51). PNO-expressing neurons are also distributed in other extra-hypothalamic areas, such as lateral septum (LS) and central amygdala (CeA). The latter is recognized as an important integrative brain region and it receives excitatory glutamatergic inputs from PEN^{AgRP} neurons, and it is also activated by CCK. PNO-expressing neurons in CeA (CeA^{PNO}) were recently identified as a novel population (52). Consumption of HFD acutely activated CeA^{PNO} neurons, and mice with prior chemogenetic inhibition of CeA^{PNO} neurons reduced their HFD consumption on first exposure. The optogenetic activation of CeA^{PNO} terminals in the ventral BNST, PBN, and NTS induced a reward-like behavior (52).

The development of tissue-clearing techniques (e.g., DISCO-based methods) combined with *Fos* staining in the whole brain have provided further progress in the field by allowing the comparison of neuronal activation in different contexts and the identification of unappreciated brain regions involved in controlling energy homeostasis. In this regard, a study identified two molecularly and anatomically distinct neuronal populations in the dorsal raphe nucleus (DRN): a vesicular GABA transporter (DRN^{VGAT}) and a vesicular glutamate transporter type 3 (DRN^{VGLT3}) (53). It was shown that fasting increased *Fos*-positive activation of DRN^{VGAT} population. Optogenetic activation of DRN^{VGAT} population increased food intake and inhibition decreased food intake. The DRN^{VGLT3} were activated by refeeding and they inhibited food intake when activated whereas photoinhibition of DRN^{VGLT3} increased food intake. Chronic chemogenetic inhibition of DRN^{VGAT} neurons in leptin-deficient *ob/ob* mice led to a significant reduction in body weight (53). Further investigation of DRN^{VGAT} neurons in controlling energy homeostasis also identified a key regulatory role in thermogenesis, as their activation suppresses energy expenditure through reduction of interscapular brown adipose tissue (IBAT) temperature (54). Using IBAT

retrograde viral tracing, the authors found that DRN^{VGAT} neurons send descending projections to raphe pallidus (RPa), which in turn innervates IBAT (54).

CONCLUDING REMARKS

Interoceptive neurons process internal-state information to control appetite. Although most of the experimental approaches in neuroscience have been useful to probe neural mechanisms and circuits, the extent to which artificial activation/inhibition of neurons recapitulate their function under physiological circumstances is still unclear. The integration of sensory cues and caloric value of food is a permanent task for neurons and how these pathways are disturbed by obesity-predisposing factors, such as the consumption of HFD, is an ongoing debate (55–57). There is also a complex CNS network that controls IBAT thermogenesis and white adipose tissue (WAT) metabolism by controlling autonomic outflow. Similarly, peripheral insulin sensitivity and glucose metabolism are also potentially, but not exclusively, governed by CNS. Finally, there is an emergent need to comprehend how the brain deciphers palatable food and drive reinforcing effects, intermingling hedonic and homeostatic feeding (58).

GRANTS

This study was supported by the São Paulo Research Foundation (FAPESP) 2019/02969-2 (to A.M.A.), the JPB Foundation (to J.M.F.), and the São Paulo Research Foundation (FAPESP) 2019/07607-8 (to L.A.V.).

DISCLOSURES

No conflicts of interest, financial or otherwise, are declared by the authors.

AUTHOR CONTRIBUTIONS

A.M.A. prepared figures; A.M.A. drafted manuscript; A.M.A., J.M.F., and L.A.V. edited and revised manuscript; A.M.A., J.M.F., and L.A.V. approved final version of manuscript.

REFERENCES

- Berthoud HR, Blackshaw LA, Brooks SJ, Gandy D. Neuroanatomy of extrinsic afferents supplying the gastrointestinal tract. *Neurogastroenterol Motil* 16: 28–33, 2004. doi:10.1111/j.1743-3150.2004.00471.x.
- Berthoud HR, Neuhuber WL. Vagal mechanisms as neuromodulatory targets for the treatment of metabolic disease. *Ann NY Acad Sci* 1454: 42–55, 2019. doi:10.1111/nyas.14182.
- Walle TMZ, Deane HJ, Lam YKT. The metabolic role of vagal afferent innervation. *Nat Rev Gastroenterol Hepatol* 15: 625–636, 2019. doi:10.1038/s41575-019-0062-1.
- Fox EA, Phillips RJ, Baronowicz EA, Byrnes MS, Jones S, Powley TL. Neuropeptide-4 deficient mice have a loss of vagal intragastric mechanoreceptors from the small intestine and a disruption of short-term satiety. *J Neurosci* 21: 8602–8615, 2001. doi:10.1523/JNEUROSCI.21-21-08602.2001.
- Chen Y, Knight ZA. Making sense of the sensory regulation of hunger neurons. *Bioessays* 38: 316–324, 2016. doi:10.1002/bies.201500167.
- Gribble FM, Reimann F. Function and mechanisms of enteroendocrine cells and gut hormones in metabolism. *Nat Rev Endocrinol* 15: 226–237, 2019. doi:10.1038/s41574-019-0168-8.
- Kaibler MM, Buchanan KL, Klein ME, Barth BB, Montoya MM, Shan X, Bohorquez DV. A gut-brain neural circuit for nutrient

- sensory transduction. *Science* 361:eart5236, 2018. doi:10.1126/science.125236
8. Williams EK, Chang RB, Strohlic DE, Umans BD, Lowell BB, Lbarria SD. Sensory neurons that detect stretch and nutrients in the digestive system. *Cell* 166: 209–221, 2016. doi:10.1016/j.cell.2016.05.011
 9. Bai L, Mesgari-zadeh S, Ramesh KS, Huey EL, Liu Y, Gray LA, Wilken TJ, Chen Y, Beutler LR, Ahn JS, Madhan L, Zeng H, Kisanow MA, Knight ZA. Genetic identification of vagal sensory neurons that control feeding. *Cell* 179: 1129–1143.e23, 2019. doi:10.1016/j.cell.2019.10.031
 10. Kim DY, Hao G, Kim M, Kim H, Jin JA, Kim HK, Jung S, An M, Ahn BH, Park JH, Park HE, Lee M, Lee JW, Schwartz GJ, Kim SY. A neural circuit mechanism for mechanosensory feedback control of ingestion. *Nature* 580: 376–380, 2020. doi:10.1038/s41586-020-2167-2
 11. D'Agostino G, Lyons D, Cifalano C, Lettieri M, Olarte-Sanchez C, Burke LK, Greenwald-Yarnell M, Cassell C, Dostikova B, Georgescu T, Martinez de Morentin PB, Myers MG Jr, Rothford JJ, Holster LK. Nucleus of the solitary tract serotonin 5-HT2C receptors modulate food intake. *Cell Metab* 28: 619–630.e15, 2018. doi:10.1016/j.cmet.2018.07.017
 12. Han W, Tollaz LA, Perkins MH, Perez IO, Qu T, Ferreira J, Ferreira TL, Quinn D, Liu ZW, Gao XB, Kaelin-Lang A, Bohorquez DV, Shamamah-Lagnado SJ, de Lartigue G, de Araujo IE. A neural circuit for gut-induced reward. *Cell* 175: 665–678.e23, 2018. doi:10.1016/j.cell.2018.08.049
 13. Tan HE, Sisti AC, Jih H, Vignovich M, Villaraincib M, Tsang KS, Goffar Y, Zuker CS. The gut-brain axis mediates sugar preference. *Nature* 580: 511–516, 2020. doi:10.1038/s41586-020-2193-7
 14. D'Agostino G, Lyons DJ, Cifalano C, Burke LK, Madara JC, Campbell JN, Garcia AP, Land BB, Lowell BB, Dibone RJ, Holster LK. Appetite controlled by a cholecystokinin nucleus of the solitary tract to hypothalamus neurocircuit. *Elife* 5: e12225, 2016. doi:10.7554/eLife.12225
 15. Cheng W, Gonzalez I, Pan W, Tsang AH, Adams J, Ndoka E, Gordon D, Khoury B, Rodolfo K, Evans SS, MacKinnon A, Wu S, Flikke-Schmidt H, Flak JN, Trevisan J, Rhodes CJ, Fukuda S, Seeley RJ, Sandoval DA, Olson DP, Bout C, Myers MG Jr. Calcitonin receptor neurons in the mouse nucleus tractus solitarius control energy balance via the non-aversive suppression of feeding. *Cell Metab* 31: 301–312.e5, 2020. doi:10.1016/j.cmet.2019.12.012
 16. Johnen H, Lin S, Kuffner T, Brown DA, Tsai VW, Bauskin AR, Wu L, Panikharat G, Jiang L, Juranek S, Hunter M, Fafile WD, Lee NJ, Enriquez RF, Baldock PA, Corey E, Apple FS, Muralani MM, Lin EJ, Wang C, Dufing MJ, Salmsbury A, Herzog H, Bratt SN. Tumor-induced anorexia and weight loss are mediated by the TGF-beta superfamily cytokine MIC-1. *Nat Med* 13: 1333–1340, 2007. doi:10.1038/nm1677
 17. Suriben R, Chen M, Higbee J, Oeffinger J, Ventura R, Li B, Mondal K, Gao Z, Ayupova D, Taskar P, Li D, Staack SR, Chen HH, McEntee M, Katow S, Phung V, Wang M, Kalkitpure A, Lakshminarasimhan D, White A, Olland A, Haldankar R, Solloway MJ, Hsu JY, Wang Y, Tang J, Lindhout DA, Allan BB. Antibody-mediated inhibition of GDF15-GFRAL activity reverses cancer cachexia in mice. *Nat Med* 26: 1264–1270, 2020. doi:10.1038/s41591-020-0945-x
 18. Emmerson PJ, Wang F, Du Y, Liu Q, Pickard RT, Gondard MD, Coakun T, Hamang MJ, Sindelar DK, Ballman KK, Foltz LA, Muppidi A, Akiba-Fernandez J, Bamard GC, Tang JX, Liu X, Mao X, Siegel R, Sloan JH, Mitchell PJ, Zhang BB, Gimeno RE, Shan B, Wu X. The metabolic effects of GDF15 are mediated by the orphan receptor GFRAL. *Nat Med* 23: 1215–1219, 2017. doi:10.1038/nm4393
 19. Mulligan SE, Lih-Schmidt X, Chin CN, Chavez JA, Furman JL, Amstong AA, Beck SC, South VJ, Dinh TG, Cash-Mason TD, Cavenshough CR, Nelson S, Huang C, Hunter MJ, Rangwala SM. GFRAL is the receptor for GDF15 and the ligand promotes weight loss in mice and nonhuman primates. *Nat Med* 23: 1150–1157, 2017. doi:10.1038/nm4392
 20. Yang L, Chang C-C, Sun Z, Madsen D, Zhu H, Pedkjaer SB, Wu X, Huang T, Hultman K, Paulsen SJ, Wang J, Bugge A, Frantzen JB, Nergaard P, Jeppesen JF, Yang Z, Sedher A, Chen H, Li X, John LM, Shan B, He Z, Gao X, Su J, Hansen KT, Yang W, Jorgensen SB. GFRAL is the receptor for GDF15 and is required for the anti-obesity effects of the ligand. *Nat Med* 23: 1158–1165, 2017. doi:10.1038/nm4394
 21. Worth AA, Shoop R, Tye K, Feitham CH, D'Agostino G, Dodd GT, Reinmann F, Gibble FM, Beebe EC, Dunbar JD, Alexander-Chacko JT, Sindelar DK, Coakun T, Emmerson PJ, Luckman SM. The cytokine GDF15 signals through a population of brainstem cholecystokinin neurons to mediate anorectic signalling. *Elife* 9: e55164, 2020. doi:10.7554/eLife.55164
 22. Bomer T, Waid HS, Ghidewon MY, Zhang B, Wu Z, De Jonghe BC, Breen D, Gilli HL. GDF15 induces an aversive visceral malaise state that drives anorexia and weight loss. *Cell Rep* 31: 107543, 2020. doi:10.1016/j.celrep.2020.107543
 23. Fortin SM, Lipicky RK, Lhamo R, Chen J, Kim E, Bomer T, Schmidt HD, Hayes MR. GABA neurons in the nucleus tractus solitarius express GLP-1 receptors and mediate anorectic effects of liraglutide in rats. *Sci Transl Med* 12: eaay8071, 2020. doi:10.1126/scitranslmed.aay8071
 24. Cheng W, Ndoka E, Hutch C, Rodolfo K, MacKinnon A, Khoury B, Magrasso J, Kim KS, Rhodes CJ, Olson DP, Seeley RJ, Sandoval D, Myers MG Jr. Leptin receptor-expressing nucleus tractus solitarius neurons suppress food intake independently of GLP1 in mice. *JCI Insight* 5: e134859, 2020. doi:10.1172/jci.insight.134859
 25. Aktan I, Sayer Atasoy N, Yavuz Y, Atas T, Coban I, Koksalar F, Filiz G, Topcu IC, Onca M, Dilaz P, Gebecoglu U, Alp M, Yilmaz B, Davit DR, Hajdukiewicz K, Sako K, Konopka W, Cui H, Atasoy D. NTS catecholamine neurons mediate hypoglycemic hunger via medial hypothalamic feeding pathways. *Cell Metab* 31: 313–326.e5, 2020. doi:10.1016/j.cmet.2019.11.016
 26. Chen J, Cheng M, Wang L, Zhang L, Xu D, Cao P, Wang F, Herzog H, Song S, Zhan C. A vagal-NTS neural pathway that stimulates feeding. *Curr Biol* 30: 3985–3998.e5, 2020. doi:10.1016/j.cub.2020.07.084
 27. Aponte Y, Atasoy D, Stenerson SM. AgRP neurons are sufficient to orchestrate feeding behavior rapidly and without training. *Nat Neurosci* 14: 351–355, 2011. doi:10.1038/nn.2739
 28. Garfield AS, Li C, Madara JC, Shah BP, Webber E, Stager JS, Campbell JN, Garibova O, Lee CE, Olson DP, Elmquist JK, Tannen BA, Krahn MJ, Lowell BB. Neural basis for melanocortin-4 receptor-regulated appetite. *Nat Neurosci* 18: 863–871, 2015. doi:10.1038/nn.4011
 29. Betley JN, Xu S, Gao ZFH, Gong R, Magnus CJ, Yu Y, Stenerson SM. Neurons for hunger and thirst transmit a negative-valence teaching signal. *Nature* 521: 180–185, 2015. doi:10.1038/nature1446
 30. Chen Y, Lin YC, Kuo TW, Knight ZA. Sensory detection of food rapidly modulates arcuate feeding circuits. *Cell* 160: 829–841, 2015. doi:10.1016/j.cell.2015.01.033
 31. Beutler LR, Chen Y, Ahn JS, Lin YC, Essner RA, Knight ZA. Dynamics of gut-brain communication underlying hunger. *Neuron* 96: 461–475.e5, 2017. doi:10.1016/j.neuron.2017.09.043
 32. Su Z, Ahadeff AL, Betley JN. Nutritive, post-ingestive signals are the primary regulators of AgRP neuron activity. *Cell Rep* 21: 2724–2736, 2017. doi:10.1016/j.celrep.2017.11.036
 33. Cryan JF, O'Brian KJ, Cowan CSM, Sandhu KV, Bastiaansen TFS, Boehme M, et al. The microbiota-gut-brain axis. *Physiol Rev* 99: 1877–2013, 2019. doi:10.1152/physrev.00018.2018
 34. Ghata MA, Ratcliffe B, Bibom SR, Goodlad RA. Fermentable dietary fibre, intestinal microflora and plasma hormones in the rat. *Clin Sci (Lond)* 93: 109–112, 1997. doi:10.1042/cs0930109
 35. Chambers ES, Morrison DJ, Frost G. Control of appetite and energy intake by SCFA: what are the potential underlying mechanisms? *Proc Nutr Soc* 74: 328–336, 2015. doi:10.1017/S002966514001657
 36. Breton J, Tannen N, Lucas N, Francois M, Legendre R, Jacquemot J, Goldron A, Guefin C, Peltier J, Pestel-Caron M, Chen P, Vaudry D, de Rego JC, Denard F, Penicaud L, Fioramonti X, Ebenzer IS, Hokfelt T, Dechelotte P, Foltasov SO. Gut commensal *E. coli* proteins activate host satiety pathways following nutrient-induced bacterial growth. *Cell Metab* 23: 324–334, 2016. doi:10.1016/j.cmet.2015.10.017
 37. Chen Y, Essner RA, Kosar S, Miller OH, Lin YC, Mesgari-zadeh S, Knight ZA. Sustained NPY signaling enables AgRP neurons to drive feeding. *Elife* 8: e46348, 2019. doi:10.7554/eLife.46348
 38. Engstrom Rhud L, Pereira MMA, de Souza AJ, Fereslau H, Bruning JC. NPY mediates the rapid feeding and glucose metabolism

- regulatory functions of AgRP neurons. *Nat Commun* 11: 442, 2020. doi:10.1038/s41467-020-14291-3.
39. Krashes MJ, Shah BP, Koda S, Lowell BB. Rapid versus delayed stimulation of feeding by the endogenously released AgRP neuron mediators GABA, NPY, and AgRP. *Cell Metab* 18: 588–595, 2013. doi:10.1016/j.cmet.2013.09.009.
 40. Krashes MJ, Lowell BB, Garfield AS. Melanocortin-4 receptor-regulated energy homeostasis. *Nat Neurosci* 19: 206–219, 2016. doi:10.1038/nn.4202.
 41. Fenselau H, Campbell JN, Varastegan AM, Madara JC, Xu J, Shah BP, Rasch JM, Yang Z, Mandelblat-Cerf Y, Lihseh Y, Lowell BB. A rapidly acting glutamatergic ARC->PVH satiety circuit postsynaptically regulated by alpha-MSH. *Nat Neurosci* 20: 42–51, 2017. [Erratum in *Nat Neurosci* 20: 1189, 2017]. doi:10.1038/nn.4442.
 42. Li C, Navarrete J, Liang-Gualpa J, Lu C, Funderburk SC, Chang RB, Uberles SD, Olson DP, Krashes MJ. Defined paraventricular hypothalamic populations exhibit differential responses to food contingent on caloric state. *Cell Metab* 29: 681–694.e5, 2019. doi:10.1016/j.cmet.2018.10.016.
 43. Li MM, Madara JC, Steger JS, Krashes MJ, Balhuvar N, Campbell JN, Rasch JM, Conley NJ, Garfield AS, Lowell BB. The paraventricular hypothalamus regulates satiety and prevents obesity via two genetically distinct circuits. *Neuron* 102: 653–667.e6, 2019. doi:10.1016/j.neuron.2019.02.028.
 44. Friedman JM. Leptin and the endocrine control of energy balance. *Nat Metab* 1: 754–764, 2019. doi:10.1038/s42255-019-0095-y.
 45. Caron A, Dungan Lemko HM, Castorena CM, Fujikawa T, Lee S, Lord CC, Ahmed N, Lee CE, Holland WL, Liu C, Elmquist JK. POMC neurons expressing leptin receptors coordinate metabolic responses to fasting via suppression of leptin levels. *Elife* 7: e33710, 2018. doi:10.7554/eLife.33710.
 46. Xu J, Bartolome CL, Low CS, Yi X, Chien CH, Wang P, Kong D. Genetic identification of leptin neural circuits in energy and glucose homeostasis. *Nature* 556: 505–509, 2018. doi:10.1038/s41586-018-0049-7.
 47. Zhu C, Jiang Z, Xu Y, Cai ZL, Jiang Q, Xu Y, Xue M, Arenkiel BR, Wu Q, Shu G, Tong Q. Profound and redundant functions of arcuate neurons in obesity development. *Nat Metab* 2: 763–774, 2020. doi:10.1038/s42255-020-0229-2.
 48. Ewbank SN, Campos CA, Chen JY, Bowen AJ, Padilla SL, Dempsey JL, Cui JY, Palmiter RD. Chronic Gq signaling in AgRP neurons does not cause obesity. *Proc Natl Acad Sci USA* 117: 20874–20880, 2020. doi:10.1073/pnas.2004941117.
 49. Furlgo JC, Teitelbaum PD, de Souza GO, Couto GCL, Romero GG, Perello M, Frazzo R, Elias LL, Metzger M, List EO, Kopchik JJ, Donato J Jr. Growth hormone regulates neuroendocrine responses to weight loss via AgRP neurons. *Nat Commun* 10: 562, 2019. [Erratum in *Nat Commun* 10(1):980, 2019]. doi:10.1038/s41467-019-08607-1.
 50. Jais A, Paeger L, Solato-Hiltschfeld T, Bremser S, Prinzansteiner M, Klamm P, Myktiluk V, Widdershooven PJM, Vesting AJ, Gzalka K, Mihare M, Cramer AL, Xu J, Komolova T, Lowell BB, Zellhofer HU, Backus H, Fenselau H, Wunderlich FT, Kloppenburg P, Buihng JC. PNO(ARC) neurons promote hyperphagia and obesity upon high-fat-diet feeding. *Neuron* 106: 1009–1025.e10, 2020. doi:10.1016/j.neuron.2020.03.022.
 51. Smith MA, Choudhury A, Giegola JA, Viskakis P, Irvine EE, de Campos Silva PCC, Khadayate S, Zellhofer HU, Wilkes DJ. Extrahypothalamic GABAergic nociceptin-expressing neurons regulate AgRP neuron activity to control feeding behavior. *J Clin Invest* 130: 126–142, 2019. doi:10.1172/JCI130340.
 52. Hardaway JA, Halladay IR, Mazzone CM, Patel D, Bloodgood DW, Kim M, Jensen J, DiBono JF, Boyd KM, Shiddapur A, Erfani A, Hon OJ, Nelin S, Stanhope CM, Sugam JA, Saddaris MP, Tipton G, McEligott Z, Zhou TC, Stuber GD, Bruchas MR, Bulik CM, Holmes A, Kash TL. Central amygdala prepro-nociceptin-expressing neurons mediate palatable food consumption and reward. *Neuron* 102: 1037–1052.e37, 2019. doi:10.1016/j.neuron.2019.03.037.
 53. Nectow AR, Schneeberger M, Zhang H, Field BC, Renier N, Azevedo E, Patel B, Liang Y, Mito S, Tessier-Lavigne M, Han MH, Friedman JM. Identification of a brainstem circuit controlling feeding. *Cell* 170: 429–442.e11, 2017. doi:10.1016/j.cell.2017.06.045.
 54. Schneeberger M, Parolaro L, Das Banerjee T, Bhawe V, Wang P, Patel B, Topfiko T, Wu Z, Choi CHJ, Yu X, Pellegrino K, Engel EA, Cohen P, Renier N, Friedman JM, Nectow AR. Regulation of energy expenditure by brainstem GABA neurons. *Cell* 178: 672–685.e12, 2019. doi:10.1016/j.cell.2019.05.048.
 55. Cai D, Rhee S. "Hypothalamic microinflammation" paradigms in aging and metabolic diseases. *Cell Metab* 30: 19–35, 2019. doi:10.1016/j.cmet.2019.05.021.
 56. Cavadas C, Avelino CA, Souza GF, Veloso LA. The pathophysiology of defective proteostasis in the hypothalamus - from obesity to ageing. *Nat Rev Endocrinol* 12: 723–733, 2016. doi:10.1038/nrendo.2016.107.
 57. Razoli DS, Moura-Assis A, Bombassaro B, Veloso LA. Hypothalamic neuronal cellular and subcellular abnormalities in experimental obesity. *Int J Obes* 43: 2361–2369, 2019. doi:10.1038/s41366-019-0451-8.
 58. Rossi MA, Stuber GD. Overlapping brain circuits for homeostatic and hedonic feeding. *Cell Metab* 27: 42–56, 2018. doi:10.1016/j.cmet.2017.09.021.